Investigating the Mechanism of Conditioning Electrical Stimulation: *Identifying Key Parameters and Signaling Pathways*

by

Paige BL Hardy

A thesis submitted in partial fulfillment of the requirements for the degree of

Master in Science

Neuroscience

University of Alberta

Abstract

Despite timely surgical intervention, regeneration following peripheral nerve injury remains insufficient for adequate functional recovery. Thus, new therapeutic interventions are necessary. Traditionally, electrical stimulation has been delivered postoperatively to promote functional recovery following peripheral nerve injury. Postoperative electrical stimulation (PES) promotes staggered regeneration (increasing axon extension across the injury site), and has been successfully integrated into clinical practice. Conditioning electrical stimulation has recently been shown to accelerate the innate rate of regeneration when administered 7 days prior to a nerve injury. Due to its non-injurious, non-inflammatory nature, CES proves a viable option for clinical translation to enhance recovery in chronic and acute nerve repair, and nerve transfer procedures. However, the parameters of CES have not yet been optimized. The minimum duration of stimulation, period between conditioning and injury (latency period) and neuronal specificity have not been investigated. Likewise, much of the mechanism of CES remains either uninvestigated, or undifferentiated in the literature from PES. However, cAMP and its downstream targets BDNF and pCREB are known to upregulate following CES. cAMP's downstream effectors PKA and EPAC have not been investigated in the context of CES.

In this study we aim to identify the minimum duration of electrical stimulation, and the minimum latency period required to elicit the pro-regenerative effects of CES. We investigate the neuronal specificity of CES, and identify key signaling pathways involved in the mechanism of CES.

To investigate the minimum duration of CES, CES was administered for 60, 30, 10 or 0 minutes either 3 days prior to DRG harvest to assess regeneration associated gene (RAG) expression, or 7 days prior to nerve repair surgery to assess regeneration. To investigate the

latency period of CES, CES was administered 7, 5, 3, or 1 days prior to either neurite extension assays or RAG analysis, and compared to unstimulated DRG controls. Neuronal specificity is investigated through immunohistochemical staining and assessment of regeneration of different neuronal subtypes, including proprioceptors, peptidergic nociceptors, and motor neurons. To investigate the involvement of cAMP and its mediators in CES, CES is administered 3 days prior to DRG harvest and culture, EPAC and PKA pathways are pharmacologically inhibited and neurite extension assessed.

Our data demonstrates that as the duration of stimulation increases, the capacity for regeneration following injury also increases. The most effective regeneration occurred with 1 hour of CES, though 30 minutes also significantly increased regeneration. Latency periods between 3 and 7 days increased neurite extension *in vitro*, coinciding with the upregulation of RAGs. CES appeared to elicit its effects non-specifically across all neuronal subtypes, despite innate differences in regenerative capacity among subtypes. Pharmacological inhibition of EPAC alone, and EPAC and PKA in combination resulted in the partial ablation of the pro-regenerative effects of CES *in vitro*, suggesting a compensatory role for both mediators, but a potentially larger role of EPAC in the mechanism of CES. CES administered for 1 hour, with a latency period between 3 and 7 days, will act upon the cAMP pathway to nonspecifically elicit pro-regenerative effects.

Preface

This thesis is an original work by Paige Hardy. The current research project was completed at the University of Alberta under the supervision of Dr. Christine Webber, Dr. Brad Kerr, and Dr. Keith Fenrich. The research project, of which this thesis is a part, received research ethics approval from the University of Alberta Research Ethics Board AUP00001871. This project received funding from a Canada Graduate Scholarship-Masters-CIHR.

Dedication

I dedicate the completion of my Master's thesis to Logan Arthur. Thank you for reminding me to slow down and to look up from my work every once in a while. I would have missed many moments of joy if it had not been for you. It is you that I owe all of my success to. I dedicate this to my wonderful parents, Patrick and Michelle Hardy, and my brother Payton. Thank you for always being my sounding boards, and showing interest when not many outside of my field would. And lastly, thank you to my friends, of which several have offered to read my thesis after its completion. I am going to hold you to that, and quiz you on it after.

I have so many incredible people in my life, and I am eternally grateful to all of you. I could not have spent so much time around rats without knowing I would have all of you to fall back on.

Acknowledgements

I have many people to thank for the completion of this project. First, I would like to thank my supervisor, Dr. Christine Webber for her guidance. Dr. Webber, the vigor in which you attack each of your many projects has always sparked my own enthusiasm in my research. You have challenged me to do more, find more, think more at each step, and you have always done so with great kindness. You invest everything into the success of your students, and I am deeply grateful to you. Thank you for showing me what it is to be not only a scientist, but a fantastic mentor.

Thank you to Dr. Brad Kerr and Dr. Keith Fenrich for taking the time to be committee members. I sincerely hope you do not regret agreeing to it once you see this document. Thank you for challenging me, and bringing a fresh perspective to every committee meeting.

My lab has been a constant source of support and positive energy. Thank you to our laboratory technician Susanne Lingrell, and her endless technical expertise. Susanne, you have salvaged more of my experiments than I would like to admit, and without you and your generosity, this project would not have been possible. I greatly enjoyed all the hours I got to spend getting to know you as we collected tissue samples-- I am indebted to you.

Thank you to the brilliant Dr. Jenna Senger, who has graciously completed hours of surgeries to make my project possible. Your drive and energy continue to amaze me, and your love for science and your work is evident. My project would not have been nearly as interesting without your masterful surgical precision.

Thank you to undergraduate students Taylor Mykto and Aryan Sharma for their contributions to my methods figures in my thesis, and thank you to undergraduate students Yousef Darwish and Rory Karbonik whose insights into their own research projects helped me to think of their applications to mine.

Thank you to all labs present at our weekly Journal Club meetings. I attribute the growth of my public speaking and scientific digestion directly to these meetings, and to everyone there. Thank you to Dr. Ming Chan and Mith Rajshekar for organizing these meetings. Dr. Chan, thank you for all of your expertise in clinic, and for your work on our publications and abstracts. Your insight is always profound and I appreciate all the time you have devoted to helping me.

Thank you to Dania Villarreal, Serena Isley, Jasmine Feddema, and Masha Sharkova for making me feel as though I was not the only graduate student in my lab. You are all incredibly hardworking, talented, and brilliant, and I cannot tell you how reassuring it was to see that I was not alone in the grad-student-esque suffering. I thank each of you endlessly, and am so excited to see all of your successes.

Thank you to the Kerr and Plemel labs for allowing me to spend many hours on their cryostat. Thank you to Dr. Andrew Simmonds, for allowing me to sit on your microscope for hours and hours. Thank you to Kiera Smith and Dr. Hilmar Strickfaden with the Cell Imaging Core for allowing me to use their new Thunder software and to Dr. Sun at the Cell Imaging Facility for his help with MetaXpress Imaging. My project would not have been possible without your guidance.

It has been incredible to discuss my research with some of the most intelligent scientists at the University of Alberta. I thank you all endlessly, and your tireless dedication to your craft will forever inspire me.

Table of Contents

List of Figures

List of Tables

List of Abbreviations

AC	Adenylate cyclase
ADPR	Adenylate-diphosphate ribosome
Akt	Protein kinase B
ANOVA	Analysis of variance
AP-1	Activator protein 1
ASIC1	Acid-sensing ion channel subunit 1
ASIC3	Acid-sensing ion channel subunit 3
ATF3	Activating transcription factor 3
Arg1	Arginine 1
BDNF	Brain derived neurotrophic factor
BMDM	Bone marrow derived monocytes
NPPB	Natriuretic peptide B
BSA	Bovine serum albumin
cADP	Cyclic adenylate-diphosphate
CALCA	Calcitonin-related polypeptide alpha
CaMK	Calmodulin kinase
cAMP	Cyclic adenylate-monophosphate
CBD	cAMP binding domain
CCL	Conditioning crush lesion
CCL2	C-C motif chemokine ligand 2
CES	Conditioning electrical stimulation
CGRP	Calcitonin gene-related peptide

ChAT	Choline acetyltransferase
CHRNA3	Cholinergic receptor nicotinic alpha 3 subunit
CMAPs	Compound muscle action potentials
CNS	Central nervous system
CPNE6	Copine 6
CREB	cAMP response element binding protein
CSPGs	Chondroitin sulfate proteoglycans
DLK	Dual-leucine zipper kinase
DMEM	Dulbecco's Modified Eagle Medium/F12
DPBS	Dulbecco’s phosphate buffered saline
DRG	Dorsal root ganglia
ECM	Extracellular matrix
Elk1	ETS-like protein 1
EPAC	Exchange protein activated by cAMP
ES	Electrical stimulation
ER	Endoplasmic reticulum
ERK	Extracellular signal-regulated kinase
FBS	Fetal bovine serum
GAB	GRB2-associated binder
GAP43	Growth associated protein 43
GDNF	Glial-derived neurotrophic factor
GDP	Guanosine diphosphate
GEF	Guanine exchange factor

GFAP	Glial fibrillary acidic protein
GFRA2	GDNF family receptor alpha 2
Gp130	Glycoprotein 13
GRB2	Growth factor receptor-bound protein-2
GSK-3	Glycogen synthase kinase 3
GTP	Guanosine triphosphate
HBSS	Hank's buffered salt solution
HGF	Hepatocyte growth factor
HRH1	H1 histamine receptor gene, histamine receptor H1
HTMRs	High threshold mechanoreceptors
HSLAS	Health Sciences Laboratory Animal Services
HTR3A	5-hydroxytryptamine receptor 3A
IB4	Isolectin B4
IFN-β	Interferon-beta
IGF-1	Insulin-like growth factor-1
IL-1α	Interleukin 1-alpha
IL-1β	Interleukin-1-beta
IL31RA	Interleukin-31 receptor A
IL-6	Interleukin-6
iNOS	Inducible nitric oxide synthase
JAK	Janus kinases
JIP	JNK-interacting protein
JNK	cJun N-terminal kinase

KCNS1	Potassium voltage-gated channel modifier subfamily S member 1
LPAR3	Lysophosphatidic acid receptor 3
LTMRs	Low threshold mechanoreceptors
MAG	Myelin associated glycoprotein
MAPK	Mitogen-activated protein kinase
MAPKK	Mitogen-activated protein kinase kinases
MAPK3	Mitogen-activated protein kinase kinase kinase
MBP	Myelin basic protein
MDMs	Monocyte derived macrophages
MEK	Mitogen‑activated and extracellular signal‑regulated kinase
MPS	Membrane-associated Periodic Skeleton
mTOR	Mammalian target of rapamycin
mTORC2	Mammalian target of rapamycin complex 2
NAD	Nicotinamide adenine dinucleotide
NF200	Neurofilament 200
NGF	Nerve growth factor
NGS	Normal goat serum
NgR	Nogo receptor
NLS	Nuclear localization signal
Nmn	Nicotinamide mononucleotide
Nmnat1	Nicotinamide mononucleotide adenylyltransferase-1
Nmnat2	Nicotinamide mononucleotide adenylyltransferase-2
NT-4	Neurotrophin type-4

OCT	Optimal cutting temperature
OMgp	Oligodendrocyte myelin glycoprotein
PBS	Phosphate buffered saline
pCREB	Phosphorylated cAMP response element binding protein
PDK1	Phosphoinositide-dependent kinase 1
PENK	Proenkephalin
PES	Postoperative electrical stimulation
PFA	Paraformaldehyde
PGE2	Prostaglandin E2
PTGER3	Prostaglandin E receptor 3
PGP9.5	Protein gene product 9.5
PIP2	Phosphatidylinositol 4,5-bisphosphate
PIP3	Phosphatidylinositol 3,4,5-trisphosphate
PI3K	Phosphatidylinositol‑3‑kinase
PKA	Protein kinase A
PMR	Preferential motoneuron reinnervation
PNS	Peripheral nervous system
pSTAT	Phosphorylated signal transducer and activator of transcription 3
PTEN	Phosphatase tensin homolog deleted on chromosome ten
PTN	Pleiotrophin
PV	Parvalbumin
P0	Myelin protein 0
P2X3R	P2X purinoceptor 3

p75NRT	p75 neurotrophic receptor
RA-LTMRs	Rapidly adapting LTMRs
Raf	Rapidly accelerating fibrosarcoma
RAGs	Regeneration associated genes
Rap1	Repressor/activator protein-1
Ras	Rat sarcoma
RET	Rearranged during transfection
ROK	Rho-kinase
RTKs	Receptor tyrosine kinases
RUNX	Runt-related transcription factor
RUNX3	RUNX family transcription factor 3
SA-LTMRs	Slowly adapting LTMRs
SARM1	Sterile-α and Toll/interleukin 1 receptor (TIR) motif containing protein 1
SCN10A	Sodium voltage-gated channel alpha subunit 10
SCN11A	Sodium voltage-gated channel alpha subunit 11
SGCs	Satellite glial cells
SLC17A7	Solute carrier family 17 member 7
Smad1	Mothers against decapentaplegic
SNI	Sciatic nerve injury
SOS	Son of sevenless
STAT	Signal transducer and activator of transcription 3
SPRY2	Sprouty2
Syd	JNK scaffold protein Sunday driver

TH	Tyrosine hydroxylase
TIR	Toll/Interleukin 1 receptor
TLRs	Toll-like receptors
TNF-α	Tumor necrosis factor alpha
TrkA	Tyrosine receptor kinase A
TrkB	Tyrosine receptor kinase B
TrkC	Tyrosine receptor kinase C
TRMs	Tissue resident macrophages
TRPM8	Transient receptor potential cation channel subfamily M member 8
UbE4B	Ubiquitination ligase E4B
URN	Urocortin
VG	Voltage gated
VGLUT1	Vesicular glutamate transporter 1
VGLUT3	Vesicular glutamate transporter 3
Wld^S	Slow Wallerian Degeneration mice
Xbp1	X-box-protein-1

CHAPTER 1: Introduction

1.1 Peripheral Nerve Injury

Unlike the central nervous system (CNS), nerves in the peripheral nervous system (PNS) have the capacity to regenerate after injury (Huebner and Strittmatter, 2009; Batty et al., 2016). While the CNS features inhibitory environmental factors, inhibitory intracellular signaling, and a lack of neurotrophic support after nerve injury, the PNS neutralizes inhibitory myelin, of which there are much less of, and promotes neurotrophins and other intracellular signaling pathways to enhance growth (Batty et al., 2016). Notwithstanding the growth promoting opportunities of the PNS, peripheral nerve regeneration often results in incomplete functional recovery (Rotshenker, 2011; Menorca et al., 2013; Grinsell and Keating, 2014). To regain function, peripheral axons must regenerate towards and reinnervate target muscles which may be up to 1 meter away (Rotshenker, 2011); peripheral injuries sustained near the dorsal root ganglia (DRG) must regenerate especially long distances, and with a slow rate of regeneration, neurotrophic support from Schwann Cells at the distal stump of regenerating axons gradually begins to decline. Muscle fibers may begin to atrophy as early as 3 weeks after injury (Fu and Gordon, 1995a; Rotshenker, 2011; Menorca et al., 2013; Scheib and Höke, 2013). Nerve reinnervation must occur 6-12 months after peripheral nerve injury before irreversible muscle atrophy, signifying the development of a ‘chronic denervation’ phenotype, unlikely to support reinnervation (Grinsell and Keating, 2014). Furthermore, axons slow their regeneration rate when crossing a site of injury, known as staggered regeneration, or may be misguided into the wrong endoneurial tubes or end organs (Sulaimen and Gordan, 2013; Shapira and Midha, 2015). With inadequate available treatments, peripheral nerve injuries can be debilitating, with a significant impact on quality of life (Menorca et al., 2013). Therefore, it is crucial to identify strategies to accelerate peripheral nerve regeneration, promote remyelination, prolong neurotrophic support for axons on the regenerative front, and delay chronic denervation of muscle.

Treatments that aim to accelerate nerve regeneration must consider peripheral nerve anatomy and supporting cell dynamics. Healthy peripheral neurons receive support from myelinating Schwann cells, tissue resident macrophages (TRMs), fibroblasts, mast cells and endothelial cells, all of which play a role in healthy regeneration and recovery after injury (Catala and Kubis, 2013). Peripheral nerves contain large myelinated α-motor and proprioceptive Aα-fibers, smaller mechanoreceptive Aβ-fibers and nociceptive Aδ-fibers, and unmyelinated nociceptive C-fibers. Schwann cells enwrap individual axons with medium and large diameter motor axons, proprioceptors, mechanoreceptors and nociceptors to form an electrically insulating sheath of the lipoprotein myelin, ensuring sufficient conduction velocity of action potentials (Catala and Kubis, 2013). Small diameter C fibers remain unmyelinated and are contained within Remak bundles, which consist of non-myelinating Schwann Cells that enwrap clusters of C fiber axons through its cytoplasmic processes (Grinsell and Keating, 2014). A Blood Nerve Barrier (BNB) is formed at the level of each axon; endothelial cells connected through tight junctions surround each myelinated axon or Remak bundle, preventing the nerve tissue from exposure to toxic blood or signaling factors external to the PNS (Palladino et al., 2017). Myelinated axons bundle together amongst vasculature, lymphatic vessels and other supporting cells, wrapped in perineurium to form fascicles, the final component of the BNB (Catala and Kubis, 2013). Fibroblasts reside within axon bundles and secrete collagen to provide mechanical support for the axon bundle (Wang et al., 2017). TRMs remain in the peripheral nerve tissue, as opposed to mast cells and bone marrow derived monocytes (BMDMs), which circulate in the blood, then infiltrate the nerve after injury (Bautista and Krishnan, 2022). Multiple fascicles of axons are subsequently bound, alongside larger vasculature, by epineurium to form the peripheral nerve (Catala and Kubis, 2013).

Peripheral nerves consist of both sensory and motor axons that are bundled separately into fascicles (Rotshenker, 2011; Catala and Kubis, 2013; Grinsell and Keating, 2014). Motor neurons exit the spinal cord through the ventral root, with cell bodies originating from the ventral horn, and afferent sensory neurons enter the spinal cord through the dorsal root (Catala and Kubis, 2013). The pseudounipolar nature of sensory neurons results in the accumulation of cell bodies known as the DRG, which resides lateral to the dorsal horn in the intervertebral foramen between vertebrae (Catala and Kubis, 2013). Motor neurons synapse onto target muscles to form neuromuscular junctions, while sensory neurons innervate cutaneous sensory organs, muscle spindles, tendons, hypodermis, and bone (Catala and Kubis, 2013).

Peripheral nerve injuries result in altered gene expression and paracellular responses to support regeneration (Chhabra et al., 2014; Grinsell and Keating, 2014). Nerve injuries can be categorized using Sunderland's and Seddan's criteria (Seddon, 1942; Sunderland, 1951): Type 1, or Neuropraxia, with focal injury to myelin only, Type 2 - 4, Axonotmesis, injury and transection of axons and varying degrees of connective tissue, and Type 5, Neurotemsis, injury and transection of all peripheral nerve tissue (Chhabra et al., 2014; Grinsell and Keating, 2014). Sunderland Type 1 injuries often include stretch or compression injuries, whereas Sunderland Type 2 and 3 injuries can be modeled as varying degrees of crush injuries. Sunderland Type 4 and 5 injuries include axotomized nerves. Despite these classifications, nerve injuries are rarely confined to one; injuries often display varying degrees of damage and are considered mixed injuries (Grinsell and Keating, 2014). Therefore, electromyography, nerve conduction studies, and magnetic resonance imaging are noninvasive imaging techniques used clinically to determine the extent of injury and degree of intervention required (Pabari et al., 2010).

Peripheral nerve injuries with classifications of Type 1 and 2 have the likeliest prognosis of recovery, even without intervention, due to the preserved integrity of most connective tissue, while Type 3 to Type 5 injuries have little to no chance of full recovery (Pabari et al., 2010; Grinsell and Keating, 2014). Type 4 and 5 injuries must undergo surgical intervention for proper recovery (Pabari et al., 2010). Injuries classified between Sunderland Type 2 and Type 5 often result in degeneration of axons distal to the injury site, a process known as Wallerian Degeneration (Rotshenker, 2011). Following degeneration of the distal stumps, peripheral axons regenerate back to their reinnervation targets. However, injuries that result in damage to connective tissue may cause nerve gaps that hinder regeneration as the regenerating axons cannot directly cross into the epineurial tube, which remains following degeneration of the distal nerve stump (Sunderland, 1951; Pabari et al., 2010). In cases of axotomy without nerve gap, or with a relatively short nerve gap, primary end to end neurorrhaphy is performed with alignment of fascicles and vasculature of the cut ends of the nerve (Pabari et al., 2010). In cases of axotomy where the nerve gap is too long and neurorrhaphy would result in excess tension, alternative surgical interventions are considered; autologous nerve grafts, or connective tissue bridges, connect the proximal injury site to the distal injury site and are considered the gold standard of intervention for long nerve gaps (Pabari et al., 2010). However, despite decades of advancements in microsurgical repair of microscopic nerve injury, functional recovery outcomes remain unsatisfactory (Pabari et al., 2010). Microsurgical techniques are insufficient for proper functional recovery due to the limitations of the intrinsic regenerative capacity of peripheral nerves. Therefore, strategies to mitigate these limitations are of interest.

1.2 Wallerian Degeneration

After peripheral nerve injury, the surrounding microenvironment undergoes changes at the site of tissue damage; these processes facilitate regeneration and reinnervation that are necessary for recovery. In cases of axonal injury, disturbances in axon membrane integrity result in an influx of extracellular Na+ and Ca2+, ultimately triggering degeneration of axons and the myelin sheath. As the axons distal to the injury site begin to degenerate, a proximal stump of regenerating axons and a distal stump of degenerating axons and other supportive tissues form (Rotshenker, 2011; Menorca et al., 2013). Disturbances in axonal structure in the distal stump are observed as early as 24 hours after injury, and fragmentation of degenerating axons is observed 2 - 3 days after injury. Within 2 days of injury, the myelin sheath enwrapping axons also begins to degrade as the myelin-producing Schwann cells separate from the axons (Rotshenker, 2011; Conforti et al., 2014). At the injury site, axon degeneration occurs 1-2 Nodes of Ranvier proximal to the injury site which allows for new regenerating axons from the proximal stump (Cullen, 1988; Rotshenker, 2011).

1.2.1 Neuronal Signaling in Wallerian Degeneration

After axotomy, axonal transport of the constitutively expressed nicotinamide mononucleotide adenylyltransferase-2 (Nmnat2) to the distal stump of the injured axon is severed, leading to the initiation of Wallerian Degeneration (Coleman & Höke, 2020). Depletion of Nmnat2 decreases expression of its downstream effector, nicotinamide adenine dinucleotide (NAD), and an increase in nicotinamide mononucleotide (Nmn), leading to the activation of sterile-α and Toll/interleukin 1 receptor (TIR) motif containing protein 1 (SARM1) (Coleman & Höke, 2020). SARM1 initiates axon degeneration by contributing to the depletion of NAD after Nmnat2 loss, and increasing cyclic adenylate-diphosphate (cADP) and adenylate-diphosphate ribosome (ADPR) to promote calcium influx (Coleman & Höke, 2020). cADP and ADPR induced calcium mobilization contributes to Ca2+ dependent protease activation and second messenger molecules (Coleman & Höke, 2020). Deletion of Nmnat2 or disruption of Nmnat2 anterograde transport prevents any new axonal growth, and even induces distal stump retraction unless SARM1 function is also disrupted (Coleman & Höke, 2020). Discovery of Nmnat2 as a neuroprotective gene led to the development of transgenic "Slow Wallerian Degeneration mice" (Wld^{S}), that express a chimeric nuclear protein nicotinamide mononucleotide adenylyltransferase-1 (Nmnat1), and ubiquitination ligase E4B (UbE4B) (Coleman & Höke, 2020). Nmnat1 is an enzyme involved in the synthesis of signaling cofactor NAD, able to compensate for Nmnat2 through NAD synthesis and Nmn degradation (Coleman & Höke, 2020; Hill et al., 2016; Laser et al., 2006). Expression of this chimeric protein inhibits the process of Wallerian degeneration (Laser, et al., 2006); with increased neuroprotection, Wallerian Degeneration does not occur, and peripheral axons display little cytoskeletal disruption following traumatic injury (Hill et al., 2006).

1.2.2 Multicellular Wallerian Degeneration

Myelin proteins released from the degenerating nerve, such as myelin basic protein (MBP), myelin protein 0 (P0), and myelin associated glycoprotein (MAG), inhibit growth of regenerating axons through activation of Nogo receptor (NgR), and downstream RhoA activation (Krishnan et al., 2016; Rotshenker, 2011). In the PNS, these myelin proteins are present in much smaller quantities than in the CNS, although initial release of myelin debris can prove to be inhibitory for peripheral nerve growth (Huebner & Strittmatter, 2009). Therefore myelin debris must be cleared for regenerating axons (Gaudet et al., 2011; Rotshenker, 2011). Schwann cells switch from a myelinating phenotype to a proliferating phenotype to facilitate myelin and axon debris clearance. Proliferating Schwann cells phagocytose debris and attract phagocytotic macrophages into the nerve tissue via cytokines and chemokines (Rotshenker, 2011; Menorca et al., 2013; Conforti et al., 2014), while upregulating TLRs (toll-like receptors) to further perpetuate injury signaling in Schwann cells and macrophages (Gaudet et al., 2011). Select inflammatory factors interleukin-1-alpha (IL-1α), interleukin-1-beta (IL-1β), tumor necrosis factor alpha (TNF-α), inducible nitric oxide synthase (iNOS), C-C motif chemokine ligand 2 (CCL2), interferon beta (IFN-β), and other cytokines are upregulated alongside TLRs (Boivin et al., 2007; Gaudet et al., 2011; Rotshenker, 2011). These factors, as well as heat shock proteins and extracellular matrix (ECM) debris bind to upregulated TLRs and induce release of CCL2 from Schwann cells to attract macrophages to the site of injury (Boivin et al., 2007; Gaudet et al., 2011; Rotshenker, 2011). Within a week of injury, TRMs and monocyte derived macrophages (MDMs) are recruited to the distal stump of the peripheral nerve (Gaudet et al., 2011). Without activation of TLRs, myelin clearance, macrophage infiltration, and functional recovery are impaired (Boivin et al., 2007; Gaudet et al., 2011).

In the weeks to months following a peripheral nerve injury, proliferating Schwann cells use the basal lamina endoneurial tubes as a scaffold to align, forming the Bands of Büngner (Rotshenker, 2011). Following alignment, Schwann cells secrete neurotrophic factors, including brain-derived neurotrophic factor (BDNF), neurotrophin type-4 (NT-4), and nerve growth factor (NGF) to guide regenerating axons through their endoneurial tubes (Naidu et al., 2009; Rotshenker, 2011). Schwann cell secretion of ECM molecule laminin also supports robust axonal regeneration and remyelination; laminin binds to axonal receptors to promote linkage between the axon actin-cytoskeleton and the ECM (Rotshenker, 2011). Though the neurotrophic support provided by Schwann cells initially assists axon regeneration, after 8 weeks the repair phenotype of Schwann cells begins to diminish (Rotshenker, 2011; Scheib and Höke, 2013).

1.2.3 Limitations of Regenerative Capacity

After nerve injury, Schwann cells undergo prolonged periods without contact with regenerating axons, resulting in their decreased neurotrophin release; deterioration of the basal lamina tubes and ECM (Scheib and Höke, 2013). Furthermore, denervated axons themselves increasingly lose the ability to regenerate and reinnervate their targets (Fu and Gordon, 1995b). Thus prolonged denervation reduces reinnervation capacity and functional recovery of muscle (Fu and Gordon, 1995a). Fu and Gordon demonstrated a significant decrease in muscle cross sectional area when muscle was denervated for 6 months. This irreversible atrophy is commonly assumed to be responsible for poor functional recovery past this time point (Gordon et al., 2011), however, it is the decline of the reinnervation capacity of chronically axotomized motoneurons and chronically denervated distal stumps that primarily begets diminished motor function recovery following chronic injury (Fu and Gordon, 1995a; 1995b; 1997; Gordon et al., 2011). Identifying strategies to overcome the consequences of chronic axotomy and denervation are crucial in supporting optimal regeneration and recovery after injury.

1.3 Injury Signal Transduction

1.3.1 Rapid Injury Signaling

Upon transection of the axolemma, transient calcium influx and retrograde transport of signaling molecules communicate the injury to the cell body (Yang et al., 2021; Ziv & Spira, 1995). Injury rapidly increases calcium concentration beyond normal physiological levels at the site of injury, though repair to the injury rapidly equilibrates the cation to physiological levels

(Ziv & Spira, 1995). In addition to the increase in membrane permeability associated with axotomy, it is proposed that injury increases microscopic mechanoporation of the axolemma to facilitate calcium influx (Khaitin, 2021). However, others suggest that calcium influx is due to the activation of voltage gated sodium channels, in turn inverting sodium-calcium ion exchangers (as voltage gated calcium channels are sparse in the axon) to result in significant calcium influx (Mandelosi et al., 2004). Treatment of axons with tetrodotoxin, a voltage gated sodium channel inhibitor, blocks injury-induced calcium influx suggesting the voltage gated sodium channels control the calcium receptors (Buki & Povlishock, 2004; Wolf et al., 2001). Whether due to increased permeability, sodium-calcium exchangers, or both, this calcium influx further increases calcium concentration by activating ryanodine receptors on the endoplasmic reticulum (ER) (Mahar & Cavalli, 2018). Calcium release from the ER signal stress in the axon, leading to activation and nuclear translocation of X-box-protein-1 (Xbp1) (Mahar & Cavalli, 2018). The calcium wave is propagated to the soma through voltage gated L-type calcium channels to promote protein synthesis, activate transcription factors and other signaling pathways, and modulate epigenetic modifiers (Mahar & Cavalli, 2018; Weng et al., 2017).

The burst of calcium activates membrane bound adenylate cyclase (AC), which dephosphorylates and activates cyclic adenosine monophosphate (cAMP) at the site of injury, in turn activating downstream effectors protein kinase A (PKA) and exchange protein activated by cAMP (EPAC) (Hao et al., 2016; Mahar & Cavalli, 2018; Murray & Shewan, 2008). cAMP activation results in downstream phosphorylation and activation of cAMP response element binding protein (pCREB), a pro-regenerative transcription factor upregulated in the nucleus (Mahar & Cavalli, 2018). To propagate the injury response, PKA activates dual-leucine zipper kinase (DLK), an important pro-regenerative mitogen-activated protein kinase kinase kinase

(MAPK3), responsible for the delayed injury-induced activation of the cJun N-terminal kinase (JNK) pathway (Shin et al., 2012; Shin et al., 2019).

Concurrently, calcium initiates degeneration through the activation of calpains and caspases, calcium-dependent cysteine proteases with roles in protein degradation (Buki & Povlishock, 2004; Khaitin, 2021). Activation of these proteolytic enzymes is necessary for disruption of the microtubule and neurofilament network that comprise the axon cytoskeleton. Cytoskeletal proteolysis occurs 1-2 hours following injury, alongside neurofilament compaction (where the interfilament space compacts as neurofilament side arms are increasingly phosphorylated or proteolyzed as the distal stump of the axon swells), microtubular loss, and mitochondrial swelling (Buki & Povlishock, 2004; Hill et al., 2016). The proteolytic targeting of spectrin, a cytoskeletal protein, plays an important role in the degradation of the cytoskeleton. Spectrin is anchored to the cytoskeletal network by an adaptor protein known as ankyrin, and α- and β-spectrin heterotetramers, which alongside actin and other molecules, form a Membrane-associated Periodic Skeleton (MPS) (Buki & Povlishock, 2004; Wang et al., 2019). The MPS forms during development, and is necessary to maintain normal morphology of microtubules, the nodes of Ranvier, and organization of membrane proteins (Wang et al., 2019). After injury induced calcium influx, calpains and caspases degrade spectrins, thereby promoting the disassembly of the MPS, and promoting a pro-degenerative retrograde signal to the cell body (Wang et al., 2019). It has been demonstrated that depletion of β-spectrin from the MPS protects axons from degeneration; it is likely that upon disassembly of the MPS, β-spectrin promotes the retrograde transport of the degenerative signal (Wang et al., 2019). Furthermore, disruption of microtubular structure due to increased tyrosinated α-tubulin stimulates retrograde transport of injury signals (Song et al., 2015). Ultimately, these cytoskeletal changes and pro-degenerative retrograde signals promote degradation of the distal stump to allow assembly of the growth cone (Mahar & Cavalli, 2018).

1.3.2 Delayed Injury Signaling

Upon injury, several signaling proteins associate with the dynein-dynactin mediated transduction of the injury signal along the microtubules to the soma (Mahar & Cavalli, 2018). Nuclear localization signal (NLS) sequences found on specific injury signaling proteins bind to importins: transport proteins necessary for associating the target protein with the retrograde transport complex (Hanz & Fainzilber, 2006). Importin-α, often constitutively expressed and bound to dynein, binds directly to the NLS sequence. Conversely, importin-β binds to importin-α to enhance NLS binding, and is only translated following injury (Hanz & Fainzilber, 2006). Once the importin heterodimer forms, injury signaling proteins with NLS sequences must be activated in order to begin the injury signaling cascade, though many kinases lacking the NLS can associate with scaffold proteins to bind to the motor complex (Hanz & Fainzilber, 2006).

Calcium dependent DLK activation (via cAMP and PKA) is necessary for downstream activation of the JNK pathway and transcriptional regulation to promote regeneration (Shin et al., 2019). Once activated, DLK activates JNK and promotes its linkage to JNK-interacting protein (JIP) or Jnk scaffold protein Sunday driver (Syd), which both facilitate retrograde transport to the soma via the dynein-dynactin motor complex, ultimately activating transcription factor cJun (Hanz & Fainzilber, 2006; Mahar & Cavalli, 2018; Shin et al., 2012; 2019). Inhibition of JNK signaling has also been demonstrated to attenuate activating transcription factor 3 (ATF3) (Lindwall & Kanje, 2005). DLK also promotes the immediate retrograde transport of phosphorylated signal transducer and activator of transcription 3 (pSTAT3), another injury dependent transcription factor (Shin et al., 2012; 2019). STAT3 mRNA is constitutively expressed in the axon; it is only upon injury that STAT3 is locally translated and phosphorylated by Janus kinases (JAK) and mitogen-activated protein kinase kinases (MAPKKs) (Mahar & Cavalli, 2018). Though JAKs are activated by membrane glycoprotein 130 (gp130), it is unclear how gp130 is activated itself. It has been proposed that macrophage-derived IL-6 and CCL2 are responsible for gp130 activation, suggesting a potential link between inflammation and injury signaling (Mahar & Cavalli, 2018). Without DLK activation of transcription factors cJun, ATF3, and STAT3, the response to injury is compromised (Gey et al., 2016; Song et al., 2015).

Other kinases involved in injury signaling are activated independent of calcium; post-injury growth factor release activates receptor tyrosine kinases (RTKs), leading to downstream activation of the rat sarcoma (Ras)‑, rapidly accelerated fibrosarcoma (Raf)‑, mitogen‑activated and extracellular signal‑regulated kinase (MEK) pathway (Ras/Raf/MEK pathway). Activation of this pathway leads to phosphorylation of extracellular-signal-regulated kinase (ERK) 1 and 2, and their subsequent binding to vimentin, an intermediate filament made available by injury-induced local translation and calcium-activated calpain cleavage (Mahar & Cavalli, 2018; Perlson et al., 2005). Though ERK1/2 does not contain NLS sequences, their capacity to bind to vimentin allows the complex to bind to importin-β1, thereby facilitating transport through the dynein-dynactin motor complex. (Hanz & Fainzilber, 2006; Mahar & Cavalli, 2018; Perlson et al., 2005). In the soma, ERK1/2 phosphorylate transcription factors like ETS-like protein 1 (Elk1), cJun, and cFos to modulate gene expression (Hausot & Klimaschewski, 2019; Perlson et al., 2005).

1.4 Peripheral Nerve Regeneration

1.4.1 cAMP Pathway

Activated downstream of injury-induced calcium influx and BDNF-TrkB interaction, cAMP significantly promotes the regenerative capacity of the peripheral axon (Gordon et al., 2009; Udina et al., 2010). Upregulation of cAMP in spinal neurons successfully overcomes the growth-inhibitory effects of CNS myelin debris (Cai et al., 2001; 2002; Hannila & Filbin, 2008). Though peripheral myelin contains much less MAG than central myelin, until macrophages can enter into the distal stump and clear proteoglycans and other inhibitory myelin debris, these molecules can interfere with the initiation of axon growth in the PNS (Shen et al., 1998; Udina et al., 2010). Rolipram induced increases of cAMP (via inhibition of phosphodiesterase) promotes regeneration of peripheral axons across proteoglycan rich extracellular matrix, suggesting a similar role of cAMP to overcome growth inhibition as in the CNS (Udina et al., 2010).

It was previously understood that cAMP activates PKA through direct binding of the regulatory cAMP binding domain (CBD) and exposure of the catalytic domain, acting as a downstream effector to activate transcription factor pCREB and inhibit GTPase RhoA (Hannila & Filbin, 2008); pCREB activation upregulates Arginase-1 (Arg1), and subsequent polyamines integral for regeneration and cytoskeletal assembly, and interleukin-6 (IL-6) gene expression to promote regeneration, while inhibition of RhoA prevents growth cone collapse (Cai et al., 2001; 2002; Hannila & Filbin, 2008). Recently, however, the guanine exchange factor (GEF) for repressor/activator protein-1 (Rap1), EPAC, has been identified as a new PKA-independent effector responsible for the pro-regenerative effects of cAMP (Batty et al., 2017; Murray & Shewan, 2008; Peace & Shewan, 2011; Wei et al., 2016). cAMP binds to a CBD, homologous to that of PKA, to activate the GEF domain found in EPAC (da Rooij et al., 1998). EPAC1 and

EPAC2 have both been identified, but EPAC2 is the isoform predominantly expressed in adult DRG neurons (Murray et al., 2008). EPAC2 will be referred to as EPAC henceforth.

EPAC, similar to cAMP, elicits attractive growth cone turning of neurons in *in vitro* assays, and selective EPAC agonists promotes neurite regeneration to the same or greater extent than PKA agonists (Murray & Shewan, 2008; Wei et al., 2016). Though it is incompletely understood, it is suggested that EPAC similarly activates pCREB and inhibits RhoA following activation via cAMP (Wei et al., 2016). Furthermore, EPAC may activate or inhibit these downstream targets more robustly than PKA, as inhibition of PKA promotes neurite outgrowth, suggesting that EPAC not only compensates for the inhibition of PKA, its role in cAMP-induced regeneration is greater (Wei et al., 2016). Additionally, the cAMP signaling pathway is linked to the ERK pathway through PKA and EPAC interactions with Rap/Raf/Ras proteins (Bos et al., 2003; Dhillon et al., 2002; Enserink et al., 2002; Schmitt & Stork, 2002). However, cAMP is proposed to have opposing effects on growth factor mediated axon outgrowth associated with ERK signaling (Dhillon et al., 2002; Enserink et al., 2002). cAMP activation of EPAC activates Rap1, which phosphorylates Raf1, leading to ERK activation (Bos et al., 2003; Schmitt & Stork, 2002). cAMP appears to promote ERK through Raf1 independent mechanisms as well; EPAC induced activation of Rap1 can lead to Rap1 binding to B-Raf to activate ERK, though this pathway must act in concert with Raf1 to significantly promote ERK (Bos, 2003; Ensurink et al., 2002). Conversely, cAMP activation of PKA leads to inhibition of Raf1, directly opposing the effects of EPAC on Rap1 (Dhillon et al., 2002; Enserink et al., 2002). However, PKA has also been demonstrated to activate Rap1 to promote ERK signaling (Vossler et al., 1997). Thus, it is clear that the interplay between cAMP effectors and ERK signaling is complicated, and context-dependent, with many levels of regulation between the two pathways.

1.4.2 MAPK Pathway

Growth factors released from neuronal and glial sources in response to injury target RTKs and influence the MAPK pathway, otherwise known as the Ras/Raf/MEK pathway (Hausot & Klimaschewski, 2019). RTKs undergo autophosphorylation to tyrosine residues in response to activation, and recruit adaptor protein growth factor receptor-bound protein 2 (GRB2) and GEF son of sevenless (SOS) (Hausot & Klimaschewski, 2019). SOS activates Ras, which recruits Raf1 to the axonal membrane to activate MEK (Hausot & Klimaschewski, 2019). MEK phosphorylates ERK on threonine and tyrosine residues to promote retrograde transport of select factors to the nucleus (Hausot & Klimaschewski, 2019). Once activated, ERK can dimerize and be retrogradely transported (aided by vimentin and importin-β1) to the nucleus to phosphorylate and ultimately activate Elk1, cJun and cFos transcription factors, positively modulating gene expression in favour of regeneration (Hausot & Klimaschewski, 2019; Perlson et al., 2005). Though spontaneous growth and pre-conditioning lesion-induced growth of DRGs in culture is not dependent on ERK expression, ERK signaling mediates promotion of growth in response to growth factors or axotomy; ERK signaling has been demonstrated to be essential for growth cone formation following injury, and the polymerization of actin filaments, with the degree of ERK signaling positively correlating with the extent of outgrowth (Hausot et al., 2022; Hausot & Klimaschewski, 2019; Traverse et al., 1992).

Sprouty2 (SPRY2) regulates activation of ERK signaling. SPRY2 binding to GRB2 interferes with SOS activation and subsequent Ras activation, and downstream to Ras, SPRY2 binds and incapacitates Raf (Hausot et al., 2009; Hausot & Klimaschewski, 2019). SPRY2 is highly expressed in adult DRGs to prevent ERK signaling, though ERK signaling overcomes SPRY2-mediated inhibition of Ras following injury; SPRY is reduced post-transcriptionally through miRNA-21 to promote outgrowth (Hauset et al., 2009; Hausott & Klimaschewski, 2019). Knockout of SPRY2 in mice with sciatic nerve injury (SNI) promotes expression of growth-associated protein-43 (GAP43) mRNA, suggesting a role of ERK in GAP43 mediated outgrowth in injury signaling (Marvaldi et al., 2015).

1.4.3 PI3K-Akt Pathway

Alongside the Ras-Raf-MEK pathway, activation of RTKs following injury in the peripheral nerve activate the phosphatidylinositol‑3‑kinase (PI3K) - protein kinase B (Akt) pathway (Hausot & Klimaschewski, 2019; Saijilafu et al., 2014; Singh et al., 2015). Growth factors that bind to RTKs also target the PI3K pathway; blocking activation of PI3K prevents the neurotrophin-mediated increase in neurite outgrowth in neurons (Hausot & Klimaschewski, 2019; Klimaschewski et al., 2013; Singh et al., 2015). Activation of RTKs recruit adaptor proteins such as GRB2-associated binder (GAB) to activate PI3K, in turn phosphorylating membrane-bound phosphatidylinositol 4,5-bisphosphate (PIP2) to become phosphatidylinositol 3,4,5-trisphosphate (PIP3) (Hausot et al., 2022). PIP3 can then recruit Akt to the membrane and enable phosphoinositide-dependent kinase 1 (PDK1) and the mammalian target of rapamycin (mTOR) complex 2 (mTORC2) to phosphorylate and activate Akt (Hausot et al., 2022). Phosphorylation of Akt increases following peripheral axon transection (Saijilafu et al., 2014), and inhibits glycogen synthase kinase 3 (GSK3) through phosphorylation; following peripheral nerve transection, phosphorylation of GSK3 also increases (Hausot et al., 2022; Saijilafu et al., 2014). Unphosphorylated GSK3 increases instability in the growth cone by blocking axon formation (Zochodne, 2009), while inhibition of GSK3 localized to the soma is suggested to be responsible for transcriptional changes promoting regeneration. In particular, increased expression and phosphorylation of mothers against decapentaplegic (Smad1) occurs downstream of the PI3K-GSK3 interaction, suggesting a role for positive modulation of genes associated with regeneration (Saijilafu et al., 2014). The PI3K pathway is regulated by protein phosphatase tensin homolog deleted on chromosome ten (PTEN), a PI3K antagonist in the axon and cell body (Krishnan et al., 2016). Though PTEN mRNA decreases its expression significantly in response to axotomy, protein levels of PTEN are preserved and continue inhibition of the PI3K pathway and promote unphosphorylated GSK3 mediated growth cone collapse, thereby stifling the pro-regenerative response (Krishnan et al., 2016; Zochodne, 2009). Inhibiting PTEN poses a potential therapeutic target to promote regeneration.

1.4.4 Regeneration Associated Gene Upregulation

After peripheral nerve injury, activated signaling pathways culminate in the activation of neuron-intrinsic regeneration associated genes (RAGs) to promote regeneration. Increased RAG expression correlates with increased axonal regeneration, and therapeutic strategies that further increase regeneration following injury upregulate RAGs further than injury alone (Senger et al., 2018; Dubový et al., 2019; Verge et al.. 1996). The most common RAGs processed and visualized in cell bodies of regenerating axons are ATF3, BDNF, cJun, cFos, GAP43, GFAP, and pCREB.

pCREB activation, often as a result of cAMP signaling, leads to transcription of Arg1 and IL-6 (Thong et al., 2014). As an enzyme integral to polyamine synthesis, Arg1 promotes the regenerative capacity of axons by increasing materials available for actin filament and microtubule formation, while IL-6 attracts T-cells necessary for myelin clearance, and activates JAK/STAT3 and PI3K/Akt regenerative signaling pathways (Chung et al., 2020; Fregnan et al., 2012). pCREB activation has also been linked to neuron-derived BDNF, a RAG protein responsible for stimulating TrkB and promoting growth pathways after its secretion (McGregor

& English, 2019; Thong & Willis, 2015). BDNF/TrkB interactions promote transcription and transport of actin mRNA to the growth cone, as well as promote neuronal survival through the PI3K-Akt pathway (Chung et al., 2020; Yao et al., 2006). BDNF expression is localized to motor neurons and select sensory neurons, but following injury, BDNF upregulates in TrkA, TrkB and TrkC neuronal populations (McGregor & English, 2019; Boyd & Gordon, 2003). Both cAMP analogues and constitutively active pCREB models have been shown to increase ATF3, cJun, and cFos through the activation of the transcription factor activator protein 1 (AP-1) (Thong et al., 2014). ATF3 overexpression is suggested to be pro-regenerative, though commonly referred to as an 'injury marker' as opposed to a RAG (Thong & Willis, 2015). Though cAMP is likely heavily involved in pCREB and BDNF upregulation, cAMP upregulation alone in *in vivo* injury models is not sufficient to promote regeneration (Blesch et al., 2012). Therefore, upregulation of these proteins may also occur independent of cAMP. Other molecular pathways have been linked to the activation of pCREB: Ca^{2+} influx and activation of Calmodulin kinases (CaMKs) (Sheng et al., 1991), and ERK (Sabbir & Fernyhough, 2018). Ca2+ influx and CaMK activation, and ERK upregulation have both been linked to increased neurite outgrowth through pCREB in DRG neurons (Sabbir & Fernyhough, 2018; Yan et al., 2016).

GAP43 is a RAG protein responsible for formation and stabilization of the growth cone (Chung et al., 2020). GAP43 expression increases with IL-6 and IL-10 cytokine release, potentially mediating GAP43 activation through the JAK/STAT3 pathway activated following injury (Chung et al., 2020). Injury significantly upregulates mRNA and subsequent phosphorylation of GAP43 to modulate actin dynamics and promote assembly of the cytoskeleton (Chung et al., 2020). Thus, increased GAP43 mRNA levels correlate with increased regenerative capacity of axons (Chung et al., 2020). Despite GAP43 acting as a marker of regeneration, GAP43 depletion alone is insufficient to hinder regeneration (Frey et al., 2000).

Glial fibrillary acidic protein (GFAP), though not localized to neuronal populations, is an intermediate filaments that supports regeneration through upregulation in satellite glial cells (SGCs) surrounding cell bodies in the DRG, and serves as a marker of glial cell activation (Avraham et al., 2020; English et al., 2000). SCGs have low levels of GFAP at baseline, and following injury upregulate within 2 days post-injury and downregulate between 7 and 14 days post-injury (Woodham et al., 1989; Xie et al., 2009). Injury-induced nerve signaling and inflammation upregulates GFAP (Blum et al., 2014; Woodham et al., 1989; Xie et al., 2009). GFAP ensures integrity of the BBB, and plays a role in the activation of SCGs (Hanani & Spray, 2020; Yang & Wang, 2015); because SCGs are functionally coupled to neuronal cell bodies, their activation enhances neuronal excitability after injury (Hanani & Spray, 2020). GFAP is also expressed in Schwann cells, similarly regulating Schwann cell cytoskeletal integrity, and promoting proliferation to support axonal regeneration (Triolo et al., 2006). GFAP null mice demonstrate impaired regeneration and remyelination following injury, likely to do deficits in Schwann cell proliferation (Triolo et al., 2006).

1.4.5 Growth Cone Dynamics

Following transection injury of axons, the proximal stump must reseal and form a growth cone to allow for regeneration (Shim & Ming, 2010). Resealing the plasma membrane is dependent on select ion channels and pumps; Na+/K+-ATPase pumps create a spatio-temporal gradient of Na+ to determine where the membrane can be resealed, while L-type VGCC are responsible for promoting activation of calcium-dependent proteases and lipases that mediate membrane resealing, and eventual growth cone formation (Shim & Ming, 2010). As the cAMP, MAPK and PI3K molecular cascades promote transcription to support increased regeneration, a growth cone forms at the proximal stump of the injured axons. The growth cone consists of several components including filopodia, which are finger-like extensions of F-actin bundles originating from the transition domain of the growth cone. Filopodia are a dynamic extension of the axon in the peripheral domain, composed of actin filaments that undergo constant polymerization, working to pull the growth cone forward (Lowery & Vactor, 2009). The lamellipodia of the growth cone refers to the bundles of actin filaments that criss-cross to create F-actin networks, forming a veil-like structure that populates majority of the peripheral domain (Dent et al., 2011; Lowery & Vactor, 2009). Microtubules from the axon shaft enter the central domain of the growth cone, which forms the major axonal cytoskeletal network. Microtubules are polarized polymers consisting of alternating α-tubulin and β-tubulin monomers, and the periphery-facing end of the polymer grows and shrinks dynamically based on the addition or GTP-hydrolysis of tubulin monomers, cycling through periods of growth or shrinkage (Lowery & Vactor, 2009). Actin arcs are present in the transition domain of the growth cone, in between the central and peripheral domains to prevent inappropriate protrusion of stable microtubules into the peripheral domain (Lowery & Vactor, 2009). Select dynamic microtubules protrude out from the central to the peripheral domain of the growth cone, accompanying F-actin bundles. Though actin dynamics are thought to be primarily responsible for growth cone guidance, asymmetric inhibition of microtubule dynamics induces growth cone turning suggesting a role for these dynamic microtubules in axon guidance (Dent et al., 2011; Lowry & Vactor, 2009).

Actin dynamics act as the main engine for growth cone motility; due to the push of F-actin polymerization in filopodia and the contractile properties of myosin (an actin motor protein) within the transition zone, F-actin undergoes retrograde flow back to the central domain.

Actin monomers polymerize on the distal ends of the filaments, and are cleaved as they near the central domain (Dent et al., 2011). Increasing the polymerization rate relative to the rate of retrograde flow favours protrusion of filaments, however protrusion is often accomplished through the slowing of retrograde flow (Dent et al., 2011). As filopodia interact with the extracellular environment, the extracellular domain of integrin receptors can act as points of attachment to extracellular matrix proteins, including collagen, laminin and fibronectin (Gomez & Letourneau, 2014; Lowery & Vactor, 2009). The anchoring points prevent retrograde flow of actin components and increase accumulation of local actin, thus resulting in protrusion of filopodia to drive the growth cone forward (Lowery & Vactor, 2009). Further, actin arcs located in the transition zone of the growth cone reposition to allow engorgement of the growth cone, in which tension created by the anchor points draws the central domain containing stable microtubules forward (Lowery & Vactor, 2009). Myosin generated tension counteracts internal compressive tension that limits microtubule polymerization, and thus promotes microtubule extension to elongate the axon shaft (Gomez & Letourneau, 2014). As one end of the microtubules elongate and are drawn forward, the distal ends of the microtubules are compacted to add to the axon shaft (Lowery & Vactor, 2009). This final process is known as consolidation.

Attractive and repulsive chemotrophins in the environment aid in guidance of the growth cone based on receptor binding. The growth cone does not only move forward; based on the environmental signals, the growth cone may shrink, protrude, or change direction (Dent et al., 2011; Gomez & Letourneau, 2014; Lowery & Vactor, 2009). Several families of molecules are implicated in growth cone guidance: netrins, ephrins, slits, semaphorins and morphogens (Thomas & Yoshikawa, 2009). These molecules are secreted from either neuronal or glial sources, binding to receptors on the growth cone to activate signal transduction molecules. These cascades induce filopodia protrusion or retraction, determining the direction of growth cone advance (Lowery & Vactor, 2009). Netrins, semaphorins, ephs/ephrins, slits and growth factors such as NGF, BDNF, FGFs, serve as guidance molecules and their ability to act as a chemoattractant or a chemorepellent depends on the receptor expression and intracellular state of the growth cone (Galko & Tessier-Lavinge, 2000; Webber et al., 2005). Chemotrophic attractants promote growth cone extension, while chemotrophic repellants act as the guard rails to prevent misdirected axon growth (Lowery & Vactor, 2009).

A notable challenge for growth cone advance after peripheral nerve injury is the inhibitory myelin debris capable of binding and hindering regeneration (Krishnan et al., 2016; Rotshenker, 2011; Shim & Ming, 2009). Though myelin proteins are much less common, and less inhibitory than those in the CNS, myelin proteins (including MBP, MP0, MAG, and oligodendrocyte myelin glycoprotein (OMgp)), cytokines, chondroitin sulfate proteoglycans (CSPGs) and neurotrophins associate with receptors present on the growth cone to act upon the RhoA molecular cascade (Cheng et al., 2008; Tan et al., 2020; Webber & Zochodne, 2010). Like the CNS, RhoA is present in peripheral nerve, and upregulates following injury (Webber & Zochodne, 2010). Inhibitory myelin, cytokines, and CSPGs act on their respective receptors to activate GEFs and facilitate the exchange of guanosine diphosphate (GDP) to guanosine triphosphate (GTP), activating RhoA (Cheng et al., 2008). RhoA-GTP phosphorylates Rho-Kinase (ROK), which is then free to disrupt actin and microtubule dynamics, induce growth cone collapse, decrease cell survival, and inhibit remyelination of regenerating axon (Bros et al., 2019; Cheng et al., 2008; Tan et al., 2020; Webber & Zochodne, 2010). Binding NGF to tyrosine receptor kinase A (TrkA) present on the growth cone inhibits activation of RhoA through cAMP-dependent pathways (Gao et al., 2003). Therefore, timely clearance of myelin debris and

Schwann cell secretion of growth factors is necessary to counteract RhoA-induced inhibition of growth cone advance (Cheng et al., 2008; Shim & Ming, 2009; Webber & Zochodne, 2010).

1.5 Strategies to Enhance Nerve Regeneration

1.5.1 Conditioning Lesions

Conditioning lesions applied to the nerve prior to injury initiates an intrinsic regenerative program involving upregulation of RAGs, resulting in accelerated regrowth ((Richardson & Issa, 1984; Sjöberg & Kanje, 1990). CCL involves administration of a crush injury to the peripheral nerve 1 week prior to a nerve transection injury and microsurgical repair (Richardson & Issa, 1984). As one of the first strategies shown to promote regeneration (Jenq et al., 1988; Richardson & Issa, 1984), the mechanism of CCL is well characterized (Richardson et al., 2009). At the time of the conditioning lesion, retrograde markers are transported from the injury site to the cell bodies to communicate membrane disruption (Kanje et al., 1991; Ying et al., 2014). Retrograde transport of importins via the dynein motor transport system signals the activation of several molecular pathways including the cAMP pathway, MEK/ERK/MAPK pathway, and JAK/STAT pathway (Mar et al., 2014). Activation of these pathways culminates with the upregulation of transcription factors associated with increased regeneration, RAGs and other signaling proteins including ATF3, BDNF, cFos, cJun, GAP43, GFAP and pCREB (Verge et al., 1996). The rate of anterograde protein and mRNA transport activated by regenerative pathways in the cell body limits the regenerative response at the site of the growth cone (Mar et al., 2014). By the time of the second injury, these regeneration associated mRNAs and proteins have already enacted pro-regenerative pathways that enable an accelerated rate of anterograde transport. Thus, actin and tubulin mRNA transport increases 4-5 fold, supporting a 3-4 fold increase in the intrinsic regeneration rate, as well as an increase in actin polymerization and assembly of the growth cone skeleton (Dubový et al., 2019; Mar et al., 2014; Senger et al., 2018a; 2018b; Sjöberg & Kanje, 1990). Conditioning lesions must be applied distal from the transection site for *in vivo* models, and can also be modeled *in vitro* by injuring the nerve prior to DRG explant and culture (Dubový et al., 2019). CCLs have proven to promote regeneration when administered 7 and 14 days prior to the test lesion, but not 2 days (Jenq et al., 1988). Though clinical translation proves elusive due to the injurious nature of CCL, the mechanistic insights have identified key pro-regenerative pathways that prime the neuronal cell body and promote the extent of regeneration and the number of axons capable of regenerating (Dubový et al., 2019; Jenq et al., 1988; Mar et al., 2014; Ying et al.,2014).

1.5.2 Electrical Stimulation

Electrical stimulation (ES) accelerates regeneration and improves functional recovery after peripheral nerve injury (Al-Majed et al., 2000a). In animal models, ES has traditionally been delivered *postoperatively* after nerve transection and repair (Al-Majed et al., 2000a). Postoperative electrical stimulation (PES) was introduced and optimized by Al-Majed et al. (2000a); 1 hour of low frequency stimulation (20Hz) delivered for a duration of 1 hour improved regeneration of motoneurons in the femoral nerve. As opposed to a CCL, PES is non-injurious and therefore has been successfully translated for clinical use (Barber et al., 2015; Gordon et al., 2010; Power et al., 2020). Though PES does not accelerate the rate of regeneration, it promotes regeneration of axons over the coaptation site (staggered regeneration), thereby increasing regeneration and promoting functional recovery (Brushart et al., 2002; Witzel et al., 2009). Furthermore, PES has been shown to increase the specificity of reinnervation by promoting preferential motor reinnervation, in which motor neurons treated with PES primarily regenerate to the appropriate motoneuron targets (Al-Majed et al., 2000a).

Recently, ES has been investigated as a conditioning strategy (Senger et al., 2018b; Senger et al.., 2019; Senger et al., 2020a; Senger et al., 2022). Administration of conditioning electrical stimulation (CES) 1 week prior to nerve injury upregulates RAGs and accelerates the rate of regeneration in a manner akin to CCL (Richardson & Issa, 1984; Verge et al., 1996). CES, introduced by Senger et al. (2018b), accelerates the innate rate of regeneration in acute and chronic models of nerve injury, and through nerve grafts and nerve transfers (Senger et al., 2020; Senger et al., 2022; Udina et al., 2008). In a direct comparison of PES and CES, CES demonstrated superior regeneration and functional recovery (Senger et al., 2020a). However, despite being non-injurious and non-inflammatory (Senger et al., 2022), clinical translation of CES has proved difficult due to the unpredictability of nerve injury. Nevertheless, clinical utility of CES lies in elective nerve reconstruction surgery that necessitates intentional nerve injury and repair. Pre-clinical investigation suggests clinical viability of CES to promote regeneration in cases of acute injury (i.e. distal nerve transfer in which healthy nerve is transected and repaired to the distal stump of a previously injured nerve) (Senger et al., 2020b), or in cases of chronic injury (i.e. chronically injured nerve with surgical interventions of nerve grafts) (Senger et al., 2022). Clinical trials for CES are currently underway. With CES only recently introduced as a clinically viable therapeutic option, much of the existing literature surrounding electrical stimulation generalizes CES and PES. Though the mechanism of PES has been investigated extensively, paradigms that distinguish between the two regenerative strategies have not been widely established. My thesis project first distinguishes between PES and CES mechanisms, and investigates key parameters and signaling pathways not yet identified. In this study we aim to identify the minimum duration of electrical stimulation, and the minimum latency period required to elicit the pro-regenerative effects of CES. We investigate the neuronal specificity of CES, and identify key signaling pathways involved in the mechanism of CES.

1.6 Thesis Statement

Hypothesis: Conditioning electrical stimulation elicits a conditioning effect as a result of the accumulation of activation of signaling pathways, including cAMP, to elicit non-specific pro-regenerative effects to all neuronal subtypes.

Aim 1: To compile a literature review distinguishing the differences between CES and PES.

Aim 2: To optimize the timeline and parameters of Conditioning Electrical Stimulation.

Aim 2.1. To determine the CES latency period (i.e., days in vivo) necessary to promote nerve regeneration.

Aim 2.2. To determine the optimal length of CES application (i.e., duration of electrical stimulation) necessary to elicit conditioning effects.

Aim 2.3 Compare electrical stimulation devices (SD9 vs Checkpoint) to elicit CES.

Aim 3: To determine if CES evokes different rates of regeneration in different neuronal subtypes

Aim 4: To determine the role of cAMP effectors EPAC and PKA in mediating the pro-regenerative effects of CES.

CHAPTER 2: Investigating the Mechanism of Conditioning vs Postoperative Electrical Stimulation to Enhance Nerve Regeneration: One Therapy, Two Distinct Effects

2.1 Abstract

Regeneration after peripheral nerve injury is often insufficient for functional recovery. Postoperative electrical stimulation (PES) following injury and repair significantly improves clinical outcomes; recently, conditioning electrical stimulation (CES), delivered prior to nerve injury, has been introduced as a candidate for clinical translation. PES accelerates the crossing of regenerating axons across the injury site, whereas CES accelerates the intrinsic rate of axonal regeneration; thus, it is likely that their mechanisms are distinct. The large body of literature investigating the mechanism of electrical stimulation has not differentiated between CES and PES. In this review, we investigate the CES and PES paradigms within the existing literature, distinguish their mechanistic insights, and identify gaps in the literature.

A systematic literature review was conducted, selecting articles identifying the pro-regenerative effects of electrical stimulation in the setting of peripheral nerve injury. As a mechanistic template, both paradigms implicate cation-channels for the initiation of numerous signaling pathways that together upregulate regeneration associated genes. CES and PES feature some overlap; activation of PI3K and MAPK signaling pathways, and upregulation of BDNF, GAP43 and GFAP are similar. Currently, the inflammatory environment in which PES is administered predominantly differentiates these mechanisms. However, gaps within the literature complicate the comparison between paradigms.

Systematic review revealed the mechanisms for both CES and PES paradigms remain fragmented; though much of the literature assumes involvement of particular signaling pathways, the evidence remains limited. Though it is likely there is overlap between mechanisms, further investigation is needed.

2.2 Introduction

Although the peripheral nervous system has the capacity to regenerate, injury often results in significant disability despite timely surgical intervention.[1] Functional recovery following neurotmesis or axonotmesis requires axonal regeneration and successful target reinnervation, and therefore functional recovery is often poor. The slow innate regenerative rate is particularly challenging for proximal nerve injuries, where the length of nerve growth required within the available recovery time frame is often insurmountable. After 6 - 12 months, axons and muscles adopt a chronically denervated phenotype that is unlikely to support reinnervation.[2,3] Loss of supporting Schwann cells and muscle atrophy lead to decreased target reinnervation.[4-6] As such, there is significant clinical need to identify perioperative strategies to decrease the time to end target reinnervation, and thereby improve motor and sensory recovery. Electrical stimulation is the most well-studied intervention to promote nerve regeneration, and one of the few techniques that has been successfully translated to clinical use.

Electrical stimulation of the peripheral nerve is a non-injurious procedure traditionally delivered *postoperatively,* following nerve injury and repair.[7] Postoperative electrical stimulation (PES) improves nerve regeneration across the coaptation site (staggered regeneration), enhances preferential motor reinnervation, and promotes early functional recovery.[8-11] Al-Majed et al., (2000a) was the first to demonstrate the pro-regenerative effects of PES with optimized parameters of 20Hz for 1 hour[7, 12-14] PES has been successfully translated to clinical practice, supported by numerous randomized control trials for improving both sensory and motor recovery following nerve transection and decompression.[15-18]

The effects of electrical stimulation on regeneration can be altered by changing the timing of stimulation relative to the time of injury. Conditioning electrical stimulation (CES) is a therapeutic paradigm in which the electrical stimulation is delivered *prior* to nerve injury and repair to induce a conditioning-like effect. In keeping with other conditioning mechanisms (traditionally a crush or cut conditioning lesion), CES upregulates regeneration associated genes (RAGs) prior to the definitive injury and repair, and accelerates the rate of axon extension. Our lab has shown improved regenerative and functional outcomes in numerous rodent models of acute and chronic nerve reconstruction surgeries.[19-22] Further, we have demonstrated that CES accelerates nerve regeneration through nerve grafts, and improves functional recovery beyond PES using a multimodal panel of immunohistochemistry and sensorimotor behavioral outcomes.[21] CES must be administered prior to nerve injury, making clinical translation less intuitive than PES, as typically nerve transections are unplanned. The clinical utility of CES lies in elective nerve reconstruction, such as prior to a scheduled distal nerve transfer, nerve decompression, or oncologic nerve resection and reconstruction.[22] Clinical trials are underway to assess functional outcomes of CES administered prior to carpal tunnel and cubital tunnel decompression surgeries.

CES and PES elicit distinct effects on regeneration; it therefore follows that the mechanisms underlying CES and PES are likely different. As the term 'CES' has only been used within the past five years,[19-22] the literature does not discern between CES and PES paradigms, but rather generalizes all research investigating the mechanism of electrical stimulation into the PES literature. Considering the timing of electrical stimulation relative to the nerve injury, we propose that many previous studies should be re-classified as CES. This differentiation is important as it provides insights into the specific effects of electrical stimulation on nerve regeneration relative to the time of injury, and may identify molecular and cellular pathways that are differently regulated. Thus, the first objective of this literature review is to define CES vs

PES treatment paradigms and to differentiate their mechanisms. Our second objective is to use this classification scheme to identify gaps and suppositions in our understanding of the mechanism of electrical stimulation, both for CES and PES. Systematically reviewing, evaluating, and classifying all available mechanistic data will generate a more comprehensive and accurate picture of these two distinct therapeutic modalities, provide greater understanding of how the same intervention can produce distinct effects on regeneration depending on the timing of delivery, and identify targets for future investigation.

2.3 Methods

2.3.1 Literature Search

A PubMed and Google Scholar literature review was conducted using the key words, “electrical stimulation”, “peripheral nerve injury”, “peripheral nerve regeneration”, “peripheral nerve repair”, “brief electrical stimulation”, “conditioning electrical stimulation”, and “postoperative electrical stimulation”. Secondary references were identified and reviewed for inclusion. In total, 112 articles were reviewed and 66 were selected for inclusion. Inclusion criteria included: i) peripheral nerve injury models (no central nervous system studies were included), ii) studies investigating the effects and/or mechanisms of CES or PES, iii) electrical stimulation parameters including a frequency of 10-30Hz, and duration between 30 minutes and 2 hours, iv) publication date January, 1976 to March, 2023. *In vitro* studies included adult primary DRG neurons or spinal neurons (embryonic neurons were excluded).

2.3.2 Defining CES and PES Paradigms

The timing of electrical stimulation relative to the nerve transection and surgical repair differentiates CES and PES. In this review, we define CES and PES *in vivo* as follows (Figure 1):

- CES *in vivo*: electrical stimulation performed a minimum of three days prior to nerve injury
- PES *in vivo*: electrical stimulation performed immediately following, or within 24 hours of nerve injury

After 4 days in vitro, DRGS are considered functionally naive.[23] Therefore, our definition of CES and PES in vitro are:

- CES *in vitro*: electrical stimulation performed i) *in vivo* prior to the DRGs placed in tissue culture, or ii) after DRG plating to uninjured neurites
- PES *in vitro*: electrical stimulation performed following neurite injury

2.4 Results and Discussion

2.4.1 Effects of CES and PES on nerve regeneration and functional recovery (Tables 1, 2).

Electrical stimulation, administered pre (CES) or post (PES) injury, significantly promotes peripheral nerve regeneration after injury. Both CES and PES increase regenerating axon density,[13,24-33] sensory functional recovery,[20,21,24,29,34,35] muscle reinnervation and compound muscle action potentials (CMAPs),[20,21,24,27,35-39] and composite functional recovery.[20,21,28-30,37,39-46] *In vitro*, CES and PES both increase neurite extension.[31,34,47-52]

A distinctive difference between CES and PES is the effect on axonal extension. PES *in vivo* increases regeneration by promoting coordinated extension of axons through the site of surgical coaptation (staggered regeneration) without affecting the rate of axonal growth.[8,12,13,29,38,53] Further, PES increases specificity of preferential motoneuron reinnervation (PMR), promoting correct reinnervation of motor targets by motoneurons and thereby contributing to improved recovery.[9,12,54] By contrast, CES accelerates the intrinsic rate of regeneration.[19-22] The effects of CES on modulating preferential motor reinnervation have not yet been studied. A direct comparison of sensorimotor reinnervation and gait restoration following nerve grafting identified superior recovery in CES animals when compared to PES; further, CES alone yielded more improved outcomes than animals treated with the combination of both CES and PES.[21]

Both CES and PES have been studied extensively in rodents, with surgical models of acute and chronic nerve repair reconstructed primarily, with nerve grafts, or with nerve transfers.[22,55] Animal models of CES studies have more thoroughly investigated kinetic (vertical peak, braking, and forces) and kinematic (duty factor and joint angles) outcomes. Human clinical trials have revealed that PES improves sensory and motor recovery in patients treated for compression neuropathies (carpal tunnel and cubital tunnel),[16,17] digital nerve transection (digital nerve),[18] and traction injuries.[15] Clinical trials for CES are underway.

2.4.2 Channels and Signaling Pathways (Table 3)

It is generally accepted that electrical stimulation, delivered at any time point, first induces a retrograde signal from the site of stimulation to the neuronal cell body, which initiates numerous molecular cascades. The effects of CES and PES on voltage-gated cation channels is therefore of considerable interest. Studies to investigate the effects of these channels have largely relied on evaluating the effects of electrical stimulation in the presence of channel blockers such as lidocaine and nifedipine. Such studies have suggested a role for voltage gated sodium channels in mediating the effects of PES. CES is more completely studied, and has been shown to be governed by voltage gated calcium channels and the CAMKII pathway.[12,13,34,48,56-59] Further, CES has been shown to activate axonal voltage gated sodium channels, which triggers activation of Schwann cell voltage gated calcium channels.[60] Cytosolic calcium release from internal stores in Schwann cells triggers mitochondrial calcium influx. The effect of electrical stimulation, either CES or PES, on ion gated channels is poorly understood, but most likely plays an important role in mediating the effects of these two treatment modalities. The net result of the resultant retrograde signal is the activation of multiple molecular pathways within the neuronal cell body.

Numerous signaling pathways have been investigated to determine the mechanism of electrical stimulation. These studies have predominantly focused on one or two individual molecules within the respective cascades, resulting in unverified inferences regarding associated molecules. Due to repetition in the literature over time, these inferences have become cited as fact. A noteworthy example is the role of cAMP in PES. Multiple studies and review articles have cited cAMP to be a key player of the mechanism of PES[61-65]; this conclusion however is based on studies confirming BDNF as a mediator of the PES effect.[7,26,36,54,59,66-73] This conclusion was further supported by a study reporting upregulation of PACAP, an adenylyl cyclase modulator that produces cAMP from ATP.[67] There remains, however, no study that has directly evaluated the effects of PES of modulating cAMP expression. The most frequently cited paper confirming a relationship between cAMP and electrical stimulation is Udina (2008). In this study, electrical stimulation was delivered to an uninjured nerve; therefore, based on our classification, we consider this to be CES and not PES (Figure 1). Authors showed that this stimulation caused increased expression of cAMP, which conditioned the neurites for regeneration when placed *in vitro.*[49] These results are supported by a second study that reported delivery of exogenous cAMP had a comparable effect on growth cone dynamics as CES.[74] Together these results support that cAMP likely is implicated in mediating the effects of CES. Based on our definition of PES *in vivo* and *in vitro,* however*,* no studies have measured cAMP or investigated the effects of modulating cAMP as it relates to PES. Although it is likely that CES and PES share cAMP as an integral effector, this relationship has yet to be confirmed.

Individual molecules of numerous other signaling pathways have been investigated following CES or PES. The inhibition of PTEN (a "brake" for the phosphatidyl-inositol-3-kinase [PI3K]) pathway) and the activation of the PI3K pathways have been demonstrated in both CES and PES.[34,69] Further, CES-induced upregulation of BDNF is mediated by MAPK/ERK; RNA sequencing similarly suggests an upregulation of MAPK following PES[59,69] Although these studies are a solid foundation, further investigation into these signaling pathways is needed to better understand the mechanism of CES and PES.

2.4.3 Regeneration Associated Genes and Neurotrophins (Tables 4, 5)

BDNF is the best studied neurotrophin in the electrical stimulation literature. Electrical stimulation affects expression of neurotrophins both within the neuronal cell bodies and the supporting glia. Upregulation of neuronal BDNF is reported as an effect of both CES and PES.[7,13,19,20,26,29,34,36,47,48,54,58,59,68-73] To date, only PES models have reported TrkB upregulation.[7,70] BDNF expression is mediated by calcium signaling in CES models of electrical stimulation, which corresponds to previously discussed studies implicating voltage-gated calcium channels in the CES effect.[48,59] BDNF expression following CES has only been investigated in sensory neuronal cell bodies; more comprehensive literature has demonstrated that PES upregulates

BDNF in both sensory and motor neurons.[7,19,20,26,29,36,54,59,67,68,70-73] BDNF expression can be mediated both within the DRG neuron, as well as in Schwann cells. Based on extremely limited research, the timing of electrical stimulation relative to the time of injury does appear to alter Schwann cell expression of BDNF. CES of Schwann cells does not alter BDNF expression *in vitro*[47] whereas PES increases Schwann cell BDNF expression.[71] The sequelae of Schwann cell expression of BDNF is largely unknown.

Similar to neuronal BDNF, expression of other neurotrophic factors in response to electrical stimulation have also been studied. Nerve growth factor (NGF) has been shown to be upregulated in Schwann cells following CES and axons following PES.[47,69,75] Only PES is reported to upregulate axonal glial-derived neurotrophic factor (GDNF)[54]; however, CES of Schwann cells did not result in GDNF upregulation.[47] The effects of CES on neuronal expression of NGF and GDNF has not been studied. Neurotrophin-3 and 4/5 are also upregulated by PES,[26,54] however the role of CES on these neurotrophins is unknown.

CES and PES both upregulate the expression of the regeneration associated genes, growth associated protein-43 (GAP-43), and glial fibrillary acidic protein (GFAP), while inhibiting the expression of the injury marker, ATF-3.[13,19,20,27,34,52,55,62-68,76] Notably, these results have been contested, with another study reported increased ATF-3 expression following PES.[29] It is therefore unclear whether this suggests a similar or different mechanism between CES and PES. Phosphorylated CREB (pCREB) is upregulated following CES,[20,55,58,75] whereas its expression following PES has not been examined. Based on our definitions (Figure 1), there have been no studies of PES *in vitro* that have examined expression of RAGs and neurotrophins.

The net effect of neurotrophin and RAG overexpression is creation of the cytoskeletal elements necessary for creation of a growth cone and a progressive reconstruction of axons.

These processes require large quantities of energy. Following nerve injury, mitochondria translocation to the injured axons is necessary for regeneration, with roles in growth cone migration.[77] Mitochondrial dynamics have been investigated after CES: mitochondrial velocity increases and anterograde transport is favored, resulting in mitochondrial accumulation at the regenerating proximal stump.[78] Further, CES mediates mitochondrial fission which increases the numbers of axonal mitochondria.[78] PES also features increased bioactivity, indicated by increased counts of mitochondria in PES-treated regenerating axons 4 weeks after injury, compared to untreated regenerating axons.[79]

In summary, Tables 3-5 and Figures 2 and 3 demonstrate that many of the same signaling pathways, neurotrophic factors, and RAGs have been partially studied in both CES and PES, with some areas of overlap, and numerous gaps identified. It is important to note that there is significant heterogeneity in methodology and the controls against which molecular expression is compared is generally either a naïve nerve or an injured nerve. No quantitative comparison of the degree of upregulation/downregulation of these individual molecules in response to PES versus CES has been performed. Similarly, given the wide variability in study design, a temporal comparison is not possible to evaluate when specifically the upregulation of these pathways occurs in CES versus PES. While our results suggest that CES and PES both utilize many of the same players, it is likely these pathways are affected differently to account for their unique effects on nerve regeneration.

2.4.4 Myelination and Inflammation (Table 6)

It is challenging to directly compare the relationship between inflammation and CES versus PES due to the timing of the injury relative to the electrical stimulation. CES is delivered to an uninjured nerve, and has been shown to be non-injurious, with no infiltration or upregulation of evoked blood born or tissue resident macrophages.[80,81] It does not appear as though the inflammatory process is implicated in the effects of CES. By contrast, PES is delivered following a nerve injury, and thus is evoked in an environment that is already injured and thus inflamed.[28,29,66,68,71,79] Whether or not these neutrophils, macrophages, and other elements of the inflammatory response are necessary to mediate the effects of PES has not yet been investigated. A relationship between the presence of inflammatory cells and enhanced nerve regeneration has previously been reported, with numerous studies showing that the pro-regenerative effects of a conditioning crush injury are ablated in CCL2 knockout models.[82] Whether or not inflammation is necessary for the effects of PES is unknown, but conversely, PES is reported to influence the type of inflammation by changing the macrophage phenotype from M1 ("pro-inflammatory") to M2 ("pro-regenerative").[66] PES further influences the local environment by influencing the rate of Wallerian degeneration. Although PES is typically delivered proximal to the nerve repair, when delivered to the distal stump of a sciatic nerve there is accelerated Wallerian degeneration with enhanced nerve regeneration.

The effects of electrical stimulation extend beyond axonal regeneration to include remyelination. As discussed above, electrical stimulation affects not only neuronal cells, but also Schwann cells. In Schwann cells, mitochondrial calcium release is induced through activity-dependent release of ATP that acts on purinergic receptors located on Schwann cells. Blocking this activation during myelination in development leads to hypomyelination of axons, though its role in remyelination after injury, or in CES specifically, is not yet established.[60] Most studies support PES as a positive modulator of post-injury remyelination. Numerous studies have reported enhanced myelination following nerve transection[24,27,29,31,35,36,38,40,71,79,83] and accelerated myelin clearance[66,68,69,71]; however, in models of surgical decompression, PES did not appear to affect remyelination.[30] The effects of CES on remyelination after injury are unknown.

2.5 Conclusions

Though electrical stimulation to promote nerve regeneration is often assumed to have been thoroughly studied,[61-65] it is clear that numerous knowledge gaps remain. On review of methodology, many stimulation paradigms assumed in the literature to correlate with PES are actually reporting mechanistic insights into CES. This distinction is important, given the unique effects of CES and PES on nerve regeneration. The complete mechanisms of either intervention remain elusive and fragmented, with numerous reviews making inferences and citing them as fact. The most striking is the presumed role of cAMP, cited in the vast majority of scientific articles and review articles about PES, that while very possibly true, has yet to be studied. Understanding the individual mechanisms of CES and PES will provide insight into how known and unknown pro-regenerative pathways affect nerve regeneration, offering information beyond "promoting regeneration" to include how these pathways affect regeneration specifically at the coaptation site, alter the speed of axonal extension, regulate preferential motor reinnervation, and influence success of reinnervation and recovery of function.

2.6 Figures

Table 2.6.1 *Electrical Stimulation and Regeneration After Peripheral Nerve Injury*

	CES IN VIVO	CES IN VITRO	PES IN VIVO	PES IN VITRO
Regeneration After PNI	CES improves length of nerve regeneration and number of regenerating axons vs. controls, and to a greater extent than PES.[19-21] CES improves regeneration through nerve transfers.[22] CES improves regeneration in chronically denervated nerves.[55] CES of the femoral nerve does not promote regeneration.[8]	CES promotes neurite extension of DRG neurons in vitro.[34,48,51,52,84] CES promotes neurite extension, increasing the number of neurites per neuron.[31] DRG neurons stimulated in vivo and harvested 7d later had a 4-fold increases in neurite extension; neurons harvested 1d after CES did not.[49] DRG neurons cultured with pre-stimulated Schwann cells increased neurite extension 3-fold; pre-stimulated fibroblasts/endothelial cells had no effect.[47]	PES of the sciatic, tibial, or common fibular/peroneal nerve after transection promoted extension of motoneurons and sensory neurons into the distal nerve segment, with increased axon counts, and reinnervation, and promoted axon fiber density.[13,24-33,35,85] PES of the sciatic nerve following sciatic nerve injury/repair increased the proportion of arborizing axons, and did not affect branching.[86] PES of the sciatic nerve promoted regeneration of axons into the spinal cord after a hemilaminectomy, though lesser than a crush lesion to the sciatic nerve.[49] RNA sequencing: PES accelerates Wallerian Degeneration after sciatic nerve injury, accelerating axonal regeneration.[35,69] PES accelerates regeneration of axons in delayed nerve injury models[27,72], but only up to one month of delayed nerve repair.[36] PES following tibial nerve repair has significantly less regenerative response than CES 7d prior to tibial nerve repair.[21] PES following femoral nerve repair did not promote regeneration of motoneurons.[40] PES following sciatic nerve injury/repair prevented a 15% initial decrease of Substance P-ergic neurons in the L4/L5 spinal cord, and a 30% decrease of Substance P-ergic neurons after 2 months.[35] PES following sciatic nerve crush promoted regeneration and normalized axon morphometry.[79] PES of the ulnar nerve after nerve injury/repair increases axon fiber density.[83]	PES and neurite axotomy of DRG neurons promoted neurite extension and number of neurites.[50]
Regeneration Rate	CES of the sciatic nerve accelerated the innate rate of regenerating axons after PNI.[19-22]		PES of the femoral, facial, sciatic, and common peroneal nerve does not alter the innate rate of regeneration of axons after injury in acutely and chronically denervated nerves.[8,11,12,32,38,53,86] PES of the ulnar nerve after nerve transection and repair increases the rate of regeneration.[83]	
Neuronal Survival		CES promotes proliferation of Schwann cells in culture with DRG neurons, and decreased apoptosis and senescence of DRG neurons.[40]	PES of the femoral nerve after nerve transection does not enhance motoneuron survival.[40] PES of the sciatic nerve after nerve transection increases apoptosis compared to injured controls receiving isografts.[25]	
Preferential Motoneuron Reinnervation			PES of the femoral nerve after nerve transection promoted PMR after injury, increasing the specificity of regenerating motor axons into the motor branch earlier than controls, and promoted specificity of sensory axons correctly reinnervating the sensory branch.[8,12,54] PES of the femoral nerve after nerve transection did not promote motoneuron reinnervation specificity.[40] PES of the femoral nerve after nerve transection and repair did not promote PMR without end organ connectivity.[54] PES increases the number of axons and the regeneration speed of axons crossing the repair site, even in nerve injury with chronically denervated Schwann cells, with chronically axotomized axons, or both.[8,12,13,29,38,53]	

Table 2.6.2 *Electrical Stimulation and Functional Recovery*

	CES IN VIVO	PES IN VIVO
Reinnervation	CES increases neuromuscular junction reinnervation to the footpad, tibialis anterior, and gastrocnemius muscles.[20] CES increases neuromuscular junction reinnervation to the gastrocnemius muscle.[55]	PES accelerated functional recovery; it did not increase reinnervation of femoral motoneurons into the quadriceps muscle after nerve injury.[40] PES promoted motoneuron reinnervation of the tibialis anterior and planar muscles after sciatic nerve transection and repair.[35]
Nerve Conduction Studies	CES accelerated CMAP recovery after tibial nerve transection and repair.[20]	H/M wave amplitude ratios of CMAPs indicated that PES of the cut/repaired tibial nerve promoted faster spinal reflex recovery and increased tibialis anterior muscle reinnervation.[24] PES of the femoral nerve accelerated nerve conduction velocity, increased CMAP amplitude and decreased CMAP latency.[37-39] CMAP recordings revealed that PES of the sciatic nerve after injury/repair promoted reinnervation of motoneurons across 13 mm nerve grafts.[27] PES of the sciatic nerve increased M amplitude of the tibialis anterior muscle, but not the plantar muscles, after sciatic nerve injury/repair.[35] In delayed (1 month) sciatic nerve injury/repair, PES increased CMAP amplitude, decreases CMAP latency, increases conduction velocity.[36] PES of the sciatic nerve after compression injury increased CMAP amplitude after injury compared to unstimulated controls.[30]
Motor Functional Recovery	CES increased muscle mass of the gastrocnemius, and promoted recovery of gait compared to control after tibial nerve transection and repair.[20] CES increased muscle mass of the tibialis anterior muscle, and promoted recovery of gait compared to control after common fibular (peroneal) distal nerve transfer.[21] CES promoted recovery of gait compared to control after chronic tibial nerve injury.[55]	PES accelerates recovery of quadricep function through gait analysis on a beam walking task after transection of the femoral nerve, but does not accelerate recovery of whisking function after facial nerve transection.[39] PES following sciatic nerve transection and repair across a 15 mm graft accelerated recovery of gait and decreased muscle atrophy.[37] PES following sciatic nerve transection and repair promoted an earlier detection of an evoked potential, although animals receiving electrical stimulation resulted in an extended recovery of the H reflex after injury compared to unstimulated animals.[45] PES following femoral nerve transection and repair accelerated recovery of gait at 4, 6 and 8 weeks compared to unstimulated controls, though PES following facial nerve transection and repair did not accelerate whisking functional recovery.[39] PES accelerated onset of functional recovery and complete functional recovery of facial nerve function after crush or nerve transection.[41-43,46] PES accelerates onset of functional recovery and complete functional recovery after laryngeal nerve crush.[44] PES following sciatic nerve compression injury accelerated recovery of gait between 2 and 8 weeks after injury.[30] PES following sciatic nerve transection injury accelerated onset and complete functional recovery in the grid walking task, and increased muscle weight of the tibialis anterior and gastrocnemius muscles.[29] PES following tibial nerve transection injury accelerated onset and complete recovery of TFI and grid walking tasks.[28]
Sensory Functional Recovery	CES promoted a decreased threshold for mechanical sensory stimuli of the footpad after tibial nerve transection and repair.[20] CES promoted a decreased threshold for mechanical sensory stimuli of the footpad after chronic tibial nerve injury.[55]	PES of the tibial nerve after nerve transection and repair decreased withdrawal latency to thermal stimuli and decreased withdrawal threshold to mechanical stimuli.[24,33] PES promoted return of nociceptive sensation, although not mechanical sensation, after sciatic nerve transection and repair.[35] PES promoted return of mechanical sensation, but not thermal sensation after sciatic nerve transection and repair.[29]

Table 2.6.3 *Channels and Signaling Pathways*

	CES IN VIVO	CES IN VITRO	PES IN VIVO	PES IN VITRO
Voltage Gated Na+ Channels	Lidocaine (VG Na+ channel inhibitor) blocks CES-mediated release of ATP and Schwann cells cytosolic and mitochondrial Ca2+ influx.[59]		Tetrodotoxin (VG Na+ channel inhibitor) blocks retrograde action potential transmission and anterograde activation of afferents, ultimately blocking PES benefits.[12,13] Lidocaine (VG Na+ channel inhibitor) decreased axon fiber density, neural tissue percentage and myelination of regeneration axons, but were not significant.[57]	
Ca2+ Release	CES induces ATP release through maxi-anion channels, leading to activation of purinergic receptors of Schwann cells. This results in Schwann cell cytosolic Ca2+ influx, and mitochondrial Ca2+ influx mediated by IP3 generation and mitochondrial Ca2+ uniporter.[59]	CES causes intracellular Ca2+ release in DRG neurons which stimulates neurite extension. Blocking T-Type low voltage gated Ca2+ channels does not block ES mediated neurite extension.[34] CES-induced BDNF upregulation is partially attenuated by inhibiting of L-type voltage gated Ca2+ channels.[59] CES-induced glutamate secretion of pudendal nerve DRG neurons coincides with Ca2+ influx and exosome release from Schwann cells.[56] CES-induced pCREB and BDNF expression and increased neurite outgrowth is abolished when Ca2+ influx is blocked.[57] When BDNF expression and pCREB levels are increased, neurite extension overcomes inhibition from Ca2+ influx inhibition.[58] CES increases intracellular Ca2+ via N and L type voltage gated Ca2+ channels. When these receptors are blocked neurite extension mediated by CES is attenuated. BDNF and c-Fos mRNA, and BDNF protein are upregulated after ES, mediated by Ca2+ influx.[48]		
Calcium/ Calmodulin Dependent Protein Kinases		CaMKII is necessary for the CES mediated increase in pCREB expression and BDNF transcription, and both CaMKK and CaMKII are required to increase neurite outgrowth.[58]		
Adenylyl Cyclase/cAMP Pathway	CES applied to the sciatic nerve resulted in upregulation of cAMP in DRGs.[49]	Addition of cAMP into cultures of spinal neurons induces an alteration of growth cone dynamics in response to different diffusible factors and myelin debris, replicating the alterations that CES induces.[74]	PES of crushed facial nerve increased PACAP expression at 1 and 2 days.[67]	
PTEN		PTEN mRNA expression is downregulated in DRG neurons after CES.[34]	PTEN mRNA expression is downregulated in DRGs after PES of sciatic nerve.[34]	
PI3K/Akt	CES activates Schwann cell purinergic receptors that generate IP3 in Schwann cells.[60]	CES mediated increase in neurite outgrowth was abolished with application of PI3K inhibitor.[34]	RNA seq analysis: PES after sciatic nerve injury activates PI3K-Akt associated genes.[69]	
MAPK/ERK/ Ras/Raf/Rap		CES mediated upregulation of BDNF in DRG neurons is attenuated with Erk inhibitor. CES induced BDNF upregulation is mediated by Erk.[59]	RNA seq analysis: PES after sciatic nerve injury activates MAPK associated genes.[69] RNA seq analysis: PES after sciatic nerve injury activates Rap1 associated genes.[69]	
miRNAs		miR-363-5p inhibition promotes neurite outgrowth in DRG neurons comparable to CES. miR-363-5p inhibits regeneration associated protein DCLK1, decreasing neurite outgrowth. This cannot be reversed by CES.[52]		

Table 2.6.4 *Neurotrophins*

	CES in VIVO	CES in VITRO	PES in VIVO	PES in VITRO
BDNF/TrkB	CES upregulates BDNF in DRG L4-L5 of sensory neurons. BDNF remains upregulated longer than unstimulated injured controls.[19,20]	CES of naive DRG neurons upregulates BDNF mRNA and protein in neurons.[34,48] This upregulation is mediated by Ca2+ influx and release from intracellular stores.[48] CES to cultured spinal neurons increases BDNF expression. This increase is partially attenuated with application of nifedipine (VG L-type Ca2+ channel inhibitor) and fully attenuated when neurons are cultured with Erk inhibitor. ES mediated upregulation of BDNF is mediated by Ca2+ dependent Erk pathways.[59] CES of cultured Schwann cells does not increase secretion of BDNF.[47] CES increases BDNF mRNA expression in neurons. Applying BDNF to ES neurons treated with calcium inhibitors reversed the inhibitory effects on neurite outgrowth. CaMKII is also necessary for the ES mediated increase of BDNF transcription.[58]	BDNF and TrkB are upregulated after PES when compared to sham stimulated injured nerves or naive uninjured nerves. BDNF is upregulated to a greater extent than TrkB.[7,26,67] Deficiency of TrkB and BDNF decreases the effect of PES; differences in HNK1 carbohydrate expression that naturally occur after injury are limited by electrical stimulation, but deficiency of TrkB returns this expression pattern to normal. PMR is reduced in animals that are deficient in TrkB that have undergone ES, and TrkB deficient mice have compromised motor functional recovery.[70] BDNF upregulated in spinal cord neurons 1-3 weeks after sciatic nerve transection surgery, and 1-2 weeks after pudendal nerve crush followed by PES.[59,69,73] . PES causes Schwann cell proliferation and neurotrophic support in the nerve after injury through increased expression of BDNF at the spinal cord[54,71] regardless of end organ connectivity.[54] PES to chronically injured motoneurons causes higher levels of BDNF and TrkB mRNA and protein compared to unstimulated injured motoneurons.[36,72] PES upregulates BDNF in sciatic nerves with demyelinating lesion, colocalizing with NF200 and GFAP.[68] PES upregulates BDNF in L3/L4 DRGs 24 hours after sciatic nerve transection.[29]	
NGF		CES of Schwann cells causes calcium release from internal stores and influx through the plasma membrane via T type VGCCs. This induces calcium mediated exocytosis of NGF from the Schwann cells.[75] Culturing DRG neurons with prestimulated SCs promotes NGF secretion into medium.[47]	PES promotes expression of NGF 7, 14 and 21 days after nerve transection.[69]	
NT-3/4/5			PES can overcome deficiencies in regeneration caused by lack of Schwann cell derived neurotrophins, induced by NT-4/5 KO grafts, or acellular grafts, and ES increases the proportion of axons with immunoreactivity to TrkB at 1 and 2 weeks.[26] PES cannot upregulate NTF3-4 without end organ connectivity.[54]	
GDNF		CES of cultured Schwann cells does not induce increased secretion of GDNF into culture media.[47]	PES upregulates GDNF regardless of end organ connectivity.[54]	

Table 2.6.5 *Regeneration Associated Genes*

	CES IN VIVO	CES IN VITRO	PES IN VIVO	PES IN VITRO
GAP43	CES upregulates GAP43 mRNA and protein expression in L4/L5 DRGs at 3 days and 14 days.[19,20]	CES increases trends of GAP43 in DRG neurons, although the upregulation is not significant.[34]	PES of the sciatic nerve upregulates GAP43 in L4/L5 DRGs in vivo.[34,76] GAP43 mRNA expression is elevated in L3 DRGs after PES of the femoral nerve, and co-localized with ATF3 mRNA expression.[13] PES of the sciatic nerve after nerve injury upregulated GAP-43 protein 2 days to 2 weeks after injury.[27] PES of the facial nerve after nerve crush increased GAP-43 expression 2 fold.[67]	
pCREB	CES upregulates pCREB protein expression in L4/L5 DRGs 3 days after conditioning.[20,55]	CES elevated pCREB DRG neuronal expression by 2 fold. Blocking pCREB upregulation, or inhibiting CaMKII, precluded CES-mediated increase in neurite extension.[58]		
ATF3	CES decreases ATF3 expression in chronic injury paradigms compared to injured controls.[55]		PES normalizes ATF3 mRNA expression in L4/L5 DRGs.[34] PES increases ATF3 protein expression in L3/L4 DRGs after sciatic nerve transection.[29]	
GFAP	CES upregulated GFAP mRNA and protein expression in satellite glial cells adjacent to L4/L5 DRGs after 3 days.[19,20,55]		PES accelerates clearance of myelin debris after a demyelinating lesion & is suggested to activate Schwann cell phagocytosis of myelin.[66] PES accelerates myelin clearance and Schwann cell proliferation (increased GFAP expression) after a demyelinating lesion.[68]	
MMP2				After DRG neurite axotomy and PES, MMP2 expression is increased in DRG neurons; abolishing MMP2 eliminates the PES mediated increase in neurite extension.[50]
FGF2			FGF-2 did not further the regeneration evoked by PES of the sciatic nerve.[27]	
Neuritin			PES of the crushed facial nerve increased expression of neuritin 6 hours to 1 week after injury compared to nerve crush alone.[67]	
Mitochond ria	CES increases mitochondrial mobilization velocity and length of mobilized mitochondria, favoring anterograde transport when nerve is stimulated at 50Hz. CES increases accumulation of mitochondria in distal nerve, and evenly distributes stationary mitochondria along the axons.[78]			

__Table 2.6.6__ Myelination and Inflammation

	CES IN VIVO	CES IN VITRO	PES IN VIVO	PES IN VITRO
Remyelination After PNI			PES enhances myelination of axons 2, 3, 4, and 8 weeks after injury.[27,29,31,71] PES increases the number of myelinated axons in the tibial nerve 2 months post transection.[24,35] PES decreases the number of myelinated fibers 4-14 days post injury (accelerated myelin clearance).[69] Delayed PES of the femoral nerve after nerve transection promotes remyelination of motoneurons.[38,40] PES does not affect remyelination of fibers after sciatic nerve compression injury.[30] PES following sciatic nerve crush increases myelin thickness of axons to closely resemble naive motoneurons, and accelerates the onset of myelination.[79] PES of the ulnar nerve increases the number of myelinated axons after nerve transection and repair.[83] In delayed (up to 1 month) sciatic nerve repair, PES increases myelin thickness.[36]	
Myelin Proteins and Schwann cell Markers	CES promotes Schwann cell proliferation in a chronic tibial nerve injury model.[55]	CES increases/promotes earlier expression of P0 and Par3 in DRG neurons and Schwann cells.[79]	PES of the sciatic nerve after nerve transection injury demonstrated downregulation of MPZ and MBP mRNA to indicate accelerated dedifferentiation of myelinating Schwann cells.[69] PES following sciatic nerve crush upregulated MPZ and Par3 in Schwann cells and promotes earlier distribution of Par3 at the axial-glial junction in Schwann cells.[79] PES accelerates myelin clearance after a demyelinating lesion, which coincided, suggesting that PES accelerated activation and Schwann cell phagocytosis of myelin.[66] PES increased protein expression of S100, P0, and Par3 in Schwann cells after sciatic nerve transection and repair.[71]	
Macrophages	CES did not upregulate macrophages in the rat tibial nerve.[80] CES does not upregulate macrophage levels at the site of stimulation (nerve) or the corresponding DRGs.[81]		PES after a sciatic demyelinating lesion accelerates macrophage clearance from the injury site.[68] PES causes earlier/increased macrophage infiltration, accelerating Wallerian Degeneration.[69] PES increased accumulation of CD68+ M1 macrophages and CD206+/CD68+ M2 macrophages.[28] PES following sciatic nerve transection upregulates IL-6, CCL2, and CSF1.[29]	

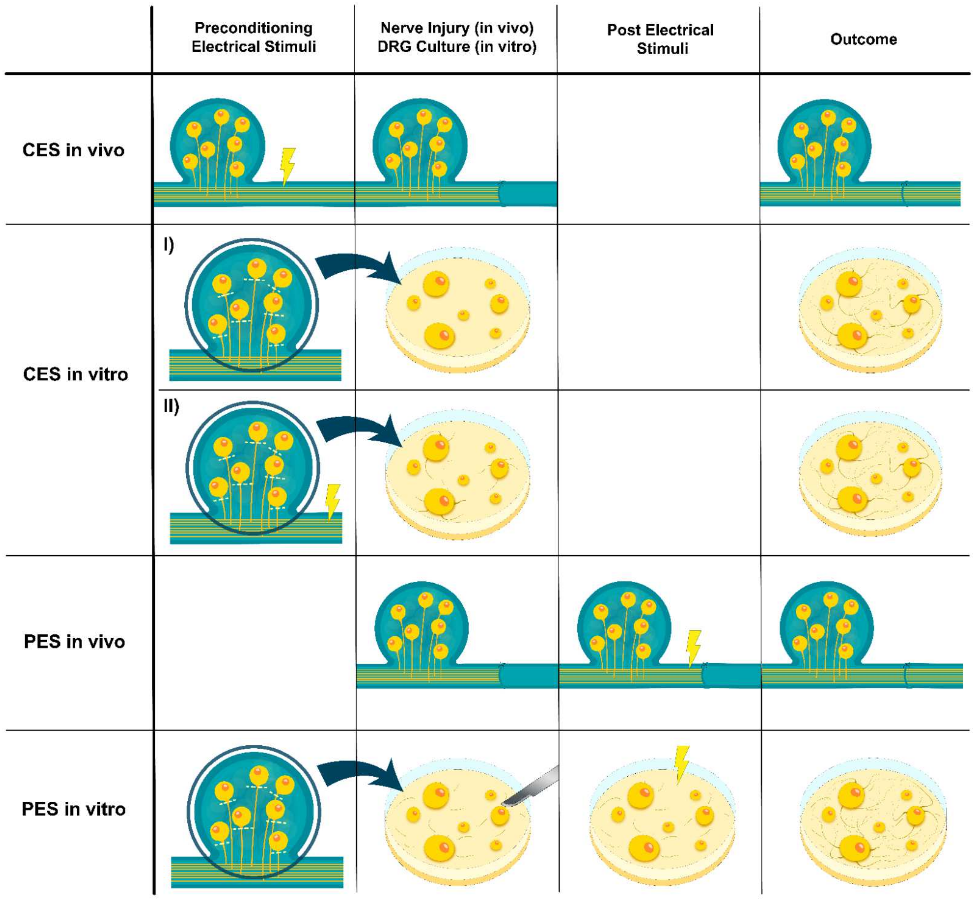

Figure 2.6.7 Defining the paradigms of conditioning and postoperative electrical stimulation in vitro and in vivo. CES constitutes administration of ES prior to injury, whereas PES is administered following injury. Dissociation of DRGs for in vitro assay is considered non-injurious; therefore, ES administered prior to and following dissociation is CES, whereas ES administered following neurite axotomy is PES.

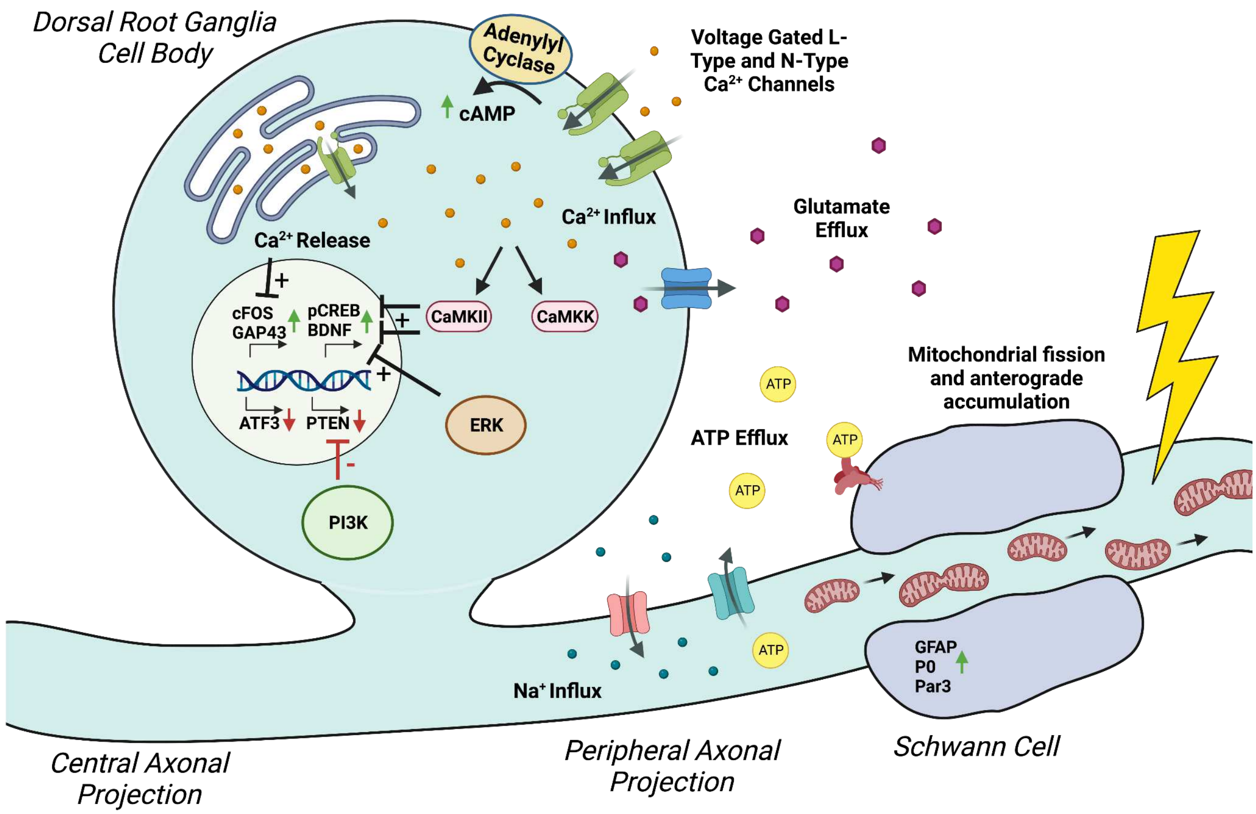

Figure 2.6.8 Mechanism of conditioning electrical stimulation in peripheral nerve. Electrical stimulation administered to the peripheral nerve prior to injury induces a series of axonal and glial events: sodium influx, ATP efflux and increases in velocity, fission and distal accumulation of mitochondria in the axon, upregulation of GFAP in satellite glial cells, and upregulation of P0 and Par3 in Schwann cells. In the soma, calcium enters the cytosol through voltage gated L and N type channels on the plasma membrane, and is released from the endoplasmic reticulum. Calcium influx increases cAMP signaling, and CaMKII and CaMKK activation. Upregulation of BDNF is dependent on CaMKII, ERK and Ca^{2+}, pCREB is dependent on CaMKII and Ca^{2+} and cFOS is dependent on Ca^{2+}. GAP43 is upregulated following CES, while ATF3 and PTEN are downregulated. PTEN downregulation is mediated by PI3K.

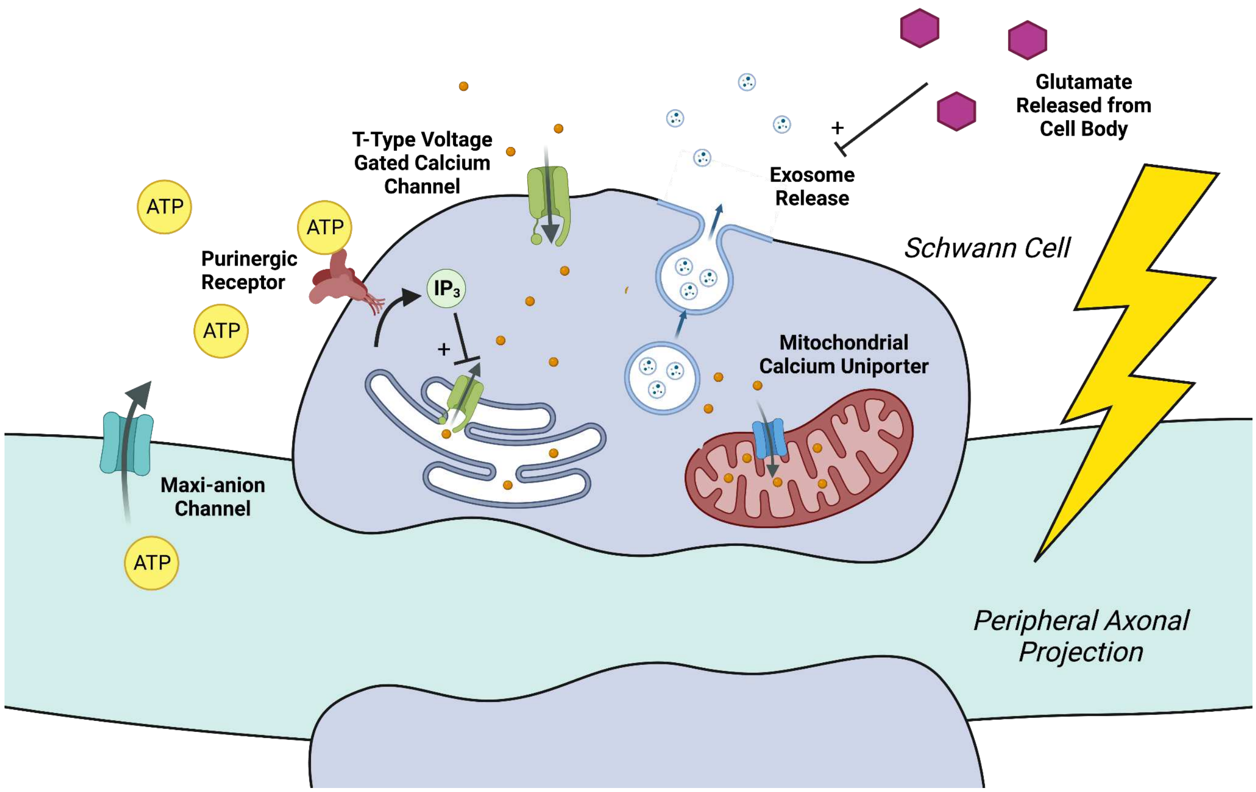

Figure 2.6.9 Mechanism of conditioning electrical stimulation in schwann cells. Electrical stimulation administered to the peripheral nerve prior to injury induces a series of events in Schwann cells. ATP, released from the axon in response to CES acts upon purinergic receptors, signaling IP3 to potentiate calcium influx into the Schwann cell cytosol, and release from the endoplasmic reticulum. Cytosolic calcium influx signals mitochondrial calcium influx through the mitochondrial calcium uniporter. CES also stimulates exosome release.

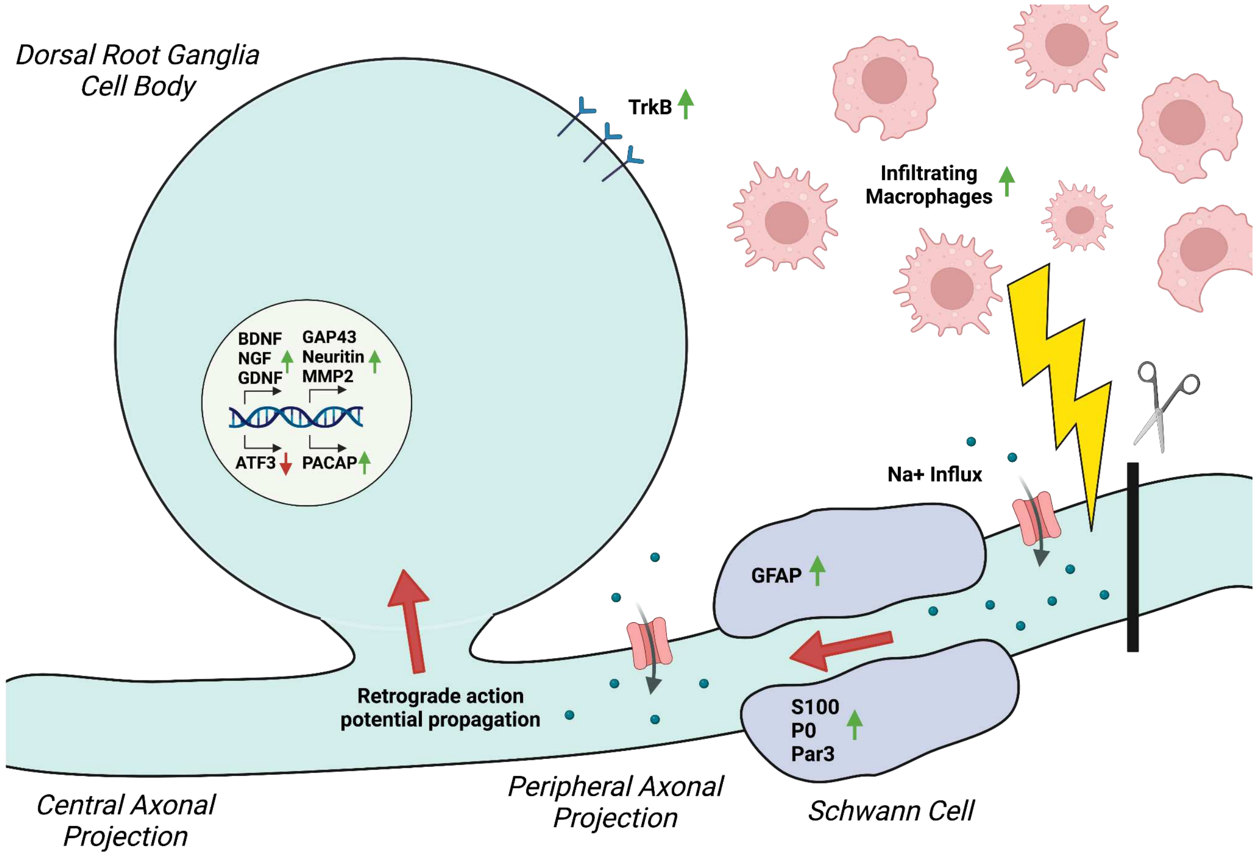

Figure 2.6.10 Mechanism of postoperative electrical stimulation in peripheral nerve. Electrical stimulation delivered to the peripheral nerve following injury induces sodium influx into the axon to mediated retrograde propagation of action potentials. Retrograde signaling results in upregulation of regeneration associated genes, neurotrophins and neurotrophin receptors, including GAP43, BDNF, NGF, GDNF, and TrkB. Neuritin, MMP2 and PACAP upregulate following PES, while PES normalizes the upregulation of ATF3 that occurs following injury. PES accelerates and increases the infiltration of macrophages to the injury site.

2.7 Bibliography

1. Ring D. Symptoms and disability after major peripheral nerve injury. Hand Clin. 2013;29(3):421-5.
2. Fu S, Gordon T. Contributing factors to poor functional recovery after delayed nerve repair: prolonged axotomy. J Neurosci. 1995b;15(5):3876-85.
3. Grinsell D, Keating C. Peripheral nerve reconstruction after injury: a review of clinical and experimental therapies. BioMed Res Int. 2014;2014, 698256.
4. Fu S, Gordon, T. Contributing factors to poor functional recovery after delayed nerve repair: prolonged denervation. J Neurosci, 1995a;15(5)3886-95.
5. Menorca R, Fussell T, Elfar J. Nerve physiology: mechanisms of injury and recovery. Hand Clin. 2013;29(3):317-30.
6. Rotshenker, S. Wallerian degeneration: the innate-immune response to traumatic nerve injury. J Neuroinflammation. 2011;108(8).
7. Al-Majed A, Brushart T, Gordon T. Electrical stimulation accelerates and increases expression of BDNF and trkB mRNA in regenerating rat femoral motoneurons. Eur J Neurosci. 2000a;12(12):4381-90.
8. Brushart T, Hoffman P, Royall R, et al. Electrical stimulation promotes motoneuron regeneration without increasing its speed or conditioning the neuron. J Neurosci. 2002;22(15):6631-8.
9. Brushart T, Jari R, Verge V, et al. Electrical stimulation restores the specificity of sensory axon regeneration. Exp Neurol. 2005; 194(1):221-9.
10. Nix W, Hopf H. Electrical stimulation of regenerating nerve and its effect on motor recovery. Brain Res. 1983;272(1):21-5
11. Witzel C, Koulaxouzidis G, Brushart T, et al. Electrical stimulation enhances distal reinnervation without increasing regeneration speed. J Plast Reconstr Aesthet Surg. 2009;62(6).
12. Al-Majed A, Neumann C, Brushart T, et al. Brief electrical stimulation promotes the speed and accuracy of motor axonal regeneration. J Neurosci. 2000b;20(7):2602-8.
13. Geremia N, Gordon T, Brushart T, et al. Electrical stimulation promotes sensory neuron regeneration and growth-associated gene expression. Exp Neurol. 2007;205(2):347-59.
14. Lu C, Ho Y, Hsu F, et al. Effects of electrical stimulation at different frequencies on regeneration of transected peripheral nerve. Neurorehabil Neural Repair. 2008;22(4):367-73.
15. Barber B, McNeely M, Chan K, et al. Intraoperative brief electrical stimulation (BES) for prevention of shoulder dysfunction after oncologic neck dissection: study protocol for a randomized controlled trial. Trials. 2015;16.
16. Gordon T, Amirjani N, Edwards D, et al. Brief post-surgical electrical stimulation accelerates axon regeneration and muscle reinnervation without affecting the functional measures in carpal tunnel syndrome patients. Exp Neurol. 2010;223(1):192-202.
17. Power H, Morhart M, Olson J, et al. Postsurgical Electrical Stimulation Enhances Recovery Following Surgery for Severe Cubital Tunnel Syndrome: A Double-Blind Randomized Controlled Trial. Neurosurgery. 2020;86(6):769-77.

18. Wong J, Olson J, Morhart M, et al. Electrical stimulation enhances sensory recovery: A randomized controlled trial. Ann Neurol. 2015;77(6):996-1006.
19. Senger J, Verge V, Macandili H, et al. Electrical stimulation as a conditioning strategy for promoting and accelerating peripheral nerve regeneration. Exp Neurol. 2018;302:75-84.
20. Senger J, Macandili H, Chan K, et al. Conditioning electrical stimulation promotes functional nerve regeneration. Exp Neurol. 2019;315:60-71.
21. Senger J, Chan K, Webber C, et al. Conditioning electrical stimulation is superior to postoperative electrical stimulation, resulting in enhanced nerve regeneration and functional recovery. Exp Neurol. 2020a:325.
22. Senger J, Rabey K, Morhart M, et al. Conditioning electrical stimulation accelerates regeneration in nerve transfers. Ann Neurol. 2020b;88(2)363-74.
23. Frey E, Valakh V, Karney-Grobe S, et al. An In Vitro Assay to Study Induction of the Regenerative State in Sensory Neurons. Exp Neurol. 2015;263:350-63.
24. Asensio-Pinilla E, Udina E, Jaramillo J, et al. Electrical stimulation combined with exercise increases axonal regeneration after peripheral nerve injury. Exp Neurol. 2009;219(1):258-65.
25. Calvey C, Zhou W, Stakleff K, et al. Short-term electrical stimulation to promote nerve repair and functional recovery in a rat model. J Hand Surg. 2015;40(2):314-22.
26. English A, Schwartz G, Meador W, et al. Electrical stimulation promotes peripheral axon regeneration by enhanced neuronal neurotrophin signaling. Dev Neurobiol. 2007;67(2):158-72.
27. Haastert-Talini K, Schmitte R, Korte N, et al. Electrical stimulation accelerates axonal and functional peripheral nerve regeneration across long gaps. J Neurotrauma, 2011;28(4):661-74.
28. Keane G, Pan D, Roh J, et al. The Effects of Intraoperative Electrical Stimulation on Regeneration and Recovery After Nerve Isograft Repair in a Rat Model. HAND. 2022;17(3):540-8.
29. Sayanagi J, Acevedo-Cintron J, Pan D, et al. Brief Electrical Stimulation Accelerates Axon Regeneration and Promotes Recovery Following Nerve Transection and Repair in Mice. J Bone Jt Surg. 2021;103(20).
30. Shapira Y, Sammons V, Forden J, et al. Brief electrical stimulation promotes nerve regeneration following experimental in-continuity nerve injury. Neurosurgery. 2019;85(1):156-63.
31. Singh B, Xu G, Franz C, et al. Accelerated axon outgrowth, guidance, and target reinnervation across nerve transection gaps following a brief electrical stimulation paradigm. J Neurosurg. 2012;116(3):498-512.
32. Sharma N, Coughlin L, Porter R et al. Effects of electrical stimulation and gonadal steroids on rat facial nerve regenerative properties. Restor Neurol Neurosci. 2009;27(6):635-46.
33. Thompson N, Sengelaub D, English A. Enhancement of peripheral nerve regeneration due to treadmill training and electrical stimulation is dependent on androgen receptor signaling. Dev Neurobiol. 2013;74(5):531-40.
34. Singh B, Krishnan A, Micu I, et al. Peripheral nerve plasticity is enhanced by brief electrical stimulation and overrides attenuated regrowth in experimental diabetes. J Neurosurg. 2015;83:134-51.
35. Vivó M, Puigdemasa A, Casals L et al. Immediate electrical stimulation enhances

regeneration and reinnervation and modulates spinal plastic changes after sciatic nerve injury and repair. Exp Neurol. 2008;211(1):180-93.
36. Xu C, Kou Y, Zhang P, et al. Electrical stimulation promotes regeneration of defective peripheral nerves after delayed repair intervals lasting under one month. PLoS ONE. 2014;9(9).
37. Huang J, Lu L, Hu X, et al. Electrical stimulation accelerates motor functional recovery in the rat model of 15-mm sciatic nerve gap bridged by scaffolds with longitudinally oriented microchannels. Neurorehabil Neural Repair. 2010a;24(8):736-45.
38. Huang J, Hu X, Lu L, et al. Electrical stimulation accelerates motor functional recovery in autograft-repaired 10mm femoral nerve gaps in rats. J Neurotrauma. 2009;26:1805-13.
39. Raslan A, Salem M, Al-Hussaini A, et al. Brief electrical stimulation improves functional recovery after femoral but not after facial nerve injury in rats. Anat Rec. 2019;302(8):1304-13.
40. Ahlborn P, Schachner M, Irintchev A. One hour electrical stimulation accelerates functional recovery after femoral nerve repair. Exp Neurol. 2007;208(1):137-44.
41. Foeking E, Fargo K, Coughlin L, et al. Single sesion of brief electrical stimulation immediately following crush injury enhances functional recovery of rat facial nerve. J Rehabil Res Dev. 2012;49(3):451.
42. Hadlock T, Lindsay R, Edwards C, et al. The effect of electrical and mechanical stimulation on the regenerating rodent facial nerve. The Laryngoscope. 2010;120(6):1094-102.
43. Hetzler L, Sharma N, Tanzer L, et al. Accelerating functional recovery after rat facial nerve injury: Effects of gonadal steroids and electrical stimulation. Otolaryngol Neck Surg. 2008;139(1)62-7.
44. Monaco G, Brown T, Burgette R, et al. Electrical stimulation and testosterone enhance recovery from recurrent laryngeal nerve crush. Restor Neurol Neurosci. 2015;(4):571-8.
45. Park S, Liu C, Ward P, et al. Effects of repeated 20-Hz electrical stimulation on functional recovery following peripheral nerve injury. Neurorehabil Neural Repair. 2019;33(9):775-84.
46. Sharma N, Moeller C, Marzo S, et al. Combinatorial treatments enhance recovery following facial nerve crush. The Laryngoscope. 2010b;120(8):1523-30.
47. Koppes A, Nordberg A, Paolillo G, et al. Electrical stimulation of Schwann cells promotes sustained increases in neurite outgrowth. 2014;20.
48. Yan X, Liu J, Huang J, et al. Electrical stimulation induces calcium-dependent neurite outgrowth and immediate early genes expressions of dorsal root ganglion neurons. Neurochem Res, 2014;39(1):129-41.
49. Udina E, Furey M, Busch S, et al. Electrical stimulation of intact peripheral sensory axons in rats promotes outgrowth of their central projections. Exp Neurol. 2008;210(1):238-47.
50. Han S, Kim D, Sung J, et al. Electrical stimulation accelerates neurite regeneration in axotomized dorsal root ganglion neurons by increasing MMP-2 expression. Biochem Biophys Res Commun. 2019;508(2):348-53.
51. Koppes A, Seggio A, Thompson D. Neurite outgrowth is significantly increased by the simultaneous presentation of Schwann cells and moderates exogenous electric fields. J Neural Eng. 2011;8(4).
52. Quan X, Huang L, Yang Y, et al. Potential Mechanisms of Neurite Outgrowth Enhanced

by Electrical Stimulation: Involvement of MicroRNA-363-5p Targeting DCLK1 Expression in Rat. Neurochem Res. 2017;42(2):513-25.
53. Elzinga K, Tyreman N, Ladak K, et al. Brief electrical stimulation improves nerve regeneration after delayed repair in Sprague Dawley rats. Exp Neurol. 2015;269:142-53.
54. Wang W, Zhu H, Li F, et al. Electrical stimulation promotes motor nerve regeneration selectivity regardless of end-organ connection. J Neurotrauma. 2009;26(4):641-9.
55. Senger J, Rabey K, Acton L, et al. Recovering the regenerative potential in chronically injured nerves by using conditioning electrical stimulation. J Neurosurg. 2022;136:1442-54.
56. Hu M, Hong L, Liu C, et al. Electrical stimulation enhances neuronal cell activity mediated by Schwann cell derived exosomes. Sci Rep. 2019;9(1).
57. Keane G, Marsh E, Hunter D, et al. Lidocaine Nerve Block Diminishes the Effects of Therapeutic Electrical Stimulation to Enhance Nerve Regeneration in Rats. HAND. 2023;18(1):119-25.
58. Yan X, Liu J, Ye Z, et al. CaMKII-mediated CREB phosphorylation is involved in Ca2+-induced BDNF mRNA transcription and neurite outgrowth promoted by electrical stimulation. PLoS ONE. 2016;11(9).
59. Wenjin W, Wenchao L, Hao Z, et al. Electrical stimulation promotes BDNF expression in spinal cord neurons through Ca2+ and ERK-dependent signaling pathways. Cell Mol Neurobiol. 2011;31:459-67.
60. Ino D, Sagara H, Suzuki J, et al. Neuronal Regulation of Schwann Cell Mitochondria Ca2+ Signaling during Myelinaiton. Cell Rep. 2015;12:1951-9.
61. Javeed S, Faraji A, Dy C, et al. Application of electrical stimulation for peripheral nerve regeneration: stimulation parameters and future horizons. Interdiscip Neurosurg. 2021.
62. Juckett L, Saffari T, Ormseth B, et al. The Effect of Electrical Stimulation on Nerve Regeneration Following Peripheral Nerve Injury. Biomolecules. 2022;12(12):1856.
63. Willand M, Nguyen A, Borschel G, et al. Electrical stimulation to promote peripheral nerve regeneration. Neurorehabil Neural Repair. 2016;30(5):490-6.
64. Zuo K, Shafa G, Antonyshyn K, et al. A single session of brief electrical stimulation enhances axon regeneration through nerve autografts. Exp Neurol. 2020;322.
65. Chu X, Song X, Li Q, et al. Basic mechanisms of peripheral nerve injury and treatment via electrical stimulation. Neural Regen Res. 2022;17(10):2185-93.
66. McLean N, Verge V. Dynamic impact of brief electrical stimulation on the neural immune axis-polarization of macrophages toward a pro-repair phenotype in demyelinated peripheral nerve. Glia. 2016;64(9):1546-61.
67. Sharma N, Marzo S, Jones K, et al. Electrical stimulation and testosterone differentially enhance expression of regeneration-associated genes. Exp Neurol. 2010a;223(1):183-91.
68. McLean N, Popescu B, Gordon T, et al. Delayed nerve stimulation promotes axon-protective neurofilament phosphorylation, accelerates immune cell clearance and enhances remyelination in vivo in focally demyelinated nerves. PLoS ONE. 2014;9(10).
69. Li X, Zhang T, Li C, et al. Electrical stimulation accelerates Wallerian degeneration and promotes nerve regeneration after sciatic nerve injury. Glia. 2022;71(3):758-74.
70. Eberhardt K, Irintchev A, Al-Majed A, et al. BDNF/TrkB signaling regulates HNK-1 carbohydrate expression in regenerating motor nerves and promotes functional recovery after peripheral nerve repair. Exp Neurol. 2006;198(2):500-10.
71. Huang J, Lu L, Zhang J, et al. Electrical stimulation to conductive scaffold promotes

axonal regeneration and remyelination in a rat model of large nerve defect. PLoS ONE. 2012;7(6).
72. Huang J, Zhang Y, Lu L, et al. Electrical stimulation accelerates nerve regeneration and functional recovery in delayed peripheral nerve injury in rats. Eur J Neurosci. 2013;38(12)3691-701.
73. Jiang H, Song Q, Gill B, et al. Electrical stimulation of the pudendal nerve promotes neuroregeneration and functional recovery from stress urinary incontinence in a rat model. Am J Physiol-Ren Physiol. 2018;315(6).
74. Ming G, Henley J, Tessier-Lavigne M, et al. Electrical activity modulates growth cone guidance by diffusible factors. Neuron. 2001;29(2):441-52.
75. Huang J, Ye Z, Hu X, et al. Electrical stimulation induces calcium-dependent release of NGF from cultured Schwann cells. Glia. 2010b;58:622-31.
76. Keane G, Marsh E, Hunter D, et al. Lidocaine Nerve Block Diminishes the Effects of Therapeutic Electrical Stimulation to Enhance Nerve Regeneration in Rats. HAND. 2023;18(1):119-25.
77. Han S, Baig H, Hammarlund M. Mitochondria Localize to Injured Axons to Support Regeneration. Neuron. 2016;92(6):1308-23.
78. Sajic M, Mastrolia V, Lee C, et al. Impulse Conduction Increases Mitochondrial Transport in Adult Mammalian Peripheral Nerves in Vivo. PLoS Biol. 2013;11(12):e1001754.
79. Wan L, Ding W, Xia R, et al. Short-Term Low-Frequency Electrical Stimulation Enhanced Remyelination of Injured Peripheral Nerves by Inducing the Promyelination Effect of Brain-Derived Neurotrophic Factor on Schwann Cell Polarization. J Neurosci Res. 2010;89(6):2578-87.
80. Webber C. Determining the mechanism through which conditioning electrical stimulation promotes nerve regeneration. Virtual Conference presented at: Proceedings of the American Society of Peripheral Nerve Conference; 2022 Jan; Carlsbad, CA.
81. Webber C. Unlike a conditioning crush lesion, conditioning electrical stimulation promotes nerve regeneration in a non-injurious and non-inflammatory manner. Nanosymposium Presentation presented at: Society for Neuroscience Conference; 2022 Nov; Miami, FL.
82. Senger J, Verge V, Chan K, et al. The nerve conditioning lesion: A strategy to enhance nerve regeneration. Annals of Neurology. 2018b;83(4):691-702.
83. Wilson D, Jagadeesh P. Experimental regeneration in peripheral nerves and the spinal cord in laboratory animals exposed to a pulsed electromagnetic field. Spinal Cord. 1976;14(1):12-20.
84. Wood M, Willits R. Applied electric field enhances DRG neurite growth: influence of stimulation media, surface coating and growth supplements. J Neural Eng. 2009;6(4).
85. Ward P, Davey R, Zajac J, et al. Neuronal androgen receptor is required for activity dependent enhancement of peripheral nerve regeneration. Dev Neurobiol. 2021;81(4):411-23.
86. Witzel C, Brushart T, Koulaxouzidis G, et al. Electrical Nerve Stimulation Enhances Perilesional Branching after Nerve Grafting but Fails to Increase Regeneration Speed in a Murine Model. J Reconstr Microsurg. 2016;32(6):491-7.

CHAPTER 3: Optimizing Parameters of Conditioning Electrical Stimulation

3.1 Introduction

CES administered *in vivo,* for *in vitro* neurite extension analysis has been demonstrated to elicit a profound conditioning effect on the length of the longest neurite 7 days, but not 1 day following conditioning (Udina et al., 2008). Further, our laboratory has shown that CES performed 7 days prior to injury elicits a conditioning effect *in vivo*, and upregulation of key regeneration genes (Senger et al., 2019, 2018a, 2020a; Udina et al., 2008). Our lab is interested in determining the minimum period between conditioning and injury (latency period) that will elicit a RAG upregulation and a conditioning effect. In this chapter, we assessed neurite extension of DRG neurons *in vitro* and the expression of BDNF, pCREB and GFAP as RAG proteins in the DRG *in vivo* at 1 day, 3 days, 5 days, and 7 days post-conditioning. Determining the latency period and RAG timeline gives insight to the overall timeline of the CES mechanism, and thus identifies key timepoints in which signaling pathways could be manipulated in *in vitro* experimental models.

Other parameters, including the minimum duration of CES necessary to promote regeneration *in vivo* have not been duly investigated. The parameters of PES, optimized by Al-Majed et al. (2000b), are widely accepted to be 1 hour at 20Hz for sufficient promotion of regeneration following injury, 20Hz previously demonstrated to promote regeneration (Pockett & Gavin, 1985), while also being the mean frequency of motor neuron action potentials (Burke, 1981). The parameters of CES have been adopted from PES, and similarly demonstrate a promotion of regeneration when administered for 1 hour at 20Hz (Senger et al., 2018a). Increasing the frequency of stimulation diminishes the pro-regenerative effects of PES, emphasizing the importance of *low-frequency* stimulation both *in vivo* and *in vitro* (Lu et al., 2008; Ming et al., 2001; Udina et al., 2008; Yan et al., 2014; Yeh et al., 2010). Pro-regenerative effects are found at frequencies as low as 2Hz (Lu et al., 2008; Ming et al., 2001; Yeh et al., 2010), though 20Hz is most commonly used. Periods of stimulation longer than 1 hour either match or diminish the pro-regenerative effects of PES, suggesting that longer periods are unnecessary or potentially injurious to the nerve (Al-Majed et al., 2000a; Geremia et al., 2007). Similar studies have not been conducted for CES, however, durations longer than 1 hour are not clinically feasible, and thus 1 hour remains standard. The utility of stimulation durations less than 1 hour have not been determined, even in PES; several labs have proposed that as little as 10-30 minutes of stimulation is sufficient to promote regeneration in pre-clinical models of PES (Aldrashan et al., 2011; Calvey et al., 2015; Foeking et al., 2012; Hetzler et al., 2008; Huang et al., 2013, 2010a; Lu et al., 2008). In considering clinical translation of CES, decreasing the minimum duration may increase availability of the intervention as clinical time is limited. Therefore, it is crucial to identify the minimum duration necessary for sufficient conditioning.

Our laboratory will also compare the Grass SD-9 stimulator to the Checkpoint stimulator in their ability to administer CES and elicit the conditioning effect to animals receiving a tibial nerve injury. SD-9 stimulators are traditionally used to administer both CES and PES in preclinical investigation (Al-Majed et al., 2000b; Senger et al., 2018a, 2019, 2020a), and have been used in clinical trials and clinical practice for PES (Barber et al., 2015; Gordon et al., 2010; Power et al., 2020). The SD-9 stimulator features stainless steel insulated wires with bared ends, with the cathode wire wrapped around the target nerve, and the anode wire inserted into muscle tissue to deliver biphasic pulses with a 0.1ms duration (Senger et al., 2018b). However, SD-9 stimulators are not commercially available. This limits the availability of both CES and PES substantially, and thus alternate stimulators have been under consideration for clinical use. Recently, a new stimulator termed Checkpoint has been approved for clinical trials to administer

PES (Juckett et al., 2022). The Checkpoint stimulator was designed originally to assist surgeons in locating motor nerves and their muscle fascicles during surgery. They place the stimulator on the nerve and look for the muscle twitch to confirm the nerve identity and function (Roh et al., 2022). Checkpoint stimulators are one-time use nerve stimulators programmed to deliver a 16 Hz frequency using a biphasic waveform to maintain sufficient stimulation of the nerve for the duration of the stimulation period. The main electrode of the stimulator is directly applied to the nerve, with a return current electrode embedded in non-muscular tissue. These stimulators provide visible feedback that contact has been maintained with the nerve with a LED light to confirm completion of the circuit (Roh et al., 2022). Recently, the Checkpoint stimulator has also been used to administer PES (Juckett et al., 2022; Roh et al., 2022). Assessment of axon regeneration and functional recovery of rats that had undergone sciatic nerve injury and repair with or without Checkpoint stimulation suggested that 10 minutes of Checkpoint stimulation was sufficient to promote regeneration and function recovery (Roh et al., 2022). The effectiveness of this stimulator has not yet been investigated in the context of CES. Our lab is interested in verifying the pre-clinical validity of Checkpoint against the traditional SD-9 stimulator, and identifying the minimum duration of stimulation required to elicit the conditioning effect using either stimulator.

3.2 Methods

3.2.1 Animals: Adult Sprague Dawley and *Thy-1-GFP* Sprague Dawley rats, between 8-12 weeks old, weighing 200g were housed with the Health Sciences Laboratory Animal Services (HSLAS) (AUP 00001871) at the University of Alberta. Animals were housed in flat-bottomed Greenline cages with ad libitum standard rat chow and water. Lighting was cycled with 12h on/off rotations. All experimental procedures were approved by the University of Alberta Animal Research Ethics Board.

3.2.2 Surgical Procedures: Animals were randomly divided into unconditioned (control) and CES (experimental) cohorts. Prior to all surgical interventions, animals were anesthetized with inhaled isoflurane (2% titrated at 1–2 L/min for maintenance of a surgical anesthetic plane) and received 0.01 mg/kg of subcutaneous buprenorphine. At the completion of all procedures, skin was closed with 4–0 Vicryl sutures (Ethicon Inc., Somerville, NJ). All surgeries were performed in a dedicated animal surgery facility at the University of Alberta.

3.2.3 Conditioning: Animals in the CES cohort received a 2 cm longitudinal incision at the right lower limb to isolate the sciatic nerve via blunt dissection proximal to the trifurcation point. CES animals received 20Hz electrical stimulation at 0.1 ms duration for either 10, 30 or 60 minutes to the sciatic nerve proximal to the trifurcation point, using an SD-9 stimulator (Grass Instruments, Quincy, MA), or received 10, 30 or 60 minutes of intraoperative current at 0.5 mA, at a pulse width of 100 μs and frequency of 16 Hz, from a Checkpoint stimulator (Checkpoint® Stimulator/Locator, Checkpoint Surgical, Inc, Cleveland, OH). Settings were based on previous studies (Jo et al., 2019; Senger et al., 2018; 2019; 2020; Wood et al., 2022). For animals stimulated with an SD-9 stimulator, a stainless-steel wire with bared ends was wrapped around the nerve, and the return electrode was placed into the tibialis anterior muscle; these were connected to the cathode and anode ports of an SD-9 stimulator. For animals stimulated with a Checkpoint stimulator, the stimulating tip was placed directly onto the nerve, and a return current electrode was placed securely in musculocutaneous facia in the dorsum of the animal just proximal to the nerve. To confirm stimulation, the device provided feedback via a LED light indicating whether current was provided and circuit complete. For both stimulators, excitation of the nerve was confirmed based on contractions of the foot. Unconditioned animals did not receive any experimental or surgical intervention. Sham electrical stimulation was not used as previous studies indicated no difference between unconditioned and sham animals (Senger et al., 2018; Senger et al., 2019).

3.2.4 Nerve Transection and Microsurgical Repair: 7 days following conditioning, unconditioned and CES animals received a 2 cm longitudinal incision in the right lower limb to isolate the sciatic nerve via blunt dissection. The sciatic nerve was traced distally and the site of trifurcation was dissected to isolate the tibial nerve from the common peroneal and sural branches. The tibial nerve was cut and immediately repaired using 9–0 silk sutures.

3.2.5 Tissue Collection: 7 days following tibial nerve transection and microsurgical repair for regeneration analysis, 1, 3, or 7 days following conditioning for RAG analysis, or 1, 3 or 7 days following conditioning for tissue culture, animals were euthanized with carbon dioxide and exsanguinated by opening the thoracic cavity and cutting the left ventricle of the heart. For the regeneration studies, the sciatic nerve was re-exposed, and the site of microsurgical repair was identified. The tibial nerve was isolated from connective tissue, and the sural and common peroneal nerve branches, and harvested approximately 2 mm proximal to the coaptation site, and 3 cm distal to the coaptation site. Harvested nerve was placed onto a wooden toothpick and put into 4% paraformaldehyde (PFA) (American MasterTech Scientific, Lodi, CA) fix for 1 hour at 4°C. For RAG analysis and tissue culture, the sciatic nerve was re-exposed and traced to the L4-L5 level of the vertebral column. L4 and L5 DRGs were exposed and harvested, and for RAG analysis, placed into 4% PFA fix for 1 hour at 4 °C. For tissue culture, L4 and L5 DRGs are placed into Hank's buffered salt solution (HBSS) modified medium (HyClone) and placed under a dissecting scope for removal of the epineurium and axon branches. Transfer processed L4/L5 DRGs into sterile HBSS medium. Following fixation, nerves and DRGs were rinsed in 30% sucrose in phosphate buffered saline (PBS) (Thermo Fisher Scientific, Waltham, MA) then stored in 30% sucrose in PBS solution at 4 °C overnight, or until tissue was saturated with sucrose. Tissue was embedded and frozen in optimal cutting temperature (OCT) (Sakura Finetek, Torrance, CA) using indirect exposure to liquid nitrogen. Tissue was stored at −80 °C, until cryosectioning. Longitudinal sections of the nerves and DRG (12 μm) were thaw-mounted onto Superfrost Plus microscope slides (Thermo Fisher Scientific, Waltham, MA) and stored at −80 °C until processing.

3.2.6 Tissue Culture: 1-7 days before culture, 500μL of 0.1 mg/mL poly-D-lysine suspended in sterile water (mol wt 70,000–100,000 kD) (Sigma) evenly distributed over bottom of well in a 24 well glass bottom plate (Cellvis). Solution left on wells for 15 minutes at room temperature, and washed wells 3x100μL with sterile water. Allowed plate to dry for several hours in sterile hood. Stored sealed at 4°C. On the day of the culture, plates coated with 500μL laminin (Mouse

1.0mg/mL) (Invitrogen) diluted in HBSS for a final concentration of 2µg/mL. Plates incubated at 37°C in tissue culture incubator for 2 hours. Laminin removed immediately before plating cells. Dissected DRGs washed by placing into sterile HBSS and tilting to wash 3 times. Sterile 1 mg/mL collagenase (Sigma Aldrich) in HBSS medium prepared and sterilized using 0.22µm low protein binding syringe filter (Thermo Fisher Scientific). Washed DRGs were placed into collagenase solution and incubated in 37°C water bath for 1 hour. Added 0.05% of filter sterilized trypsin (Sigma Aldrich) in HBSS, and continued incubation for 15 minutes. Used sterile 1mL pipette tips to aspirate DRGs with 10 passes through sterile tip for mechanical digestion. Incubated for 15 minutes in water bath if DRGs did not aspirate through 1mL tips. Continued aspiration with 1mL tips until DRGs passed easily through tips, then aspirated DRGs with 200µL tips for 10 passes. Incubated ganglia for 5 minutes in water bath. Repeated aspiration and incubation of ganglia until cells were in suspension. Added 100µL fetal bovine serum (FBS) (Sigma Aldrich). Centrifuged cell suspension at 800-1000 rpm for 7 minutes. Removed supernatant and resuspended cells in HBSS medium. Repeated centrifugation, removed supernatant, and resuspended cells in cell medium: Dulbecco's Modified Eagle Medium/F12 (DMEM) (Gibco), 5% FBS, 1% N2 supplement (Thermo Fisher Scientific), and 1% pen-strep (HyClone). Plated cells with approximate concentration of 700 neurons per well. Stored plate in 37°C tissue culture incubator for 48 hours. After 1 day, pipetted out half of solution in well and pipetted in fresh cell medium.

3.2.7 Immunohistochemistry: Slides were warmed to room temperature for 15 minutes before undergoing 3 by 5 minute washes in 0.01M PBS (Thermo Fisher Scientific), and permeabilized in 0.01% Triton-100x (Thermo Fisher Scientific). Sections were then blocked in 10% normal goat serum (MP Biomedicals, Santa Ana, CA) and 3% bovine serum albumin (BSA) (Sigma Aldrich, St. Louis, MO) in 0.01 M PBS for 90 min. Antibodies and concentrations used are represented in Table 1. Primary antibodies included ATF3, BDNF, GAP43, GFAP, pCREB and NF200 and were applied to sections overnight at 4°C in a solution of 3% BSA and 0.01M PBS (Table 3.5.1). The following day, slides were washed two times in 0.05% Tween in PBS followed by two washes for five minutes in PBS. Secondary antibodies were applied for 60 minutes at room temperature in a solution of 3% BSA and 0.01M PBS (Table 3.5.1). Washes in 0.05% Tween in PBS and in PBS were repeated after secondary antibody application. The nuclei were stained with DAPI (NucBlue) (Thermo Fisher Scientific) which was applied to DRG sections in PBS for five minutes before a final PBS rinse was applied to slides. Slides were sealed with AquaMount (Polysciences) and stored at -20°C.

3.2.8 Immunocytochemistry for Tissue Culture: At experimental endpoints, an equivalent volume of 8% PFA was added to the media for an end concentration of 4%. Wells were incubated for 15-20 minutes at room temperature and wells washed with Dulbecco's phosphate buffered saline (DPBS) (Gibco) 3 times. Cells were permeabilized and blocked with 250μL 0.2% Triton X-100 in DPBS with 10% normal goat serum (NGS) (LifeTech) for 60 minutes at room temperature, then incubated overnight 4°C with primary antibody solution of β-III tubulin in DPBS (Table 3.5.1). The following day, cells were washed with DPBS 3 times, then incubated with DAPI (Invitrogen) and a secondary antibody solution of Cy3 in DPBS for 60 minutes at room temperature (Table 3.5.1). Following incubation, cells were washed 3 times with DPBS.

3.2.9 Imaging: All digital images of longitudinal tibial nerve were processed in a parallel manner with identical fluorescent exposures with 20X objective with a Leica widefield epifluorescent microscope with THUNDER imaging software for large volume computational clearing. Two representative longitudinal tibial nerve sections were analyzed using Thunder Imaging software. For length of nerve regeneration and axon count analysis, Thunder Imaging software identified an ROI and z-stack of the section, and automatically imaged the selected ROI. Z-stack images were combined automatically to enable analysis of each individual axon within the 12µm sections. All digital images of DRGs were captured with identical fluorescent exposures with a 20X objective with a Leica widefield epifluroescent microscope (Leica Microsystems, Wetzlar, Germany). Two representative DRG sections were analyzed for each animal using Image J software. BDNF was analyzed through cytosolic pixel intensity (a.u.), whereas pCREB and GFAP were analyzed through binary evaluation (positive or negative nuclei). *In vitro* DRG neurons were imaged at 20X using High Content Screening Analysis ImageXpress Micro AI imaging system (MetaXpress XLS, Molecular Devices, San Jose, CA, USA). Total neurite outgrowth and length of primary neurite was analyzed using Image J software. Individual neurites were traced and measured to calculate total neurite outgrowth, and the longest neurite per DRG neuron was considered the primary neurite. DRG neurons overlapping neurite extension with other DRG neurons were excluded.

3.2.10 Statistical Analysis: Experimental results are written as the mean ± standard error mean *(s.e.m).* Significance of RAG analysis, neurite outgrowth, and length of regeneration was determined using a one-way analysis of variance (ANOVA) to determine any differences in the mean between groups followed by a post-hoc Dunnett's test to compare experimental groups against unconditioned animals. A level of $p<0.05$ was the cut-off for statistical significance. To determine statistical significance between axon counts, a two-way ANOVA was completed to determine differences between the mean of each group in a paired data set followed by Dunnett's post-hoc for comparison against unconditioned animals. A paired t-test was conducted to determine differences between the length of regeneration of different biomarkers. Statistics were completed using Prism 9.3.1 (GraphPad Software, San Diego, CA).

Table 3.2.1 Primary and Secondary Antibody Protocols for Immunohistochemistry

Primary Antibody	**Antigen Retrieval** 40 minutes in 60 °C citrate buffer (10mM sodium citrate, 0.05% Tween-20, pH 6.0)	**Primary Antibody Dilution**	**Secondary Antibody**	**Secondary Antibody Dilution**
BDNF (rabbit) Abcam Ab108319	Yes	1:1000	Cy3 goat anti-rabbit Jackson Labs 111-167-003	1:1000
CGRP (rabbit) Millipore PC205L	No	1:4000	Cy3 goat anti-rabbit Jackson Labs 111-167-003	1:1000
GAP43 (rabbit) Millipore/Chemicon AB5220	No	1:500	Cy3 goat anti-rabbit Jackson Labs 111-167-003	1:1000
GFAP (rabbit) DAKO Z0334	Yes	1:500	Cy3 goat anti-rabbit Jackson Labs 111-167-003	1:1000
NF200 (mouse) Sigma-Aldrich N4142	No	1:1000	Cy5 donkey anti-mouse Abcam ab15067	1:1000
pCREB (rabbit) Cell Signaling 9198	Yes	1:1000	Cy3 goat anti-rabbit Jackson Labs 111-167-003	1:1000
SMI-32 (rabbit)	No	1:1000	AlexaFluor 488 goat anti-rabbit Invitrogen, Carlsbad, CA A-11008	1:1000
β Tubulin-III (rabbit) Sigma T2200	No	1:1000	Cy3 goat anti-rabbit Jackson Labs 111-167-003	1:1000

3.3 Results

3.3.1 Latency periods between 3 and 7 days allow CES to promote neurite extension of DRG neurons.

CES administered *in vivo*, for *in vitro* neurite extension analysis has been demonstrated to elicit a profound conditioning effect on neurite growth 7 days, but not 1 day following conditioning (Udina et al., 2008). To determine the minimum period required for CES to elicit a conditioning effect, the sciatic nerve of *Thy-1-GFP* Sprague Dawley rats received 1 hour of CES to the sciatic nerve. The L4/L5 DRGs were collected 7 days, 5 days, 3 days, or 1 day after conditioning (n=6/cohort) to be cultured for 48 hours. The average neurite extension and average length of the longest neurite were quantified, normalized and compared to unconditioned DRGs. Replicate *in vitro* experiments revealed latency periods ranging from 3 to 7 days promoted similar neurite outgrowth and primary neurite extension (Figure 3.5.2). Control (naive) DRG neurons reported an average total neurite extension of 542.2 µm ± 181.4 µm, and an average length of longest neurite of 194.7 µm ± 37 µm. Outgrowth of CES-administered DRG neurons was thereby normalized to the respective control of each replicate experiment. CES latency periods of 1 day revealed no significant differences in either average neurite extension (167% ± 23.1% of control ($p>0.05$)), or average length of longest neurite, as previously reported in Udina et al (2008) (125% ± 15.4% of control ($p>0.05$)). Also consistent with previous literature, a CES latency period of 7 days was sufficient for the pro-regenerative effects to increase neurite extension; average total neurite extension increased to 271.3% ± 38.9% of control, and the average length of the longest neurite increased to 211.9% ± 32.6% of control (*$p<0.05$; **$p<0.01$). Latency periods of 3 and 5 days have not previously been reported. At 3 days, average total neurite extension increased to 308.7% ±71.9%% of control (**$p<0.01$), and the

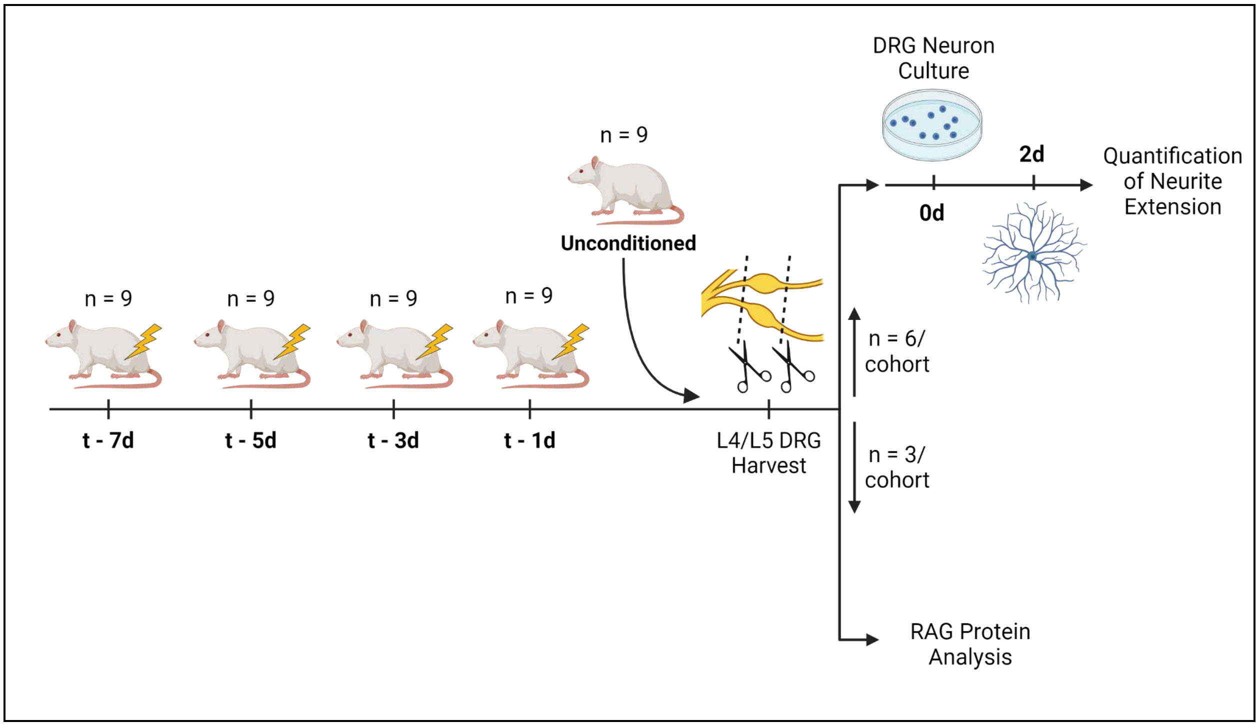

Figure 3.3.1 Experimental design to determine latency period of *in vitro* conditioning effect and *in vivo* RAG expression.

average length of the longest neurite increased to 190.3% ± 20.4% of control (**p*<0.05). At 5 days, average total neurite extension increased to 316% ± 39.2% of control (**p*<0.05) and the average length of the longest neurite increased to 242.9% ± 62.2% of control (****p*<0.001).

3.3.2 CES upregulates RAGs between 1 and 3 days post-conditioning.

CES has been previously shown to upregulate RAGs 3 days following stimulation (Senger et al., 2018; 2019; 2020) including BDNF, GFAP and pCREB. To determine the timeline of RAG upregulation, *Thy-1-GFP* Sprague Dawley rats received 1 hour of CES to the sciatic nerve, and 7 days, 5 days, 3 days or 1 day following conditioning, animals were euthanized, and L4/L5 DRGs were harvested (n=3/cohort). DRGs were sectioned for immunohistological

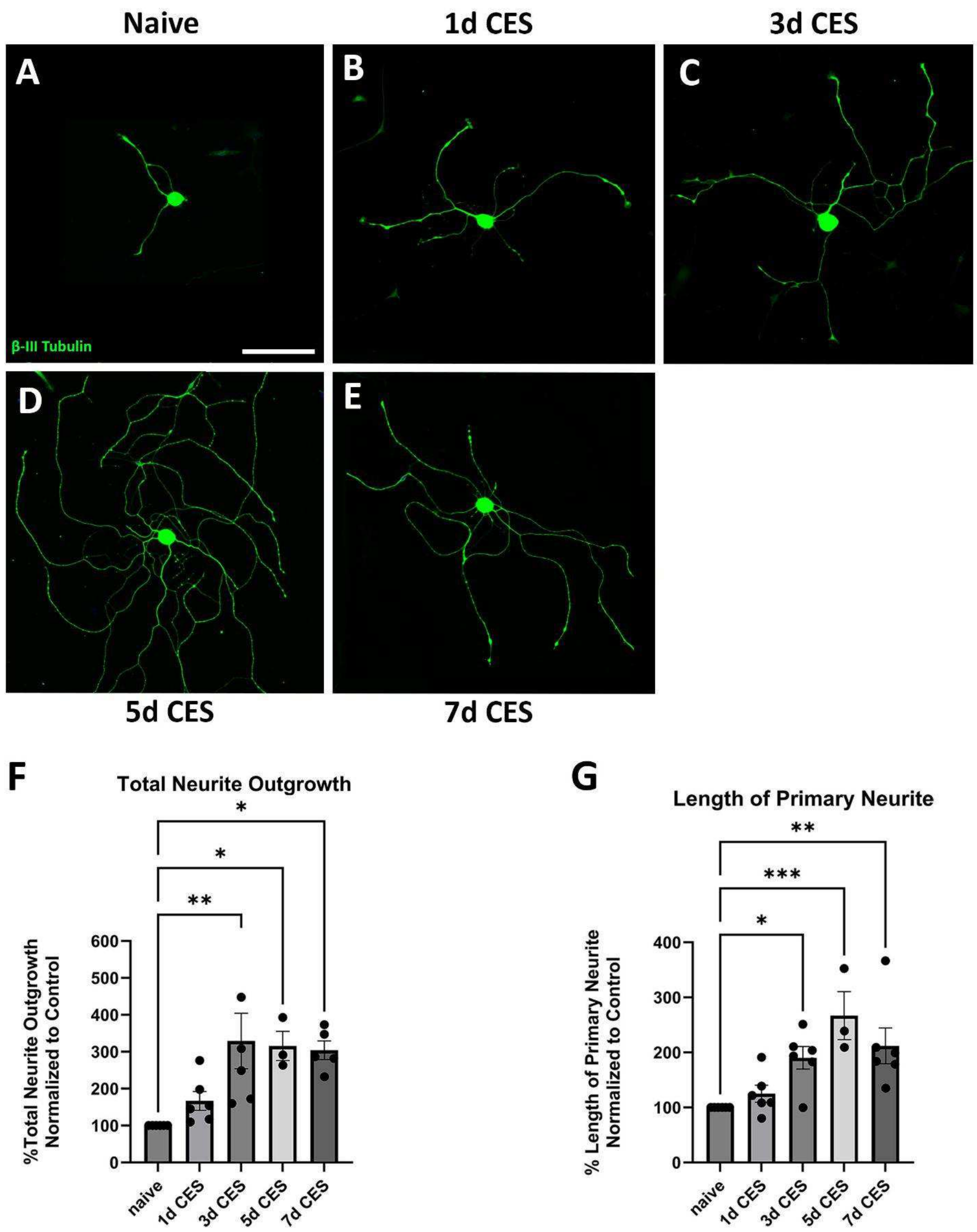

Figure 3.3.2 Latency periods between 3 and 7 days are sufficient for CES to upregulate neurite extension *in vitro*. (A-E) β-III tubulin immunostained 48 hour cultured DRG neurons *in vitro* either (A) unconditioned, or conditioned with latency periods of (B) 1 day (n=6), (C) 3 days (n=6), (D) 5 days (n=3), or (E) 7 days (n=6). (F-G) Latency periods of 3, 5, and 7 days promoted total average neurite outgrowth (*$p<0.05$; **$p<0.01$; *$p<0.05$) and average extension of primary neurites (*$p<0.05$; ***$p<0.001$; **$p<0.01$). Scale bar in A indicates a length of 100μm.

analysis. DRG demonstrated consistent upregulation of RAGs either 1 day or 3 days post-conditioning, persisting until at least 7 days post-conditioning (Figure 3.5.3). At timepoints of 3, 5, and 7 days post-conditioning, DRGs demonstrated increased cytosolic expression of BDNF (13.1 a.u. ± 0.85 a.u. $^{**}p<0.01$; 14.06 a.u. ± 0.9 a.u. $^{***}p<0.001$; 12.57 a.u. ± 0.3 a.u. $^{**}p<0.01$) compared to the baseline expression of BDNF in unconditioned DRGs (7.93 a.u. ± 0.84 a.u.). One day post-conditioning appeared to trend upwards, but was not significantly different compared to unconditioned DRGs (10.14 a.u. ± 0.85 a.u. $p>0.05$) (Figure 3.5.3). Immunohistochemical analysis of pCREB demonstrated an increase of pCREB expressing DRG neurons between 1 and 7 days post-conditioning compared to unconditioned DRG.One day post-conditioning increased the proportion of pCREB positive neurons to 56.1% ± 3.9% compared to 16.8% ± 5.8% in unconditioned DRG ($^{**}p<0.01$). At 3, 5 and 7 days post-conditioning, the proportion of pCREB positive neurons were maintained (55.5% ± 3.1% $^{**}p<0.01$; 55.1% ± 3.% $^{**}p<0.01$; 56.6% ± 6.5% $^{**}p<0.01$). Similarly, 1 day post-conditioning increased GFAP expression in SCGs surrounding neuronal cell bodies; the proportion of GFAP positive SCGs coupled to DRG neurons increased from 9% ± 0.5% to 23.9% ± 2.9% compared to unconditioned (naive) DRG ($^{*}p<0.05$). GFAP expression in surrounding SCGs remains upregulated at 3 and 7 days post-conditioning (24.4% ± 3.3% $^{*}p<0.05$; 25.4% ± 2.1% $^{*}p<0.05$). At 5 days post-conditioning, GFAP expression decreased to 21.2% ± 5.9% and was not significantly different from naive ($p>0.05$) (Figure 3.3.3).

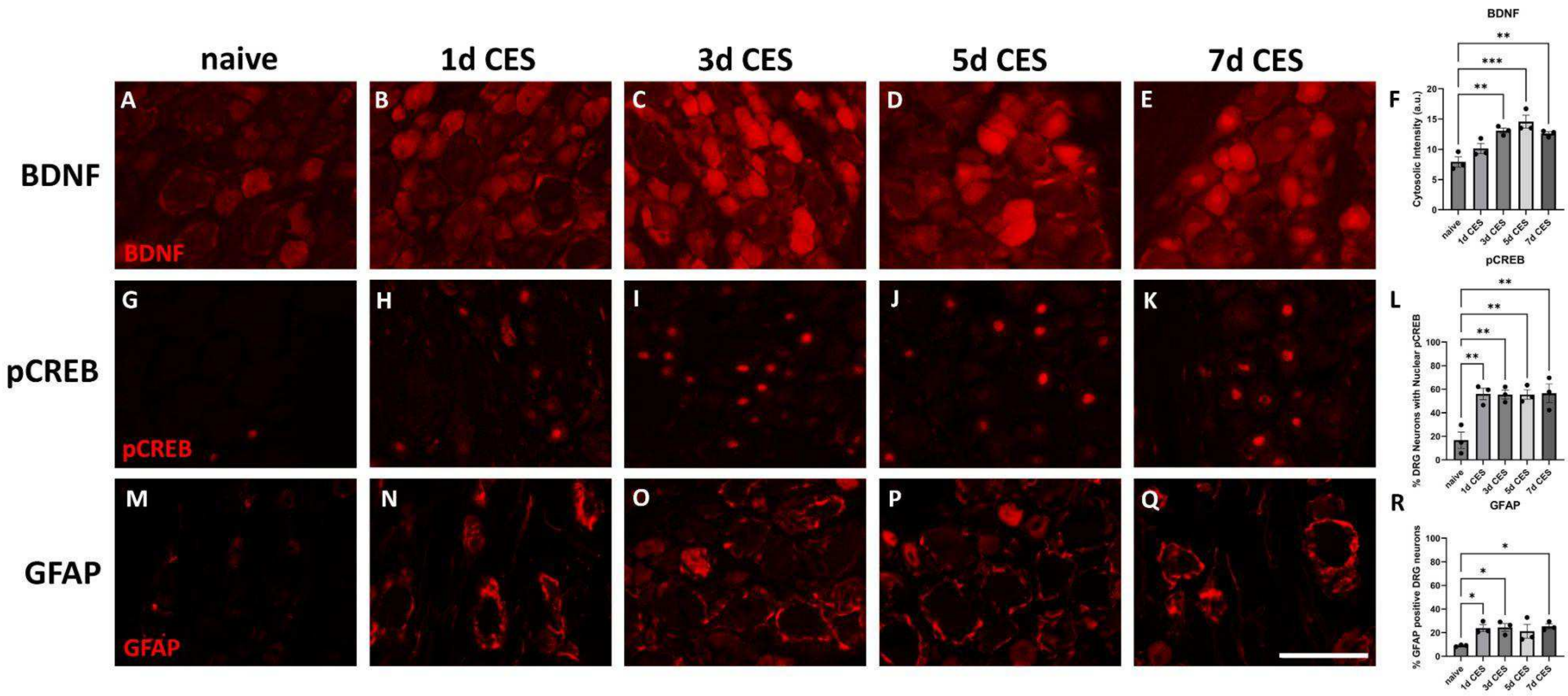
naive
1d CES
3d CES
5d CES
7d CES
BDNF
pCREB
GFAP
A
B
C
D
E
F
G
H
I
J
K
L
M
N
O
P
Q
R
BDNF
Cytosolic Intensity (a.u.)
pCREB
% DRG Neurons with Nuclear pCREB
GFAP
% GFAP positive DRG neurons

Figure 3.3.3 CES upregulates RAGs between 1 and 3 days post-conditioning, and are maintained until at least 7 days post-conditioning. (A-E) BDNF immunofluorescence of unconditioned DRG cell bodies (n=3) (A), or conditioned with CES 1 day (n=3) (B), 3 days (n=3) (C), 5 days (n=4) (D), or 7 days prior (n=3) (E). BDNF cytosolic intensity in arbitrary units (a.u.) increases 3 days, 5 days and 7 days post-conditioning (**p<0.01; ***p<0.001; **p<0.01) (F). (G-K) pCREB immunofluorescence of DRG cell bodies left unconditioned (n=3) (G), or conditioned with CES 1 day (n=3) (H), 3 days (n=3) (I), 5 days (n=4) (J), or 7 days prior (K). The proportion of pCREB positive nuclei in DRG neurons increases 1 day, 3 days, 5 days, and 7 days post-conditioning (**p<0.01; **p<0.01;**p<0.01; **p<0.01; **p<0.01) (L). (M-Q) GFAP immunofluorescence of SCGs surrounding DRG cell bodies left unconditioned (n=3) (M), or conditioned with CES 1 day (n=3) (N), 3 days (n=3) (O), 5 days (n=4) (P), or 7 days prior (n=3) (Q). The proportion of DRG neurons surrounded by GFAP positive SCGs increased at 1 day, 3 days, and 7 days post-conditioning. An increase was observed at 5 days post-conditioning, but was not significant (R). The scale bar in Q indicates a length of 100μm.

3.3.3 Increasing the duration CES promotes regeneration in a stepwise manner with optimal regeneration elicited with 1 hour in NF200+ and CGRP+ axons.

To determine the optimal duration of CES required to elicit pro-regenerative effects, Sprague Dawley rats received 1 hour, 30 minutes, or 10 minutes of CES, or no CES (n=4/cohort). Seven days after conditioning, animals underwent a tibial nerve transection and repair. Animals were left to recover for 7 more days before they were euthanized and the tibial

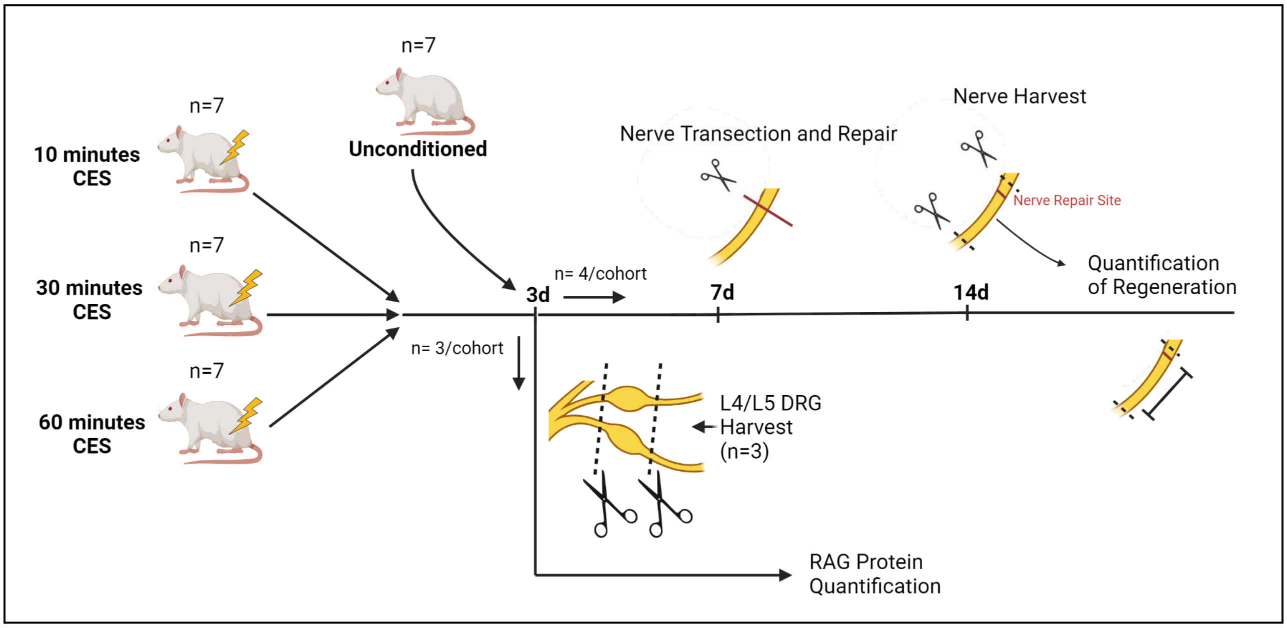

Figure 3.3.4 Experimental design to determine the minimum duration of CES required to promote regeneration and RAG protein expression in DRG neurons.

nerves were harvested for nerve regeneration analysis. As regenerating and degenerating axons have different morphologies, neurofilament 200 (NF200) labeling allowed for quantification of axons regenerating past the coaptation site (Figure 3.5.2; Figure 3.5.3). One hour of CES served as the positive control, as 1 hour has been previously determined to significantly increase the regeneration of axons following sciatic nerve injury (Senger et al., 2018b), while unconditioned animals were the control group.

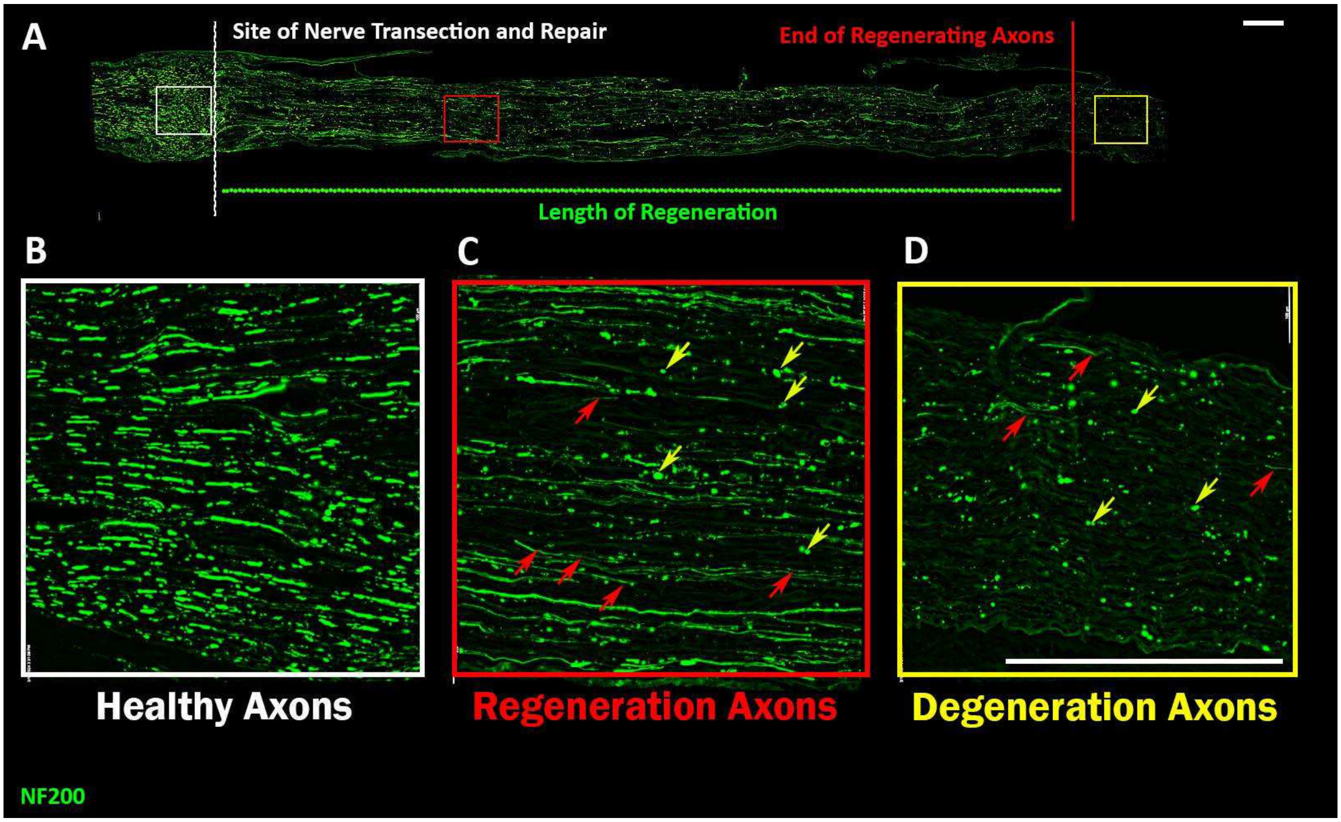

Figure 3.3.5 Distinguishing between regenerating and degenerating axons in a longitudinal section of tibial nerve repair. (A) NF200 immunofluorescence on longitudinal tibial nerve sections depict nerve repair site from which healthy axons transition to regenerating axons. The site of the end of regeneration is identified and marked as the site from which less than 10 regenerating axons remain. The distance between these points is identified as the extent of regeneration. Scale in A indicates length of 0.5mm. (B-D) Morphology of healthy (B), regenerating (C), and degenerating (D) axons are depicted. Red arrows indicate regenerating axons. Yellow arrows indicate degenerating axons. Scale bar in D indicates a length of 0.5mm for images (B-D).

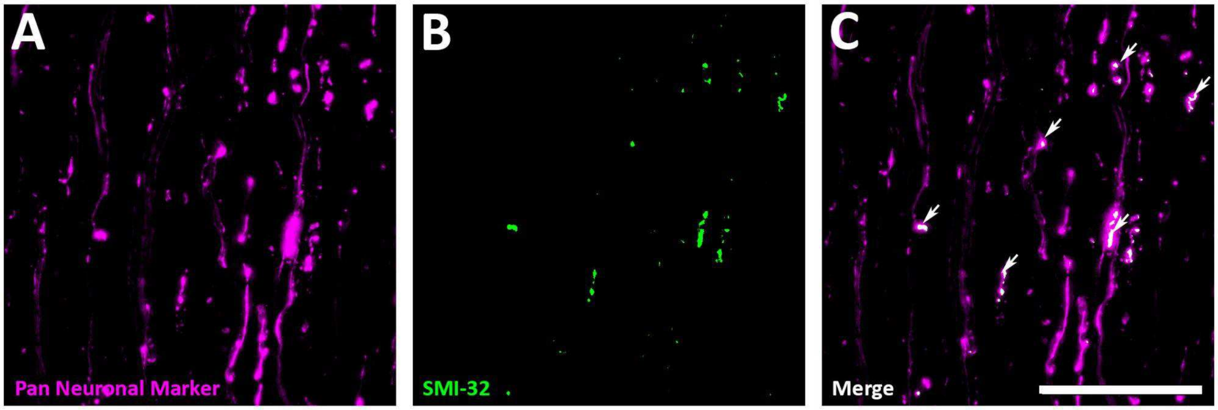

Figure 3.3.6 Confirming morphology of degenerating axons. (A) Pan-neuronal marker immunofluorescence of regenerating and degenerating axons, (B) SMI-32 immunofluorescence of degenerating axons, and (C) merge. Arrows in C indicate overlap between (A) and (B). Scale bar in C indicates a length of 0.1mm.

One hour of CES was determined to significantly increase regeneration of NF200+ fibers compared to 10 minutes of CES and unconditioned cohorts (8.6mm ± 0.4 mm; 4.3 mm ± 1.0 mm ***p<0.001; 3.3 mm ± 1.3 mm **p<0.01). Thirty minutes of CES significantly increases regeneration compared to unconditioned (6.3 mm ± 1.0 mm; 3.3 mm ± 1.3 mm; *p<0.05), but not 10 minutes of CES. Numbers of regenerating axons were also assessed at just proximal to the site of nerve repair, and every 0.5 mm following the nerve repair until less than 10 regenerating axons remained. Durations of 10 minutes and 1 hour significantly increased the number of axons crossing the site of nerve repair (100 axons ± 26 axons **p<0.01; 101 axons ± 16 axons**p<0.01) compared to unconditioned nerve (66 axons ± 14 axons). Thirty minutes of CES had increased axon counts 1 mm distal to the nerve repair site, and both 1 hour and 30 minute durations of CES promoted the number of regenerating axons until the end of regeneration (significance of at least p<0.05). Ten minutes of CES promoted axon extension over the nerve

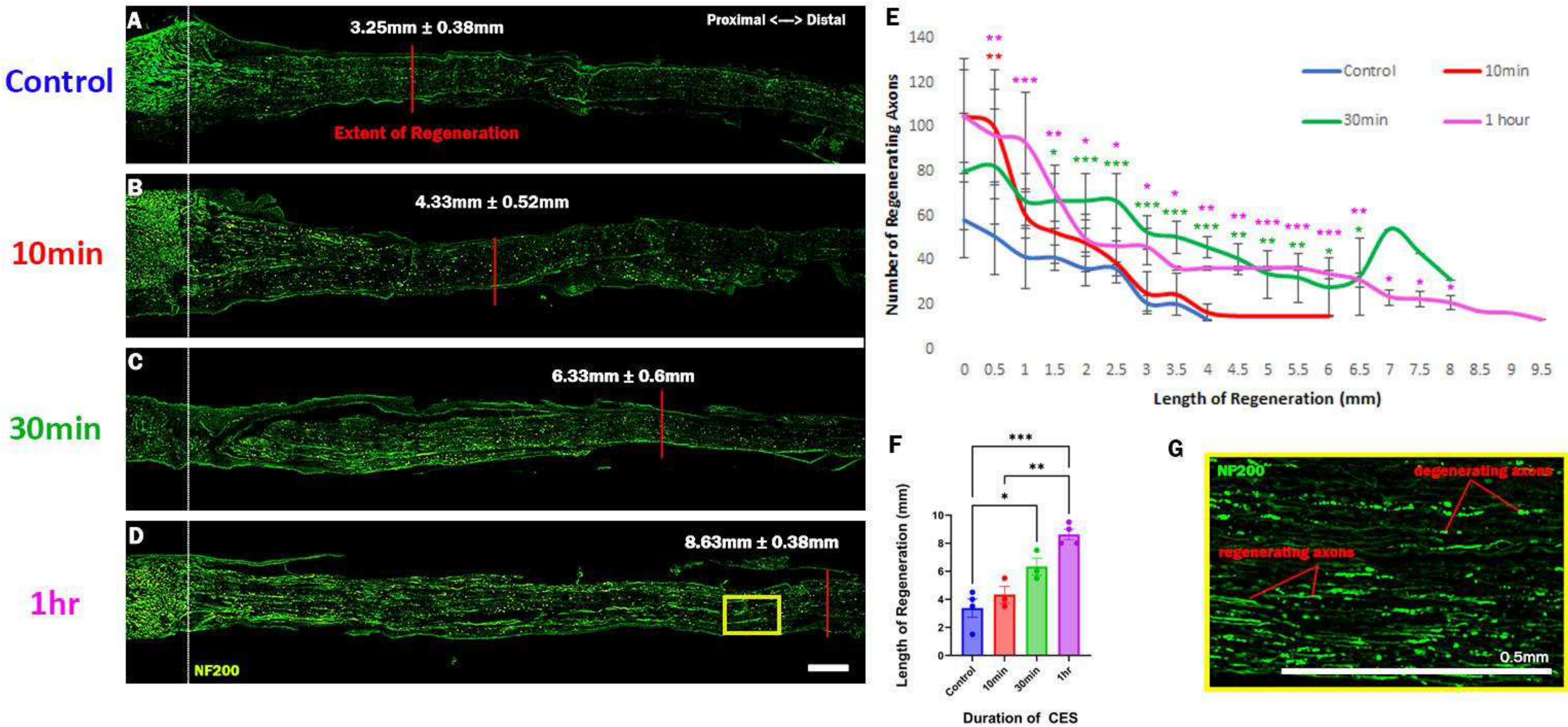
Control
10min
30min
1hr
A
3.25mm ± 0.38mm
Proximal <—> Distal
Extent of Regeneration
B
4.33mm ± 0.52mm
C
6.33mm ± 0.6mm
D
8.63mm ± 0.38mm
NF200
E
Number of Regenerating Axons
Length of Regeneration (mm)
Control
10min
30min
1 hour
F
Length of Regeneration (mm)
Duration of CES
Control
10min
30min
1hr
G
NF200
degenerating axons
regenerating axons
0.5mm

Figure 3.3.7 Regeneration of NF200+ fibers following nerve repair increases incrementally as the duration of CES increases. (A-D) NF200 immunofluorescence on longitudinal tibial nerve sections depict nerves left unconditioned (n=4) (A), nerves conditioned for 10 minutes (n=3) (B), nerves conditioned for 30 minutes (n=3) (C), and nerves conditioned for 1 hour of CES (n=4) (D). White lines indicate the site of surgical repair. Red lines indicate the length at which less than 10 axons were counted. (E) Axon counts beginning at the nerve transection site, and quantified every 0.5mm until the end of regeneration. Statistical significance at each 0.5mm length where the number of axon counts of CES animals were different than the unconditioned axon counts is indicated on the graph (*$p<0.05$, **$p<0.01$, ***$p<0.001$). (F) Durations of 1 hour and 30 minutes of CES promote regeneration of NF200+ fibers compared to unconditioned, but not 10 minutes of CES. (G) Depiction of regeneration and degenerating axons within a longitudinal nerve section. The scale bar in D indicates a length of 0.5mm

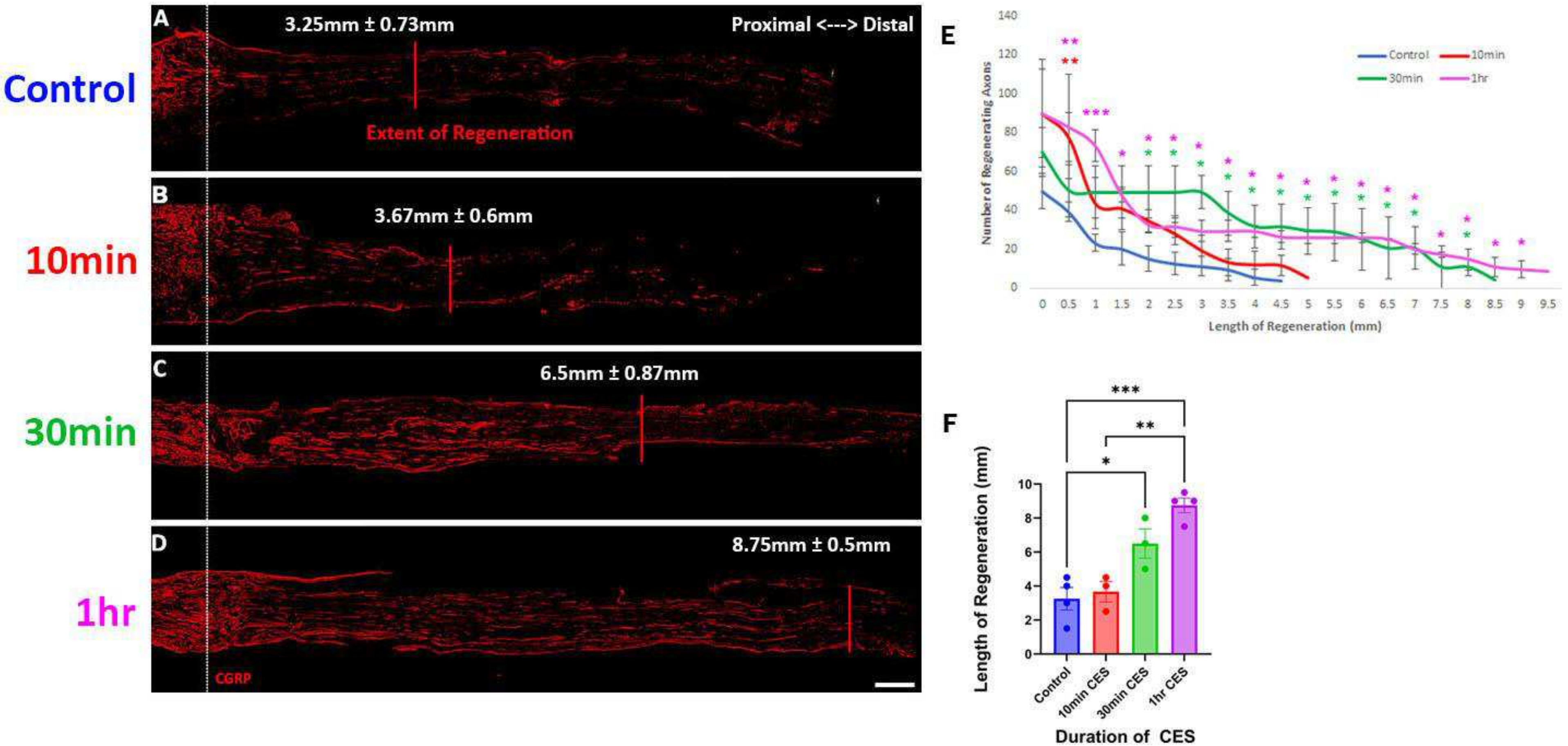

Control
10min
30min
1hr
A
3.25mm ± 0.73mm
Proximal <---> Distal
Extent of Regeneration
B
3.67mm ± 0.6mm
C
6.5mm ± 0.87mm
D
8.75mm ± 0.5mm
CGRP
E
Number of Regenerating Axons
Length of Regeneration (mm)
Control
10min
30min
1hr
F
Length of Regeneration (mm)
Control
10min CES
30min CES
1hr CES
Duration of CES

Figure 3.3.8 Regeneration of CGRP+ fibers following nerve repair increases incrementally as the duration of CES increases. (A-D) CGRP immunofluorescence on longitudinal tibial nerve sections depict nerves left unconditioned (n=4) (A), nerves conditioned with 10 minutes (n=3) (B), nerves conditioned with 30 minutes (n=3) (C), and nerves conditioned with 1 hour of CES (n=4) (D). White lines indicate the site of surgical repair. Red lines indicate the length at which less than 10 axons were counted. (E) Axon counts beginning at the nerve transection site, and quantified distally every 0.5mm until the end of regeneration. Statistical significance at each 0.5mm length where the number of axon counts of CES animals were different than the unconditioned axon counts is indicated on the graph (*$p<0.05$; **$p<0.01$; ***$p<0.001$). (F) Durations of 1 hour and 30 minutes of CES promote regeneration of CGRP+ fibers compared to unconditioned, but not 10 minutes of CES. The scale bar in D indicates a length of 0.5mm.

repair site, but did not increase the number of regenerating axons past the transection site (*p*>0.05).

Similarly, the length of 1 hour of CES significantly increased regeneration of calcitonin gene related peptide (CGRP)+ fibers compared to 10 minutes of CES and unconditioned cohorts (8.8 mm ± 0.5 mm; 3.7 mm ± 0.6 mm $^{**}p<0.01$; 3.3 mm ± 0.7 mm $^{***}p<0.001$). Thirty minutes of CES significantly increases regeneration compared to unconditioned (6.5 mm ± 0.9 mm; 3. 5mm ± 0.7 mm $^{*}p<0.05$), but not 10 minutes of CES. Durations of 10 minutes and 1 hour significantly increased the number of axons crossing the site of nerve repair (78 axons ± 23 axons $^{**}p<0.01$; 83 axons ± 28 axons $^{**}p<0.01$) compared to unconditioned nerve (39 axons ± 9 axons). Starting at 1.5mm distal from the nerve repair site, 30 minutes of CES increased the number of regenerating axons until the end of regeneration. A paired t-test conducted to compare NF200+ and CGRP+ fiber length of regeneration revealed no significant difference between regeneration at each duration of CES ($p>0.05$).

3.3.4 RAG expression increases as the duration of stimulation increases.

To further investigate the optimal duration of CES administration to elicit pro -regenerative effects, *Thy-1-GFP* Sprague Dawley rats were conditioned with 0, 10, 30, or 60 CES, and euthanized 3 days post-conditioning. L4/L5 DRGs were harvested (n=3/cohort), and processed for RAG immunohistochemical analysis. As the duration of CES increased, the expression of BDNF, pCREB, and GFAP increased (Figure 3.5.7). Cytosolic expression of BDNF increases from a baseline of 3.6 a.u. ± 1.4 a.u. to 8.0 a.u. ± 0.5 a.u. with 60 minutes of CES ($^{*}p<0.05$). Ten minutes and 30 minutes of CES was insufficient to promote BDNF expression (3.7 a.u. ± 0.1 a.u. $p>0.05$; 4.9 a.u. ± 0.4 a.u. $p>0.05$). Thirty minutes and 60 minutes

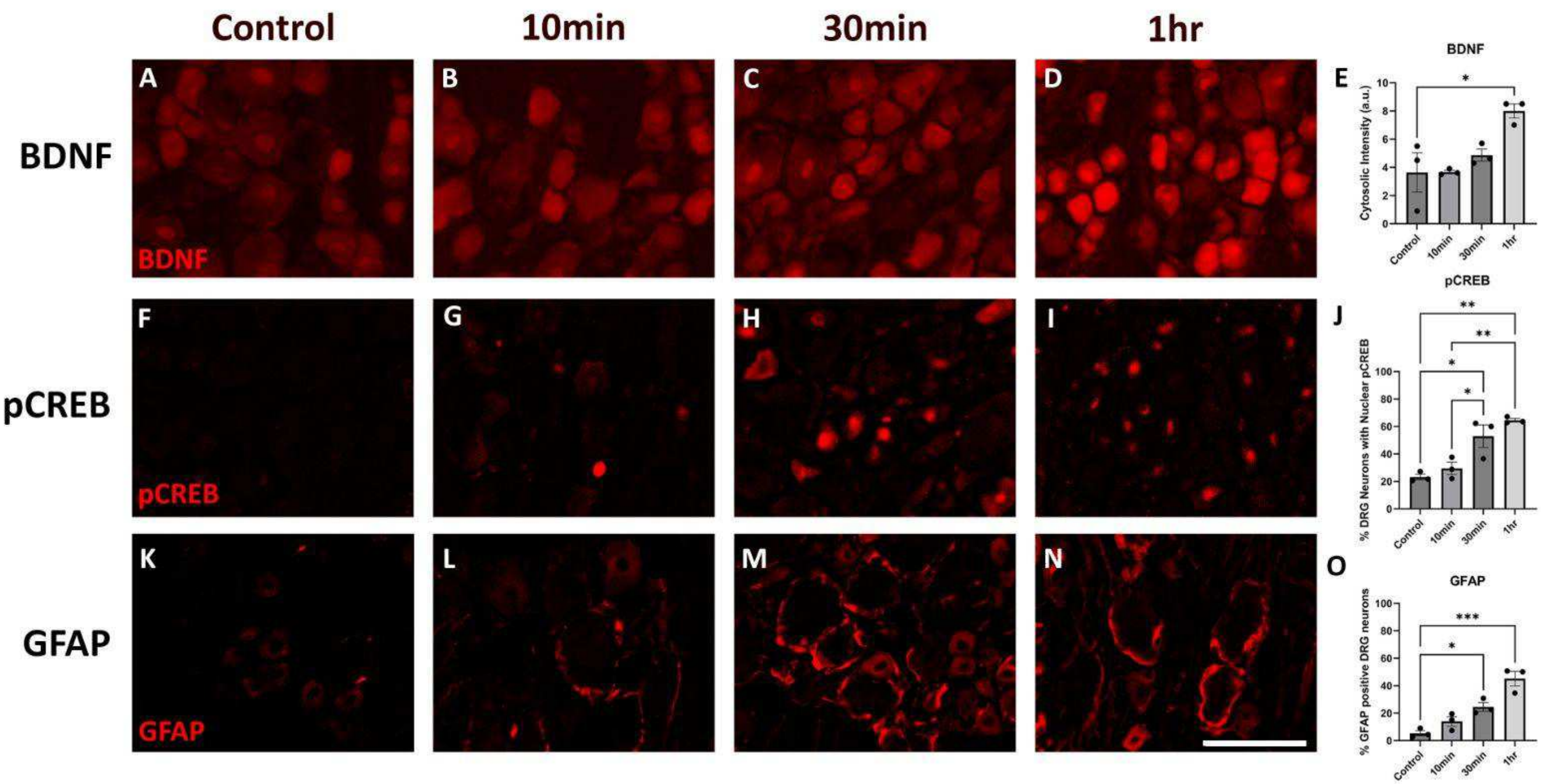

Control
10min
30min
1hr
BDNF
pCREB
GFAP
A
B
C
D
E
F
G
H
I
J
K
L
M
N
O
BDNF
pCREB
GFAP
BDNF
Cytosolic Intensity (a.u.)
pCREB
% DRG Neurons with Nuclear pCREB
GFAP
% GFAP positive DRG neurons
Control
10min
30min
1hr

Figure 3.3.9 CES requires a duration of between 30 and 60 minutes to upregulate RAG proteins in DRG neurons 3 days post-conditioning. (A-D) BDNF immunofluorescence in arbitrary units in DRG cell bodies left unconditioned (n=3) (A), or conditioned with CES for 10 minutes (n=3) (B), 30 minutes (n=3) (C), or 1 hour (n=3) (D). 1 hour of CES significantly increases BDNF cytosolic intensity (a.u.) in DRG neurons 3 days post-conditioning (*p<0.05) (E). (F-I) pCREB immunofluorescence of DRG neurons left unconditioned (n=3) (F), or conditioned for 10 minutes (n=3) (G), 30 minutes (n=3) (H), or 1 hour (n=3) (I). 30 minutes and 1 hour of CES significantly increase the proportion of DRG neurons with nuclear pCREB expression 3 days post-conditioning (*p<0.05; **p<0.01) (J). GFAP immunofluorescence in DRG neurons left unconditioned (n=3) (K), or conditioned with CES for 10 minutes (n=3) (L), 30 minutes (n=3) (M), or 1 hour (n=3) (N). 30 minutes and 1 hour of CES significantly increase the proportion of DRG neurons surrounded by GFAP positive SCGs ((*p<0.05; ***p<0.001) (O). Scale bar in N indicates a length of 100μm.

of CES was sufficient to increase the proportion of DRG neurons with nuclear pCREB expression compared to 23.2% ± 2.1% of unconditioned (naive) DRGs (52.9% ± 8.2% *$p<0.05$; 64.5% ± 1.3% **$p<0.01$) and 29.2% ± 4.5% of DRGs stimulated only 10 minutes (*$p<0.05$; **$p<0.01$). Though 10 minutes of CES appeared to increase compared to unconditioned DRGs, the difference was not significant ($p>0.05$). GFAP expression in SCGs coupled to neuronal cell bodies increased after durations of 10, 30 and 60 minutes; the proportion of DRG neurons coupled to GFAP positive SCGs increased to 25.8% ± 3.2% (*$p<0.05$) and 45.1% ± 5.3% (***$p<0.001$) in 30 minute and 60 minute durations of CES respectively. Unconditioned DRGs featured a baseline proportion of DRG neurons associated with GFAP expressing SCGs of 5.3% ± 1.9%, and 10 minutes of CES revealed an average proportion of 14% ± 3.5% ($p>0.05$) (Figure 3.5.7).

3.3.5 The SD-9 Grass Stimulator and Checkpoint Stimulator deliver CES and promote regeneration to the same extent when 1 hour of CES is administered.

Traditionally, CES has been performed using a Grass SD-9 Stimulator (Senger et al., 2018b). To determine if the Checkpoint Stimulator delivers CES and promotes regeneration akin to the SD-9 stimulator, the tibial nerve was stimulated for 1 hour or 10 minutes and compared to unconditioned nerve. Seven days after conditioning, animals underwent a tibial nerve transection and repair. Animals were left to recover for 7 days before they were euthanized and the tibial nerves were harvested for nerve regeneration analysis. One hour of stimulation delivered by the Checkpoint stimulator promoted regeneration compared to unconditioned nerve (7.0 mm ± 0.5 mm; 3.3 mm ± 0.4 mm, ***$p<0.001$), nerve conditioned for 10 minutes with the Checkpoint stimulator (4.5 mm ± 0.5 mm, **$p< 0.01$), and nerve conditioned for 10 minutes with the SD-9

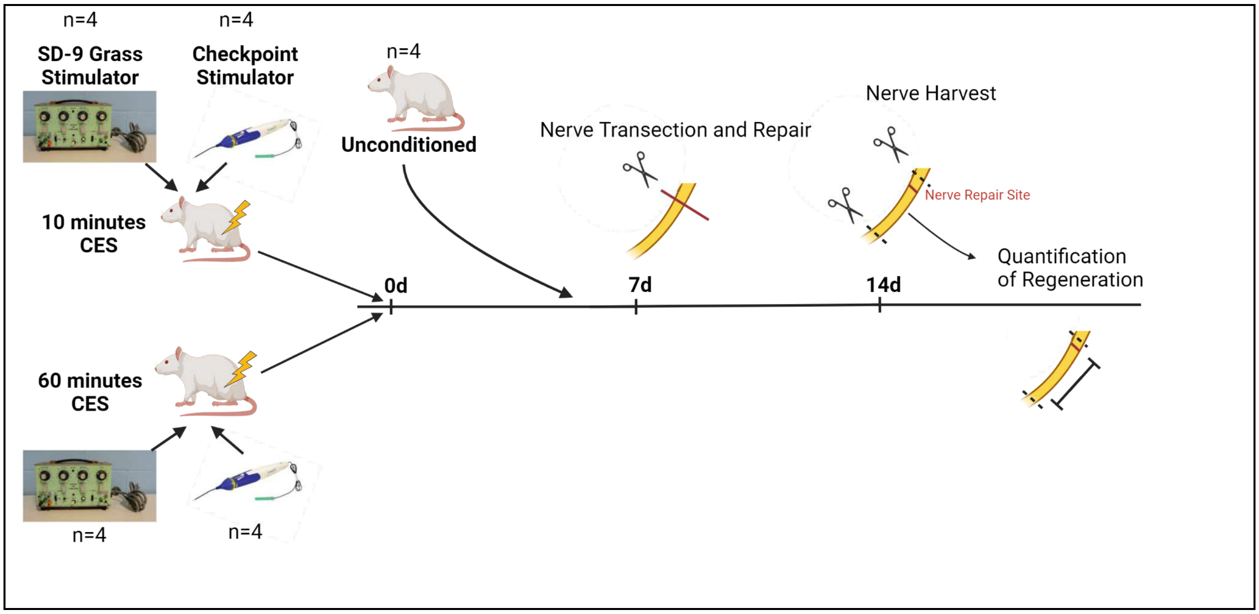

Figure 3.3.10 Experimental design to investigate the validity of the Checkpoint stimulator to deliver CES in comparison with the SD-9 Grass Stimulator.

stimulator (4.3 mm ± 0.5 mm, $^{**}p<0.01$). One hour of stimulation delivered by SD-9 stimulator promoted regeneration compared to nerve conditioned for 10 minutes with Checkpoint stimulator (8.6 mm ± 0.4 mm; 4.6 mm ± 0.5 mm, $^{**}p<0.01$), but not nerve conditioned for 1 hour with the Checkpoint stimulator (8.6 mm ± 0.4 mm; 7.0 mm ± 0.5 mm $p>0.05$). Administering CES with Checkpoint for both 10 minutes and 1 hour promoted axon extension across the site of nerve repair (96 axons ± 17 axons $^{**}p<0.01$; 118 axons ± 10 axons $^{***}p<0.001$) compared to unconditioned nerve (66 ± 14 axons). Ten minutes of CES promoted the number of regenerating axons until 1.5mm distal to the nerve repair site. One hour of CES promoted the number of regenerating axons from 4mm until the end of regeneration.

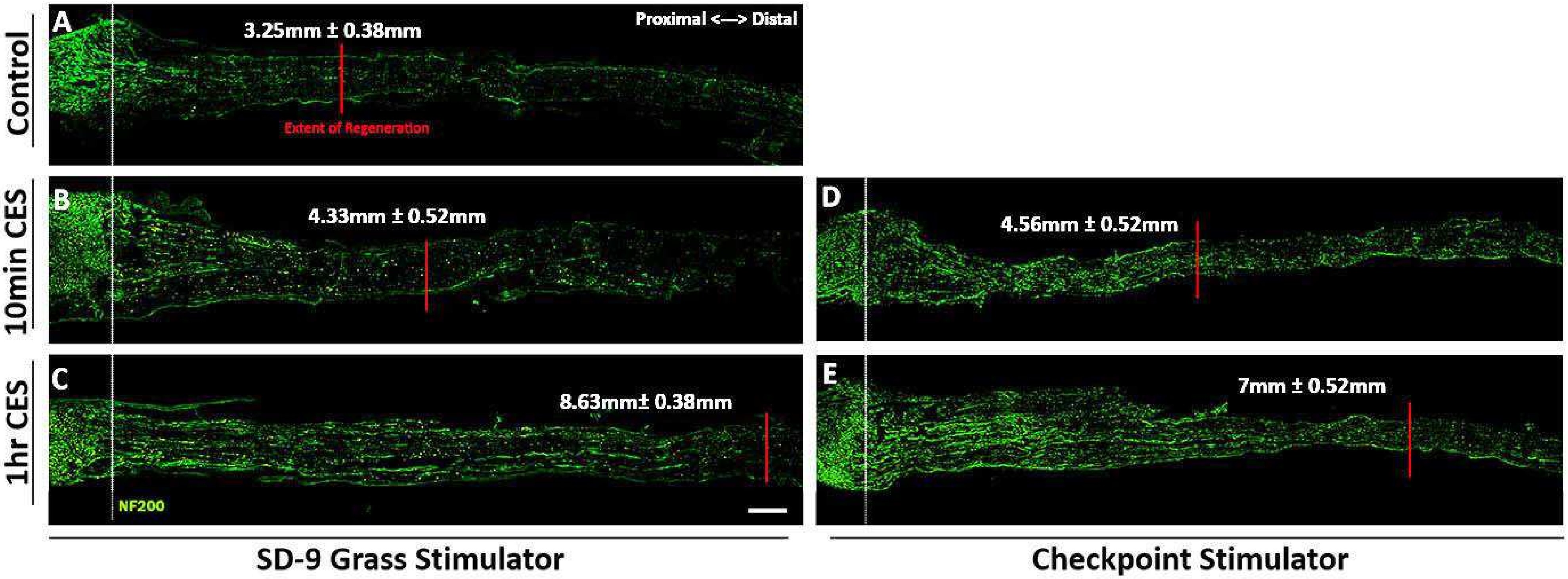
Control
10min CES
1hr CES
A
Proximal <—> Distal
3.25mm ± 0.38mm
Extent of Regeneration
B
4.33mm ± 0.52mm
C
8.63mm± 0.38mm
NF200
D
4.56mm ± 0.52mm
E
7mm ± 0.52mm
SD-9 Grass Stimulator
Checkpoint Stimulator

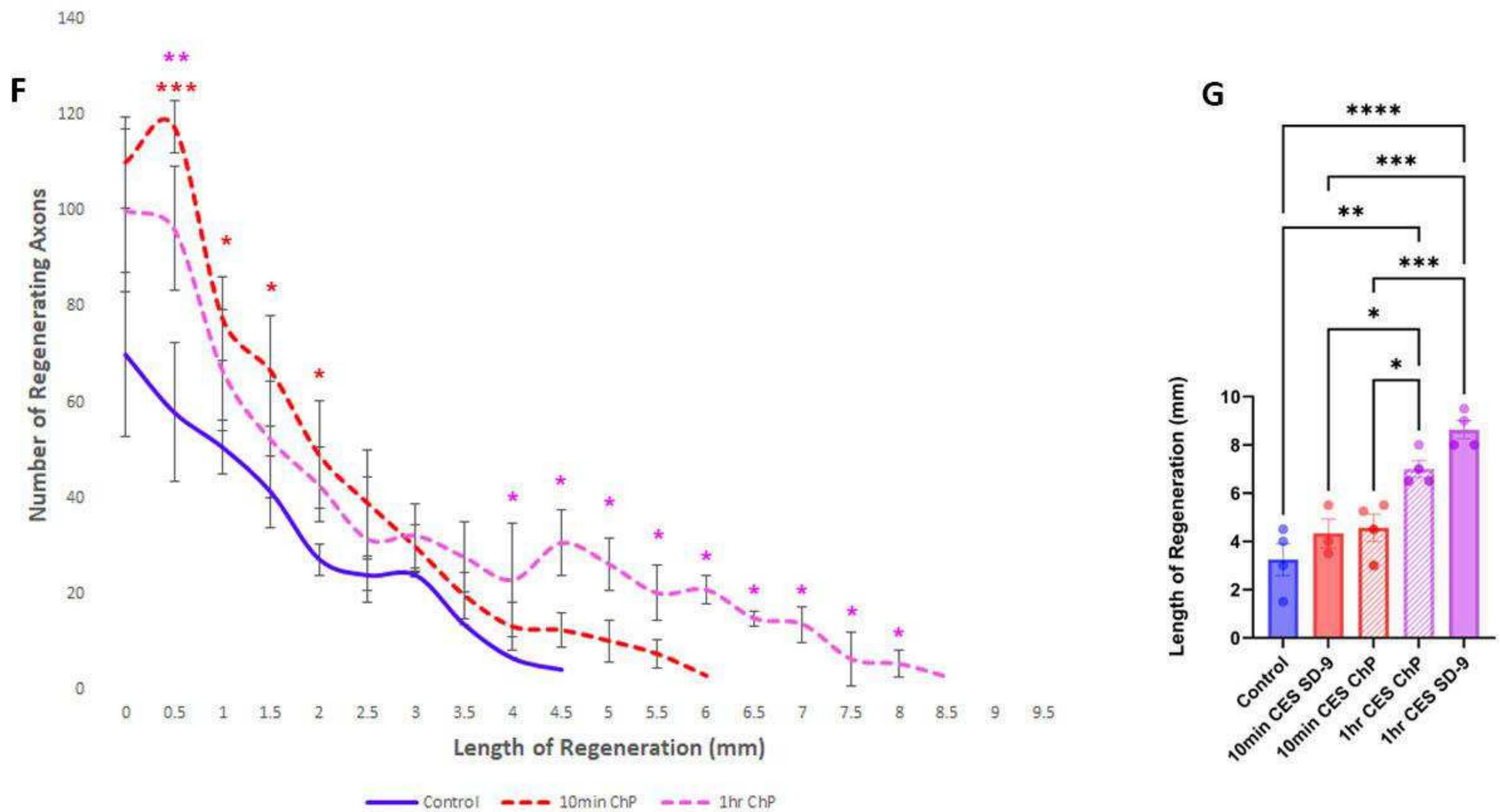

F
140
120
100
80
60
40
20
0
Number of Regenerating Axons
**
***
*
0
0.5
1
1.5
2
2.5
3
3.5
4
4.5
5
5.5
6
6.5
7
7.5
8
8.5
9
9.5
Length of Regeneration (mm)
Control
10min ChP
1hr ChP
G
****
***
**
*
Length of Regeneration (mm)
10
8
6
4
2
0
Control
10min CES SD-9
10min CES ChP
1hr CES ChP
1hr CES SD-9

Figure 3.3.11 CES administered with either an SD-9 Grass Stimulator or Checkpoint Stimulator promotes regeneration to the same extent when delivered for 1 hour, but not 10 minutes. (A-E) NF200 immunofluorescence on longitudinal tibial nerve sections depict nerves left unconditioned (n=4) (A), nerves conditioned with 10 minutes using the SD-9 stimulator (n=3) (B), nerves conditioned with 1 hour using the SD-9 stimulator (n=4) (C), nerves conditioned with 10 minutes using the Checkpoint stimulator (n=4) (D), and nerves conditioned with 1 hour using the Checkpoint stimulator (n=4). White lines indicate the site of surgical repair. Red lines indicate the length at which less than 10 axons were counted. (F) Axon counts of Checkpoint stimulated nerve beginning at the nerve transection site, and quantified distally every 0.5mm until the end of regeneration. Statistical significance at each 0.5mm length where the number of axon counts of CES animals were different than the unconditioned axon counts is indicated on the graph (*$p<0.05$; **$p<0.01$; ***$p<0.001$; ***$p<0.001$). (G) Duration of 1 hour of CES using either stimulator promotes regeneration of NF200+ fibers compared to unconditioned, but not a duration of 10 minutes using either stimulator. The scale bar in C indicates a length of 0.5mm.

3.4 Discussion

3.4.1 RAG protein expression precedes the conditioning effect of CES

Our data demonstrates that cultured DRG neurons treated with CES *in vivo* for 3-7 days promote total neurite outgrowth and the length of the longest neurite. A latency period of 1 day CES was insufficient to influence neurite extension compared to naive, unconditioned DRGs. This suggests CES requires a 3-day period to upregulate key pathways *in vivo* before cytoskeletal component transport and assembly are sufficiently accelerated at the site of the growth cone. This increased regenerative capacity is sustained at 5 and 7 days post-conditioning, suggesting that CES induces a lasting mechanistic change beginning 3 days post-conditioning and persisting until at least 7 days post-conditioning *in vitro*. Analysis of protein expression of RAGs at these time points supports the timeline of regenerative capacity; BDNF and pCREB expressing DRG neurons and GFAP positive SCGs surrounding neurons increase between 1 and 3 days post-conditioning. The upregulation of RAG proteins, potentially part of the mechanism of CES, precedes the onset of its pro-regenerative effects, and both BDNF and pCREB have been previously implicated in the mechanism of CES (Yan et al., 2014). The upregulation of both pCREB and BDNF may suggest the involvement of the cAMP pathway, as cAMP is also shown to upregulate in DRG neurons 1 day post-conditioning, preceding the pro-regenerative effects of CES (Udina et al., 2008). CES-induced BDNF expression is also dependent on ERK1/2 signaling (Yan et al., 2014). GFAP thus far has not been directly implicated in the mechanism of CES, but serves as a marker of SGC activation to indicate a regenerative phenotype of glial cells in the DRG (Hanani et al., 2020). Regardless, the upregulation of RAGs precedes the earliest emergence of the conditioning effect.

3.4.2 CES as a cumulative activation of signaling pathways

A 1 hour duration of CES administered to sciatic nerve accelerates regeneration of NF200+ fibers following a nerve repair surgery in rats, as previously demonstrated by Senger (2018; 2019; 2020b; 2022). Though existing literature suggests that 10 minutes of PES may be sufficient to improve regeneration (Aldrashan et al., 2011; Calvey et al., 2015; Foeking et al., 2012; Hetzler et al., 2008; Huang et al., 2013, 2010a; Lu et al., 2008), this does not translate to CES. My results indicate 10 minutes of CES does not produce a conditioning effect. Thirty minutes of CES improves regeneration following injury, and was not significantly different from 1 hour of CES. However, 30 minutes was not statistically different from 10 minutes of CES. This suggests that though 30 minutes produces a conditioning effect, it is unclear whether or not 30 minutes promotes regeneration to the same extent as 1 hour. Rather, it is likely that as duration increases, the pro-regenerative effects of CES also increases incrementally. Studies in PES suggest the pro-regenerative effects peak at a duration of 1 hour (Al-Majed et al., 2000b), and as the parameters of CES have been adopted from PES, this assumption has remained. However, it is unknown if the pro-regenerative effects peak at a duration of 1 hour, similar to PES, or if the pro-regenerative effects may continue to increase with duration. Due to limitations of clinical time, increasing the duration of CES past 1 hour would be of limited interest; however, determining if CES durations longer than 1 hour continue to promote regeneration may contribute to our understanding of its mechanism, and further differentiate CES from PES.

The conditioning effect of 1 hour of CES increases the number of regenerating axons at and beyond the repair site. Due to inhibitory scar tissue and extracellular matrix, injury sites cause a delay of regeneration. PES is known to accelerate regenerating axons across the injury site (termed staggered regeneration) to promote regeneration (Brushart et al., 2002). Conversely, CES appears to counteract the delay of regeneration by increasing the number of axons crossing the injury site. It is unknown if CES also accelerates regeneration across the injury site apart from the accelerated rate of regeneration observed outside of the injury site. Ultimately, increasing the number of axons capable of regeneration improves the likelihood of successful reinnervation and functional recovery (as demonstrated in Senger et al., 2019).

Thirty minutes of CES did not increase the number of regenerating axons crossing the nerve repair site, though it increased the number of axons distal to the nerve repair site. Post-hoc observation of tissue revealed rips that prevented complete analysis of axon regeneration at the site of nerve repair. As the effect of increased regenerating axons persists until the end of regeneration, it is likely there is also an increase across the injury site. To confirm this, analysis would need to be completed at the site of nerve repair. Without complete analysis, it is unknown whether the effect of increased regenerating axons is comparable to that of 1 hour.

Surprisingly, 10 minutes of CES promoted an increased number of axons crossing the nerve repair site, despite not affecting the length of regenerating axons. This may suggest that the promotion of the number of regenerating axons precedes the effect of CES on the length of regeneration. This data supports the idea that the pro-regenerative effects of CES accumulate incrementally; the initial effects of CES are likely the recruitment of axons to cross the inhibitory milieu that is the injury site.

As a conditioning strategy, the general mechanism of CES to promote regeneration lies in the early activation of signaling pathways and upregulation of key proteins required for regeneration. This is supported by evidence of upregulation of RAGs as early as 3 days following conditioning (Senger et al., 2018; 2019) (Figure 3.5.4). Increasing the duration of conditioning likely increases the duration of time in which the stimulated axon can signal the cell body through retrograde action potentials, activate key signaling pathways responsible for the upregulation of RAGs, and result in an increased capacity for regeneration. Thus, as the duration of stimulation increases, signaling pathway activation accumulates until a 1 hour duration has been reached; increasing the duration past 1 hour provides no benefit (Al-Majed et al., 2000b).

Regeneration trends upwards from a duration of 30 minutes to 1 hour, but no significant difference between 30 minutes and 1 hour is found in the current sample size. To reveal differences between 1 hour and 30 minutes, and 30 minutes and 10 minutes, the sample size in each cohort should be increased. As 10 minutes of CES was insufficient to upregulate BDNF, pCREB, and GFAP, the increase of regenerating axons across the nerve repair site does not correlate to the expression of these RAG proteins, unlike the length of regeneration. The increased number of axons regenerating across the nerve repair site suggests 10 minutes of CES promotes the regenerative capacity of the axons to some degree. The mechanism of which 10 minutes of CES promotes the extension of axons across the nerve repair site is unclear. It is possible that with a shorter duration of stimulation, fewer effectors are immediately recruited following stimulation, and thus pro-regenerative signaling pathways are activated less robustly. Ten minutes of CES may induce a small upregulation of RAG proteins at 3 days, and a larger sample size may reveal slight differences.

3.4.3 CES promotes length and number of regenerating axons in small sensory CGRP+ fibers

A significant limitation to the research indicating the pro-regenerative effects of CES is the population of axons visualized to assess regeneration. Traditionally, longitudinal nerve sections are stained to visualize and assess regeneration of large and medium diameter axons (NF200+), leaving out a large population of small sensory fibers, primarily nociceptive fibers. To assess sensory outcomes associated with CES, Senger (2019) conducted von Frey behavioural tests, and evaluated cutaneous reinnervation following injury. The behavioural test in particular suggests CES promotes reinnervation and recovery of nociceptive fiber function to detect noxious stimuli at the end of an 8 week recovery period following a nerve transection injury. CES was also found to promote epidermal reinnervation of sensory fibers at the end of an 8 week recovery period, though this experiment did not distinguish between low threshold mechanoreceptor and nociceptive recovery. Thus, if CES promotes reinnervation of nociceptive fibers at 8 weeks, it is likely that regeneration of small nociceptive fibers is also promoted by CES. However, this has not been previously demonstrated outside of functional measures. In addition to my assessment of large and medium diameter axons, I assessed the regeneration of a population of small peptidergic nociceptors (CGRP+) in association with CES. Similar to large and medium diameter fibers, CES promoted the regeneration of small diameter fibers with a duration of 1 hour and 30 minutes, but not 10 minutes. The regeneration of small fibers follows a similar trend, in which there is an incremental increase in regeneration as the duration of CES increases. Likewise, it is unclear if 30 minutes of CES promotes regeneration to the same extent as 1 hour, and thus an increased sample size is needed to elucidate this. Assessment of axon counts revealed a similar pattern of increasing the number of regenerating axons across the nerve repair site when stimulated for 1 hour and 10 minutes. Ten minutes was only sufficient to increase the regenerating fibers at the injury site, while 1 hour promoted the number of regenerating fibers until the end of regeneration. It is likely that 30 minutes is sufficient to increase the number of regenerating peptidergic nociceptive fibers across the injury site, similar to NF200+ fibers.

At each duration of CES, there is no significant difference in the length of regeneration between medium/large diameter fibers, and small peptidergic fibers. CES elicits the same pattern of pro-regenerative effects on both subpopulations for the length of regeneration, and the number of regenerating fibers, suggesting CES elicits a nonspecific pro-regenerative effect. However, when assessing the population of nociceptors, axon size must also be considered; peptidergic nociceptor populations overlap largely with C-fiber populations. Axon diameters of C-fibers can be as small as 0.2μm in diameter, and as unmyelinated fibers, form Remak bundles (McGlone & Reilly, 2010). Methods of immunohistochemistry to visualize regenerating C-fibers may be insufficient to distinguish between individual fibers due to imaging with limited resolution. Because C-fibers regenerate within their Remak bundles, longitudinal sections of nerve may further complicate the visualization; it is likely that multiple fibers within the Remak bundle are indistinguishable. Thus, when counting the number of regenerating peptidergic nociceptive fibers, the number of Remake bundles are quantified instead of individual fibers, potentially masking significant CES-induced increases of regenerating fibers. Additionally, this may also influence the length of regeneration of CGRP+ fibers. If individual axons are indistinguishable, the length of regeneration may continue far past our perceived limit of 10 axons. NF200+ fibers are myelinated fibers with diameters ranging from 2.5 to 20μm in diameter. Larger axon diameter increases the likelihood of adequate visualization using immunohistochemical methods as compared to the much smaller CGRP+ fibers. To further investigate differences between subtypes, higher power visualization, such as electron microscopy, should be used to visualize cross sections of regenerating nerve.

It is important to note that the population of peptidergic nociceptive fibers is only a small fraction of the total small diameter fibers that must regenerate following an injury. My investigation into peptidergic nociceptors does not inform on the regeneration of other populations of nociceptors. In later experiments, I further investigate the specificity of CES on different neuronal subtypes.

3.4.4 Checkpoint as an alternate stimulator

As CES has only been preclinically investigated using the SD-9 Grass stimulator, an alternative stimulator was investigated. SD-9 Grass-stimulators are not commercially available, and alternate stimulators, including the Checkpoint stimulator, have been proposed as candidates to deliver PES in clinic (as CES has not yet been translated into clinical practice). The Checkpoint stimulator was found to match the pro-regenerative effects of the SD-9 stimulator at durations of 10 minutes and 1 hour; neither stimulator promoted regeneration with 10 minutes, while both stimulators promoted regeneration with 1 hour. Current literature has only investigated the use of the Checkpoint stimulator in the context of PES; Roh (2022) suggests that 10 minutes of PES is sufficient to promote regeneration following injury. Our results indicate 10 minutes of CES delivered with either the SD-9 stimulator or Checkpoint stimulator are insufficient to promote regeneration. Rather, in order to promote regeneration using either stimulator, it must be used for 1 hour. Regeneration length after 1 hour of Checkpoint-delivered CES appears to trend downwards, though no significant difference between SD-9 1 hour and Checkpoint 1 hour is found. Increasing the sample size may reveal a small difference in regeneration length.

Akin to 1 hour of SD-9-delivered CES, 1 hour of Checkpoint-delivered CES promoted axon extension across the nerve repair site, and distal to the nerve repair site. Though SD-9 stimulation appeared to promote the number of regenerating axons more consistently, Checkpoint stimulation increased regeneration distal to the nerve repair site until the end of regeneration. It is likely that differences between the two result from issues in tissue quality in the middle sections of the nerve, and 1 hour of Checkpoint stimulation also consistently increases the number of regenerating axons. Interestingly, 10 minutes of Checkpoint-delivered CES increased the number of regenerating axons further than just past the repair site, unlike 10 minutes of SD-9-delivered CES (10 minutes of SD-9 stimulation only increased axon extension across the transection site, and no further). It is unclear why a difference between stimulators only emerges at shorter durations of CES. However, the length of regeneration is unaffected by the increase of regeneration axons, as the increase does not persist to the end of regeneration. Further, there does not appear to be a difference between Checkpoint and SD-9 with 1 hour of stimulation. Ultimately, the difference does not appear to positively impact regeneration, and impacts on recovery would likely be minimal if not non-existent. Therefore, we propose Checkpoint and SD-9 stimulation deliver CES and promote regeneration to the same extent.

Differences in the programming of the stimulators may confound the results described. Checkpoint stimulators are programmed to deliver stimulation at a 16Hz frequency, as opposed to a 20Hz frequency, of which is the standard for CES. Thus, all Checkpoint stimulated animals received stimulation at a frequency of 16Hz instead of 20Hz. The frequency of Checkpoint stimulators is pre-set, unable to be altered. Though the frequency of SD-9 stimulation is alterable, 20Hz is the standard frequency of CES, and current clinical trials administer CES at 20Hz. The goal of the experiment was to compare the efficacy of stimulators as they would be used in clinic, and so different frequencies were administered by the stimulators.

Despite our reasoning, the difference in frequencies may alter the pro-regenerative effects of CES. Frequencies as low as 2Hz have been used to deliver PES in which it was found that decreasing the frequency appeared to promote regeneration more effectively than higher frequencies (Lu et al., 2008). PES primarily improves regeneration through accelerating staggered regeneration; lower frequencies may have specifically increased axon extension across the nerve repair site to improve regeneration (Lu et al., 2008). Decreasing the frequency of stimulation to 16Hz in our CES model may have had similar effects, as we have previously demonstrated CES to improve the number of regenerating axons crossing the injury site at 10 minutes. Further, a frequency of 20Hz was initially chosen due to it being the mean frequency of motor axon action potentials. Decreasing the frequency of stimulation may preferentially target different neuronal subpopulations. Different neuronal subtypes have different compositions within the peripheral nerve; the tibial nerve is a mixed nerve, containing smaller diameter sensory neurons.

The Checkpoint stimulator is a handheld device, as opposed to the SD-9 stimulator in which wires are wrapped around the nerve of interest. Though the handheld stimulator allows for ease of use in identifying nerve tissue and differentiating between fascicles as the stimulator was intended, this also proves to be a limitation when using this device to administer CES. Holding the stimulator in place for 10 minutes may prove reasonable in the clinic. However, as we have demonstrated that 1 hour of stimulation is needed to induce a pro-regenerative response, holding the stimulator in place for 1 hour is likely not feasible in the clinic. Increasing the duration of use of the Checkpoint stimulator increases the likelihood of user error. The user must stay vigilant during stimulation: ensuring the stimulator tip remains in contact with the appropriate tissue, and ensuring the appropriate degree of muscle twitch. This may be difficult to achieve with a handheld device, as opposed to the SD-9 stimulator whose wires easily remain in place. As the SD-9 stimulator is not commercially available, the Checkpoint stimulator may prove useful as an alternative stimulator if necessary. However, new stimulators that consider the minimum duration of 1 hour of stimulation should be developed and made clinically available to best administer CES once clinically translated.

CHAPTER 4: Investigating the Neuronal Specificity of the Pro-Regenerative Effects of Conditioning Electrical Stimulation

4.1 Introduction

4.1.1 Classification of Neuronal Subtypes in the PNS

Traditional classifications of peripheral neurons consider soma and axon diameter, degree of myelination, and the type of information transmitted to the brain from sensory organs, or from the brain to motor endplates. α motor fibers, which are large diameter motor axons (13-20µm), with soma diameters of 20-30µm, exhibit high myelination and fast conduction speeds (80-120m/s), facilitating the transmission of motor impulses to the muscle motor end plates they innervate (Accornero et al., 1977; Friese et al., 2009). These fibers primarily innervate extrafusal muscle, contributing to muscle contraction force (Friese et al., 2009). In contrast, γ motor fibers, comprising a smaller portion of motor fibers, innervate intrafusal muscle fibers found in muscle spindles (Burke et al., 1977; Friese et al., 2009). γ fibers modulate muscle spindle sensitivity to muscle stretch and have smaller axon diameters (5-8µm), soma diameters (10-20µm) and slower conduction velocity (4-24m/s) compared to α fibers (Burke et al., 1977; Friese et al., 2009).

Sensory afferents are categorized into proprioceptive, mechanoreceptive, and nociceptive fiber types. Proprioceptors, identified as Aα fibers, are the largest sensory fibers in terms of axon diameter (13-20µm), and cell diameter (20-30µm), with conduction speeds comparable to α motor fibers (80-120m/s) (Accornero et al., 1977; Dietrich et al., 2022). Proprioceptors relay positional information from muscles, further classified by their synaptic connections to muscle spindles (type Ia or II) or golgi tendon organs (type Ib) (Dietrich et al., 2022).

Mechanoreceptors can be categorized as low threshold or high threshold. Low threshold mechanoreceptors (LTMRs), traditionally represented by large diameter Aβ-LTMRs, but also a population of Aδ LTMRs and C LTMRs are responsible for sensing non-noxious stimuli such as light touch, temperature, stretch, and vibration (Cain et al., 2001; Handler & Ginty, 2021). Aβ

LTMRs, the second largest sensory afferents, have slightly smaller axon diameters (6-12µm) and soma diameters (10-20µm) and conduction velocities slightly slower than proprioceptive afferents (33-75m/s) (Cain et al., 2001; Handler & Ginty, 2021). These LTMRs can be further subdivided into slow adapting LTMRs (SA-LTMRs) and rapidly adapting LTMRs (RA-LTMRs) based on their response to stimuli (Handler & Ginty, 2021). Aβ RA-LTMRs respond only at the onset or removal of stimuli, quickly adapting to changes, while Aβ SA-LTMRs maintain responsiveness over the duration of stimulation (Handler & Ginty, 2021; Olson et al., 2017). Aβ RA-LTMRs are particularly useful for detecting changes in stimulus intensity (Djouhri & Lawson, 2004). Mechanoreceptors can be further divided based on the sensory end organs of the axons and the type of skin innervated (Handler & Ginty, 2021; Olson et al., 2017). Aδ LTMRs, intermediate in axon diameter (1-5µm), soma diameters (5-10µm), and conduction velocity, (3-30m/s) primarily innervate hair follicles and detect changes in the direction of hair follicles (Crawford & Catarina, 2020). C-LTMRs are believed to convey low threshold mechanosensation to the dorsal horn to modulate pain perception and potentially contribute to the development of allodynia (Larsson & Nagi, 2022).

High threshold mechanoreceptors, or nociceptors, primarily consist of small diameter fibers that detect painful stimuli such as intense pressure, tissue damage, or extreme temperatures (Cain et al., 2001; Dubin & Patapoutian, 2010). Aδ HTMRs are lightly myelinated, intermediate diameter fibers (1-5µm), intermediate diameter somas (5-10µm) with intermediate conduction velocities (3-30m/s) (Cain et al., 2001). C HTMRs are small axon diameter (0.2-1.5µm), cell soma diameter (1-5µm) unmyelinated fibers with slow conduction velocities (0.5-2.0m/s) (Cain et al., 2001). Aδ HTMRs are associated with the rapid onset of pain due to their intermediate conduction velocity, while C HTMRs are associated with a slower onset of pain due to their slow conduction velocity (Cain et al., 2001). Itch-sensing pruriceptors constitute another class of C-fibers, as well as closely related "silent nociceptors," which innervate deep tissues such as internal organs, muscle, and joints, and are unresponsive to mechanical nociception but are activated by inflammation, potentially playing a role in itch (Crawford & Caterina, 2020; Prato et al., 2017). Aβ nociceptors have also been identified, potentially involved in itch sensation (Luo et al., 2015).

4.1.2 Expression Profiles of Neuronal Subtypes

Due to the diversity in function within large, medium and small diameter axons, identifying differences in mRNA and protein expression in the cell body has further differentiated neuronal subtypes. Motor axons can be distinguished from sensory axons based on positive expression of choline acetyltransferase (ChAT). Expression of the transcription factor Err3 differentiates between α and γ motor neurons; small γ motor neurons feature high Err3 expression, while larger α motor neurons do not (Friese et al., 2009). Differentiation of sensory neurons is less straightforward. Large diameter Aα proprioceptors express parvalbumin (PV), but also express tyrosine receptor kinase C (TrkC), solute carrier family 17 member 7 (SLC17A7) (formally known as vesicular glutamate transporter 1 (VGLUT1)), acid-sensing ion channel subunit 1 (ASIC1), potassium voltage-gated channel modifier subfamily S member 1 (KCNS1), runt-related transcription factor (RUNX) family transcription factor 3 (RUNX3) (known to suppress TrkB) and NF200 (Olson et al., 2017; Tavares-Ferreira, 2021). Aβ RA-LTMRs can be differentiated based on their expression of rearranged during transfection (RET) and alongside SLC17A7 and NF200 (Olson et al., 2017). Currently few molecular markers exist to differentiate Aβ SA-LTMRs; Aβ SA-LTMRs also express TrkC, SLC17A7, PV and NF200, similar to proprioceptive fibers. However, it may be possible to differentiate Aβ SA-LTMRs from other large diameter populations with expression of receptor activity modifying protein 1 (RAMP1), a receptor component for the CGRP receptor (Tavares-Ferreira et al., 2021). Aδ LTMRs primarily express TrkB, but not NF200 (Tavares-Ferreira et al., 2021; Olson et al., 2017). C LTMRs express vesicular glutamate transporter 3 (VGLUT3), tyrosine hydroxylase (TH), and GDNF family receptor alpha 2 (GFRA2), distinguishing themselves from other tactile C fibers, though all delineations of C fibers express TrkA. Interestingly, transcriptional profiling reveals increased overlap between C LTMRs and A LTMRs when compared to other C tactile fibers (Handler & Ginty, 2021; Larsson & Nagi, 2022; Olson et al., 2017; Tavares-Ferreira et al., 2021). Apart from size, nociceptive fibers in mice can be classified as peptidergic and nonpeptidergic; peptidergic neurons expressing neuropeptides such as CGRP and substance P, while nonpeptidergic neurons bind to isolectin B4 (IB4) on the extracellular facing membrane (Crawford & Catarina, 2020; Stucky & Lewin, 1999). These fibers can be distinguished by their responsiveness to neurotrophic factors: peptidergic neurons express TrkA and respond to NGF, whereas nonpeptidergic neurons express the GDNF receptor complex and respond to GDNF (Stucky & Lewin, 1999). Nonpeptidergic fibers have also been found to highly express TRPA1 on their membrane, an ion channel closely related to nociceptive mechano- and cold- sensation, whereas peptidergic fibers do not (Barbaras et al., 2012). P2X purinoceptor 3 (P2X3R) is a non-peptidergic nociceptive marker (Shiers et al., 2021). Tavares-Ferreira and colleagues (2021) further identified different human nociceptor groups based on mRNA expression and cell diameter. Aδ HTMRs expressed TrkC, Copine 6 (CPNE6), sodium voltage-gated channel alpha subunit 10 (SCN10A), calcitonin- related polypeptide alpha (CALCA) and lysophosphatidic acid receptor 3 (LPAR3). Cold sensing C-fiber nociceptors were identified based on expression of transient receptor potential cation channel subfamily M member 8 (TRPM8), a receptor known to transmit noxious cold sensation, as well as SCN10A (Tavares-Ferreira et al., 2021). Another C-fiber nociceptive group had expression of Proenkephalin (PENK), urocortin (UCN), and prostaglandin E2 (PGE2) receptor PTGER3 (Tavares-Ferreira et al., 2021). Interestingly, neuropeptides were widely expressed among all nociceptive groups. TRPA1 co-expressed highly with tachykinin precursor 1 (TAC1), which encodes for substance P, and CALCA, which encodes for CGRP. This contradicts the results found in mice, in which TRPA1 was primarily expressed in non-peptidergic, IB-4 binding nociceptor groups. Further, P2X3R (non-peptidergic marker) and neuropeptides were highly co-expressed in human DRG neurons. Tavares-Ferreira and colleagues (2021) therefore argue that peptidergic and nonpeptidergic nociceptive classifications are not consistent in human nociceptor populations. This is supported by Shiers et al (2021), who assessed protein levels in human DRG neurons. Silent nociceptors were also identified based on expression of cholinergic receptor nicotinic alpha 3 subunit (CHRNA3), serotonin receptor 5-hydroxytryptamine receptor 3A (HTR3A), P2RX3, acid sensing ion channel subunit 3 (ASIC3), and H1 histamine receptor gene, histamine receptor H1 (HRH1) (Tavares-Ferreira et al., 2021). Lastly, a C-fiber population enriched for pruritogen receptors was identified based on expression of natriuretic peptide B (NPPB), GDNF family receptor alpha 2 (GFRA2), interleukin-31 receptor A (IL31RA), and sodium voltage-gated channel alpha subunit 11 (SCN11A), likely involved with itch-sensation (Tavares-Ferreira et al., 2021). The last nociceptive population identified were Aβ nociceptors, found to be large in diameter, but also express TRKC and SCN10A (common nociceptive markers) (Tavares-Ferreira et al., 2021).

4.1.3 Innate Rate of Regeneration Between Neuronal Subtypes

The inherent rate of regeneration among nerve types and neuronal subpopulations remains a subject of debate. Several early studies have identified differences in regeneration between motor, mixed and sensory nerves, suggesting that motor and mixed nerves regenerate faster than pure sensory (da Silva et al., 1985; Jenq and Coggeshall, 1985). Within the mixed sciatic nerve in both rat and rabbit, sensory axons have been found to regenerate faster and earlier than motor axons (Kawaski et al., 2020; Madorsky et al., 1998; Sanger et al., 1991; Suzuki et al., 1998). However, other studies have shown that the innate rate of regeneration between motor and sensory neurons are the same (Forman & Berenberg, 1978; Forman et al., 1979; Moldovan et al., 2006). Thus, it is unclear whether or not sensory and motor regeneration differs. Furthermore, it is unknown whether nociceptive, mechanoreceptive, or proprioceptive neurons differ in rate of regeneration. A study in which the tibial branch of the sciatic nerve was transected and regeneration into the footpad demonstrated that nociceptors derived from the sural branch of the sciatic nerve were capable of sprouting collaterals and reinnervating mechanoreceptive end targets (Gangadharan et al., 2022). Collaterally sprouting nociceptors were capable of following the exact trajectory of tibial nociceptors at baseline by using blood vessels as scaffolding. Though Aβ mechnoreceptive neurons were present in the sural nerve, only nociceptive neurons were capable of collateral sprouting, potentially suggesting a higher regenerative capacity for the unmyelinated sensory fibers as compared to larger myelinated sensory fibers (Gangadharan et al., 2022). Likewise, Song et al. (2019) demonstrates that conditional knockout of Piezo, a Ca^{2+}-permeable non-selective cation channel responsible for mechanosensation, accelerates regeneration of mechanoreceptors. This further suggests mechanoreceptive neurons may have a reduced regenerative capacity compared to other sensory populations that do not express Piezo (Song et al., 2019).

Environmental factors have the potential to affect regeneration between motor and sensory neurons. Motor and sensory Schwann cells feature different neurotrophin expression patterns following peripheral nerve injury; as reviewed in Bolívar et al (2020), motor Schwann cells express and release pleiotrophin (PTN), and insulin-like growth factor-1 (IGF-1), and sensory Schwann cells express BDNF, NGF, and hepatocyte growth factor (HGF) (Höke et al., 2006). Differences in glial neurotrophin expression and secretion influence preferential motor reinnervation, and may influence differences in sensory and motor regeneration, though only speculative. Basal markers of non-myelinating Schwann cells (forming Remak bundles) differ from those of myelinating Schwann cells, with expression of select markers that partially resemble immature Schwann cell expression, such as the p75 neurotrophic receptor (p75NRT) (Bosse et al., 2006). It is unclear to what degree neurotrophin and neurotrophin receptor expression of Schwann cells influences axon regeneration. However, Schwann cell neurotrophic expression profiles are important to consider, as cell-cell interactions between Schwann cell and axons are integral for axon guidance and reinnervation following injury. Many factors, including ion channel expression, Schwann cell neurotrophin expression, and myelination may affect the intrinsic regenerative capacity of neuronal subtypes.

To date, CES has only been investigated in NF200+ populations. Differences between neuronal subpopulations may influence the efficacy of CES as a treatment on different axons. To investigate if CES elicits pro-regenerative effects on additional neuronal subpopulations, conditioning, tibial nerve repair, and tibial nerve harvest was performed, as previously described in Chapter 3. Immunohistochemical analysis assessed the regeneration of all axons, motor axons, peptidergic nociceptive axons, and proprioceptive axons. For the purposes of this study, ChAT is used to identify motor axon populations, PV is used to identify proprioceptive axon populations, and CGRP is used to identify peptidergic nociceptive populations. NF200 is a broad marker that is present in Aα, Aβ, and populations of Aδ fibers, and has been previously used to assess the extent of regeneration following administration of CES (Senger et al., 2018a; 2019; 2020a; 2022). Despite the increasingly complex classifications of DRG and motor neurons, identification of regenerating neuronal populations was limited based on the availability of immunohistochemical antibodies. Our lab acknowledges that these classifications do not account for all neuron populations and overlap between selected populations is highly likely.

4.2 Methods

4.2.1 Animals: Adult Sprague Dawley and *Thy-1-GFP* Sprague Dawley rats 8-12 weeks old, weighing 200g were housed with the Health Sciences Laboratory Animal Services (HSLAS) (AUP 00001871) at the University of Alberta. Animals were housed in flat-bottomed Greenline cages with ad libitum standard rat chow and water. Lighting was cycled with 12h on/off rotations. All experimental procedures were approved by the University of Alberta Animal Research Ethics Board.

4.2.2 Surgical Procedures: Animals were randomly divided into unconditioned (control) and CES (experimental) cohorts. Prior to all surgical interventions, animals were anesthetized with inhaled isoflurane (2% titrated at 1–2 L/min for maintenance of a surgical anesthetic plane) and received 0.01 mg/kg of subcutaneous buprenorphine. At the completion of all procedures, skin was closed with 4–0 Vicryl sutures (Ethicon Inc., Somerville, NJ). All surgeries were performed in a dedicated animal surgery facility at the University of Alberta.

4.2.3 Conditioning: Animals in the CES cohort received a 2 cm longitudinal incision at the right lower limb to isolate the sciatic nerve via blunt dissection proximal to the trifurcation point. CES animals received 20Hz electrical stimulation at 0.1 ms duration for either 10, 30 or 60 minutes to the sciatic nerve proximal to the trifurcation point, using an SD-9 stimulator (Grass Instruments, Quincy, MA), or received 10, 30 or 60 minutes of intraoperative current at 0.5 mA, at a pulse width of 100 µs and frequency of 16 Hz, from a Checkpoint stimulator (Checkpoint® Stimulator/Locator, Checkpoint Surgical, Inc, Cleveland, OH). Settings were based on previous studies (Jo et al., 2019; Senger et al., 2018; 2019; 2020; Wood et al., 2022). For animals stimulated with an SD-9 stimulator, a stainless-steel wire with bared ends was wrapped around the nerve, and the return electrode was placed into the tibialis anterior muscle; these were connected to the cathode and anode ports of an SD-9 stimulator. For animals stimulated with a Checkpoint stimulator, the stimulating tip was placed directly onto the nerve, and a return current electrode was placed securely in musculocutaneous facia in the dorsum of the animal just proximal to the nerve. To confirm stimulation, the device provided feedback via a LED light indicating whether current was provided and circuit complete. For both stimulators, excitation of the nerve was confirmed based on contractions of the foot. Unconditioned animals did not receive any experimental or surgical intervention. Sham electrical stimulation was not used as previous studies indicated no difference between unconditioned and sham animals (Senger et al., 2018; Senger et al., 2019).

4.2.4 Nerve Transection and Microsurgical Repair: 7 days following conditioning, unconditioned and CES animals received a 2 cm longitudinal incision in the right lower limb to isolate the sciatic nerve via blunt dissection. The sciatic nerve was traced distally and the site of trifurcation was dissected to isolate the tibial nerve from the common peroneal and sural branches. The tibial nerve was cut and immediately repaired using 9–0 silk sutures.

4.2.5 Tissue Collection: 7 days following tibial nerve transection and microsurgical repair for regeneration analysis, animals were euthanized with carbon dioxide and exsanguinated by opening the thoracic cavity and cutting the left ventricle of the heart. The sciatic nerve was re-exposed, and the site of microsurgical repair was identified. The tibial nerve was isolated from connective tissue, and the sural and common peroneal nerve branches, and harvested approximately 2 mm proximal to the coaptation site, and 3 cm distal to the coaptation site. Harvested nerve was placed onto a wooden toothpick and put into 4% paraformaldehyde (PFA) (American MasterTech Scientific, Lodi, CA) fix for 1 hour at 4°C. For tissue culture, L4 and L5 DRGs were placed into Hank's buffered salt solution (HBSS) modified medium (HyClone) and placed under a dissecting scope for removal of the epineurium and axon branches. L4/L5 DRGs were then transferred into sterile HBSS medium. Following fixation, nerves were rinsed in 30% sucrose in phosphate buffered saline (PBS) (Thermo Fisher Scientific, Waltham, MA) then stored in 30% sucrose in PBS solution at 4 °C overnight, or until tissue was saturated with sucrose. Tissue was embedded and frozen in optimal cutting temperature (OCT) (Sakura Finetek, Torrance, CA) using indirect exposure to liquid nitrogen. Tissue was stored at −80 °C, until cryosectioning. Longitudinal sections of the nerves (12 μm) were thaw-mounted onto Superfrost

Plus microscope slides (Thermo Fisher Scientific, Waltham, MA) and stored at −80 °C until processing.

4.2.6 Tissue Culture: 1-7 days before culture, 500µL of 0.1 mg/mL poly-D-lysine suspended in sterile water (mol wt 70,000–100,000 kD) (Sigma) evenly distributed over bottom of well in a 24 well glass bottom plate (Cellvis). Solution left on wells for 15 minutes at room temperature, and wells washed 3x100µL with sterile water. Plate was allowed to dry for several hours in sterile hood, and stored sealed at 4°C. On the day of the culture, plates are coated with 500µL laminin (Mouse 1.0mg/mL) (Invitrogen) diluted in HBSS for a final concentration of 2µL/mL of HBSS. Plates are incubated at 37°C in tissue culture incubator for 2 hours. Laminin is removed immediately before plating cells. Dissected DRGs are washed by placing them into sterile HBSS and tilting to wash 3 times. Sterile 1 mg/mL collagenase (Sigma Aldrich) in HBSS medium is prepared and sterilized using a 0.22µm low protein binding syringe filter (Thermo Fisher Scientific). The washed DRGs were placed into collagenase solution and incubated in 37°C water bath for 1 hour. 0.05% of filter sterilized trypsin in HBSS (Sigma Aldrich) is added after 1 hour, and the incubation is continued for 15 minutes. Sterile 1mL pipette tips are used to aspirate DRGs with 10 passes through sterile tip for mechanical digestion. DRGs are incubated for 15 minutes in water bath if DRGs do not aspirate through 1mL tips. Aspiration continued with 1mL tips until DRGs passed easily through tips, then aspirated DRGs with 200µL tips for 10 passes. Incubated ganglia for 5 minutes in water bath. Repeated aspiration and incubation of ganglia until cells in suspension. 100µL fetal bovine serum (FBS) (Sigma Aldrich) was added to stop further enzyme reactions. Cell suspension then centrifuged at 800-1000 rpm for 7 minutes. Removed supernatant and resuspended cells in HBSS medium. Repeated centrifugation, removed supernatant, and resuspended cells in cell medium: Dulbecco's Modified Eagle Medium/F12 (DMEM) (Gibco), 1% N2 supplement (Thermo Fisher Scientific), and 1% pen-strep (HyClone). Plated cells with approximate concentration of 1000 neurons per well. Stored plate in 37°C tissue culture incubator for 48 hours or 5 days. Day of culture is considered Day 0. On Day 1 of the 48 hour cultures, 250µL of growth medium is pipetted out of each well and 250µL of fresh medium is pipetted in along with the full concentration of inhibitors for each respective treatment.

5.2.7 Immunocytochemistry for Tissue Culture: At experimental endpoints, an equivalent volume of 8% PFA was added to the media for an end concentration of 4%. Wells were incubated for 15-20 minutes at room temperature and wells washed with Dulbecco's phosphate buffered saline (DPBS) (Gibco) 3 times. Cells were permeabilized and blocked with 250µL 0.2% Triton X-100 in DPBS with 10% normal goat serum (NGS) (LifeTech) for 60 minutes at room temperature, then incubated overnight 4°C with primary antibody solution of β-III tubulin in DPBS (Table 5.5.1). The following day, cells were washed with DPBS 3 times, then incubated with DAPI (Invitrogen) and a secondary antibody solution of Cy3 in DPBS for 60 minutes at room temperature (Table 5.5.1). Following incubation, cells were washed 3 times with DPBS, and sealed and stored at 4°C.

4.2.8 Immunohistochemistry: Slides were warmed to room temperature for 15 minutes before undergoing 3 by 5 minute washes in 0.01M PBS (Thermo Fisher Scientific), and permeabilized in 0.01% Triton-100x (Thermo Fisher Scientific). Sections were then blocked in 10% normal goat serum (MP Biomedicals, Santa Ana, CA) and 3% bovine serum albumin (BSA) (Sigma

Aldrich, St. Louis, MO) in 0.01 M PBS for 90 min. Antibodies and concentrations used are represented in Table x. Primary antibodies included CGRP, ChAT, NF200, and Parvalbumin and were applied to sections overnight at 4°C in a solution of 3% BSA and 0.01M PBS (Table 4.5.1). The following day, slides were washed two times in 0.05% Tween in PBS followed by two washes for five minutes in PBS. Secondary antibodies were applied for 60 minutes at room temperature in a solution of 3% BSA and 0.01M PBS. Washes in 0.05% Tween in PBS and in PBS were repeated after application of secondary antibodies (Table 4.5.1). Slides were sealed with AquaMount (Polysciences) and stored at -20°C.

4.2.9 Imaging: All digital images of longitudinal tibial nerve were taken were processed in a parallel manner with identical fluorescent exposures with 20X objective with a widefield epifluorescent microscope (Leica) with THUNDER imaging software for large volume computational clearing (Leica Microsystems, Wetzlar, Germany). Two representative longitudinal tibial nerve sections were analyzed using Thunder Imaging software. For length of nerve regeneration and axon count analysis, Thunder Imaging software identified an ROI and z-stack of the section, and automatically imaged the selected ROI. Z-stack images were combined automatically to enable analysis of each individual axon within the 12µm sections. *In vitro* cells were imaged at 20X using High Content Screening Analysis ImageXpress Micro AI imaging system (MetaXpress XLS, Molecular Devices, San Jose, CA, USA). Total neurite outgrowth and length of primary neurite was analyzed using Image J software. Individual neurites were traced and measured to calculate total neurite outgrowth, and the longest neurite per DRG neuron was considered the primary neurite. Cell body area was traced and measured for each DRG neuron. DRG neurons overlapping neurite extension with other DRG neurons were excluded.

4.2.7 Statistical Analysis: Experimental results are written as the mean ± standard error mean *(s.e.m).* Significance of neurite outgrowth and length of regeneration was determined using unpaired t-test to determine any differences in the mean between the two groups. A level of $p<0.05$ was the cut-off for statistical significance. To determine statistical significance between axon counts and axon marker proportions, a two-way ANOVA was completed to determine differences between the mean of each group in a paired data set followed by Dunnett's post-hoc for comparison against unconditioned animals. A paired t-test was conducted to determine differences between the length of regeneration of different biomarkers. To compare between neurite outgrowth and cell body area, a linear Pearson correlation was conducted. Statistics were completed using Prism 9.3.1 (GraphPad Software, San Diego, CA).

Table 4.2.1 Primary and Secondary Antibody Protocols for Immunohistochemistry

Primary Antibody	**Antigen Retrieval** 40 minutes in 60 °C citrate buffer (10mM sodium citrate, 0.05% Tween-20, pH 6.0)	**Primary Antibody Dilution**	**Secondary Antibody**	**Secondary Antibody Dilution**
CGRP (rabbit) Millipore PC205L	No	1:4000	Cy3 goat anti-rabbit Jackson Labs 111-167-003	1:1000
ChAT (rabbit) Invitrogen PA5-29653	No	1:200	Cy3 goat anti-rabbit Jackson Labs 111-167-003	1:1000
Parvalbumin (rabbit) Gene Tex GTX134110	No	1:1000	Cy3 goat anti-rabbit Jackson Labs 111-167-003	1:1000
Pan Neuronal Marker (mouse) Millipore MAB2300	No	1:1000	Cy5 donkey anti-mouse Abcam ab15067	1:1000
NF200 (mouse) Sigma N0142	No	1:1000	Cy5 donkey anti-mouse Abcam ab15067	1:1000

4.3 Results

4.3.1 CES promotes axon regeneration in pan-axonal, PV+, and ChAT+ populations alongside NF200+ and CGRP+ populations.

Traditionally, our lab has used NF200 as an axonal marker when determining the extent of regeneration and number of regenerating axons. However, this biomarker excludes smaller diameter axon populations. In order to assess the regenerative capacity of the total axons in the peripheral nerve with and without CES, Sprague Dawley rats (n=4/cohort) were either conditioned with CES for 1 hour or remained unconditioned. Seven days post-conditioning, animals underwent a tibial nerve transection and repair. Animals were left to recover for 7 more

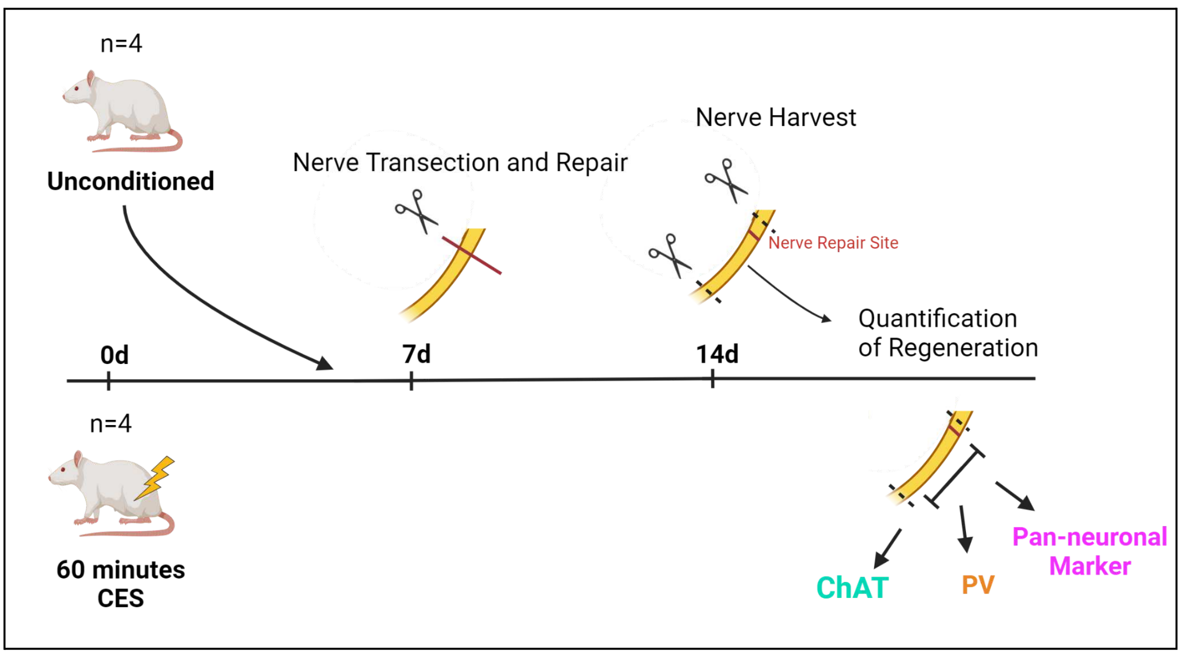

Figure 4.3.1 Experimental design of *in vivo* analysis of the effect of CES on different neuronal subtypes.

days before they were euthanized, and the tibial nerves were harvested for nerve regeneration analysis. Tibial nerves were longitudinally sectioned, and axons were immunohistochemically visualized with a pan-neuronal marker. As expected, CES significantly increased the extent of regeneration from 3.9mm ± 0.7mm to 10.1 mm ± 0.9mm (***$p<0.001$). Further, the number of regeneration axons increased across the nerve repair site with CES (79 axons ± 12 axons; 129 axons ± 16 axons; ***$p<0.001$) The pattern of increased regeneration axons continues until the end of regeneration (significance of at least $p<0.05$) (Figure 4.3.2).

To assess the regenerative capacity of specific subpopulations of axons in response to CES, PV+ and ChAT+. axons were visualized and the length of regeneration and the number of regenerating axons assessed. Proportions of each neuronal subtype proximal to the coaptation site were calculated, with the consideration of NF200 and CGRP+ fibers previously assessed. Neuronal subtypes found to have significantly smaller proportions of axons compared to NF200+ axons had thresholds for axon counting decreased to accurately represent the length of regeneration. In axons proximal to the transection site in both unconditioned and conditioned nerves (n=8/cohort), ChAT+ axons represented a significantly smaller proportion of total axons as compared to NF200+, PV+ and CGRP+ axons. ChAT+ axons proximal to the coaptation site consisted of 12.9% ± 1.1% of total axons, while NF200+ axons consisted of 53.1% ± 7.3% of total axons (***$p<0.001$). PV+ axons consisted of 38%% ± 3.9% of total axons, and CGRP+ axons consisted of 42.6% ± 8.1% of total axons, not different from the proportion of NF200+ axons ($p>0.05$; $p>0.05$). Due to a high degree of overlap between markers, the combined proportions of each marker do not add to 100%. The parameters to determine the length of regeneration of ChAT+ axons were adjusted to a value of 2 axons to accurately represent the proportion of ChAT+ axons compared to other subtypes. (Figure 4.3.4).

CES significantly increased the length of regeneration for all neuronal subtypes assessed. Unconditioned PV+ axons reported an average length of regeneration of 3.4mm ± 0.4mm. CES

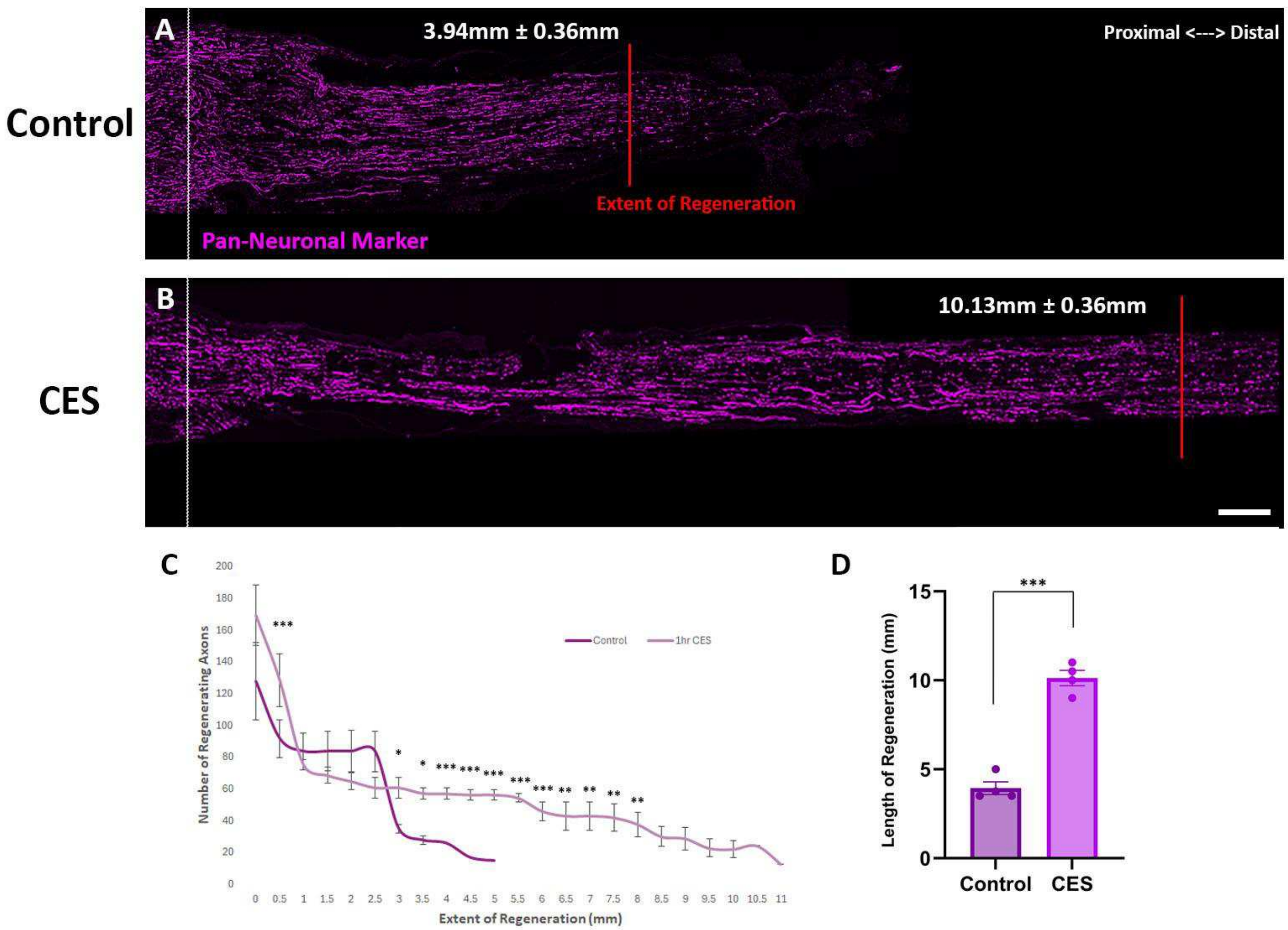

Figure 4.3.2 CES promotes regeneration in axons stained with a pan-neuronal marker. (A-B) Pan-neuronal marker immunofluorescence on longitudinal tibial nerve sections depict nerves left unconditioned (A), or conditioned with CES for 1 hour (B) (n=4/cohort). Red lines indicate the length at which less than 10 axons were counted. (C) Axon counts beginning at the nerve transection site, and quantified every 0.5mm until the end of regeneration. Statistical significance at each 0.5mm length where the number of axon counts of CES animals were different than the unconditioned axon counts is indicated on the graph (*p<0.05, **p<0.01, ***p<0.001). (D) CES promotes the length of regeneration in axons stained with a pan-neuronal marker (***p<0.001). Scale bar in B indicates a length of 0.5mm.

significantly increased the length of regeneration to 8.2mm ± 0.2mm (***p<0.001). (Figure 4.3.3). CES increased the number of regeneration PV+ axons distal to the nerve repair site until the end of regeneration (significance of at least p<0.05), but not at the site of nerve repair (p>0.05). Unconditioned ChAT+ axons reported an average length of regeneration of 2.4mm ± 0.4mm. CES significantly increased the length of regeneration to 7.7mm ± 1.2mm (**p<0.01). CES also significantly increased the number of regeneration axons across the nerve repair site (7 axons ± 1 axon; 16 axons ± 1 axon; ***p<0.001) (Figure 4.3.4).

4.3.2 Cell body area has a weak, positive correlation with neurite outgrowth in conditioned DRG neurons

Cell body size is often used as an indicator of neuronal subtype. To determine the effect of CES on neurite extension of different DRG neuron cell body areas, the sciatic nerve of *Thy-1-GFP* Sprague Dawley rats received 1 hour of CES to the sciatic nerve. The L4/L5 DRGs were collected 3 days prior to 48 hour culture. The regenerative capacity of DRG neuron subtypes was assessed *in vitro* through linear Pearson correlational analyses between neurite extension or primary neurite extension and cell body area. Naive and DRG neurons conditioned with a 1 day latency period (1d CES) were grouped as "Unconditioned DRG Neurons" DRG neurons conditioned with a latency period of 3, 5, and 7 days (3d, 5d, 7d CES) were grouped as "Conditioned DRG Neurons." Linear Pearson correlation analysis revealed no correlation between cell body area and neurite outgrowth in unconditioned DRG neurons (r^2=0.0009, p>0.05), wherass conditioned DRG neurons showed a weak positive correlation between cell body area and neurite outgrowth (r^2=0.015, *p<0.05). In both unconditioned and conditioned

DRG neurons, observational analysis revealed the majority of DRG neurons that grew over 100µm were considered 'medium' in size, between 300µm^2 and 600µm^2 (Figure 4.3.5).

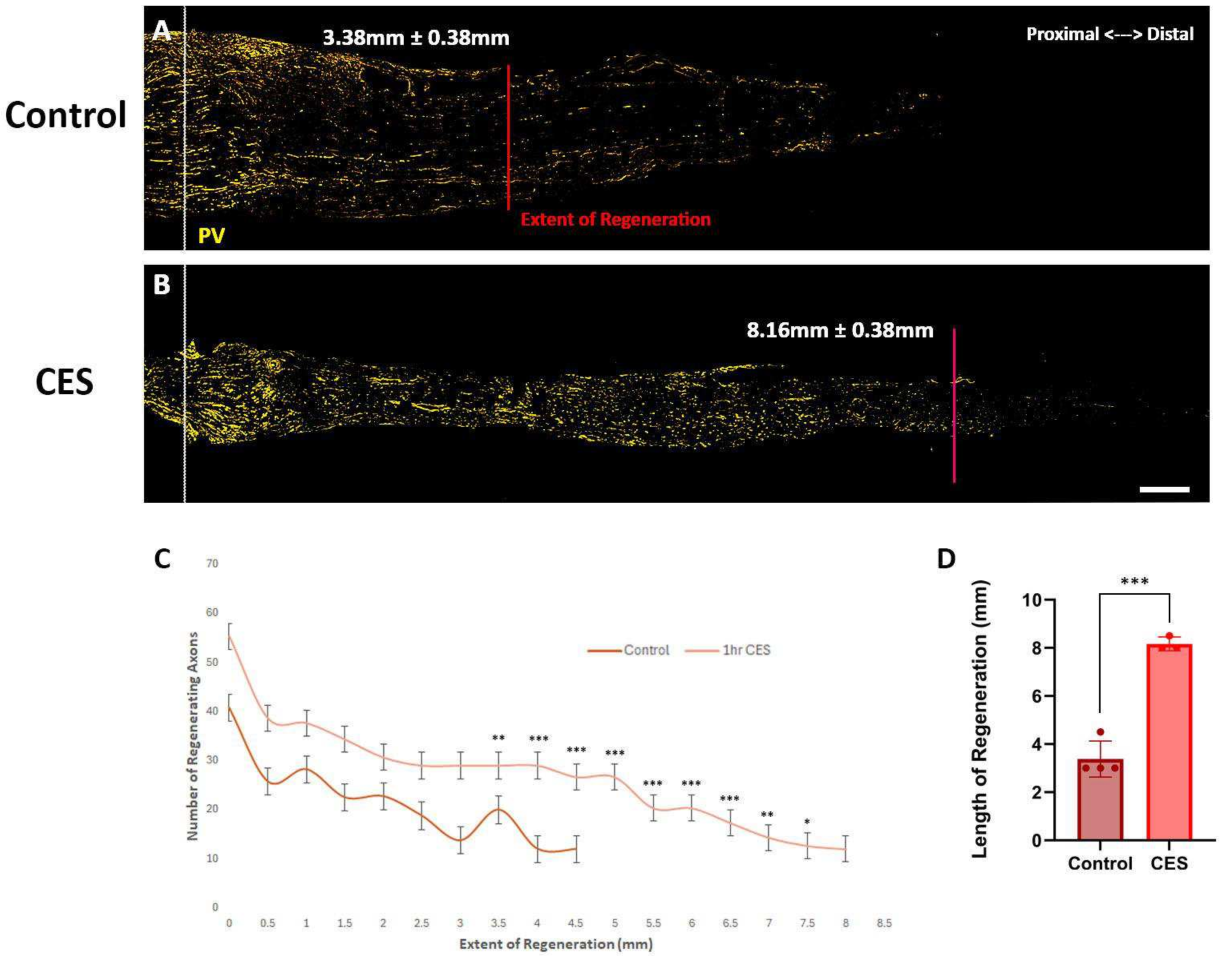

Figure 4.3.3 CES promotes regeneration in PV+ axons. (A-B) Parvalbumin (PV) immunofluorescence on longitudinal tibial nerve sections depict nerves left unconditioned (n=4) (A), or conditioned with CES for 1 hour (n=3) (B). Red lines indicate the length at which less than 10 axons were counted. (C) Axon counts beginning at the nerve transection site, and quantified every 0.5mm until the end of regeneration. Statistical significance at each 0.5mm length where the number of axon counts of CES animals were different than the unconditioned axon counts is indicated on the graph (*p<0.05, **p<0.01, ***p<0.001). (D) CES promotes the length of regeneration in PV+ axons (***p<0.001). Scale bar in B indicates a length of 0.5mm.

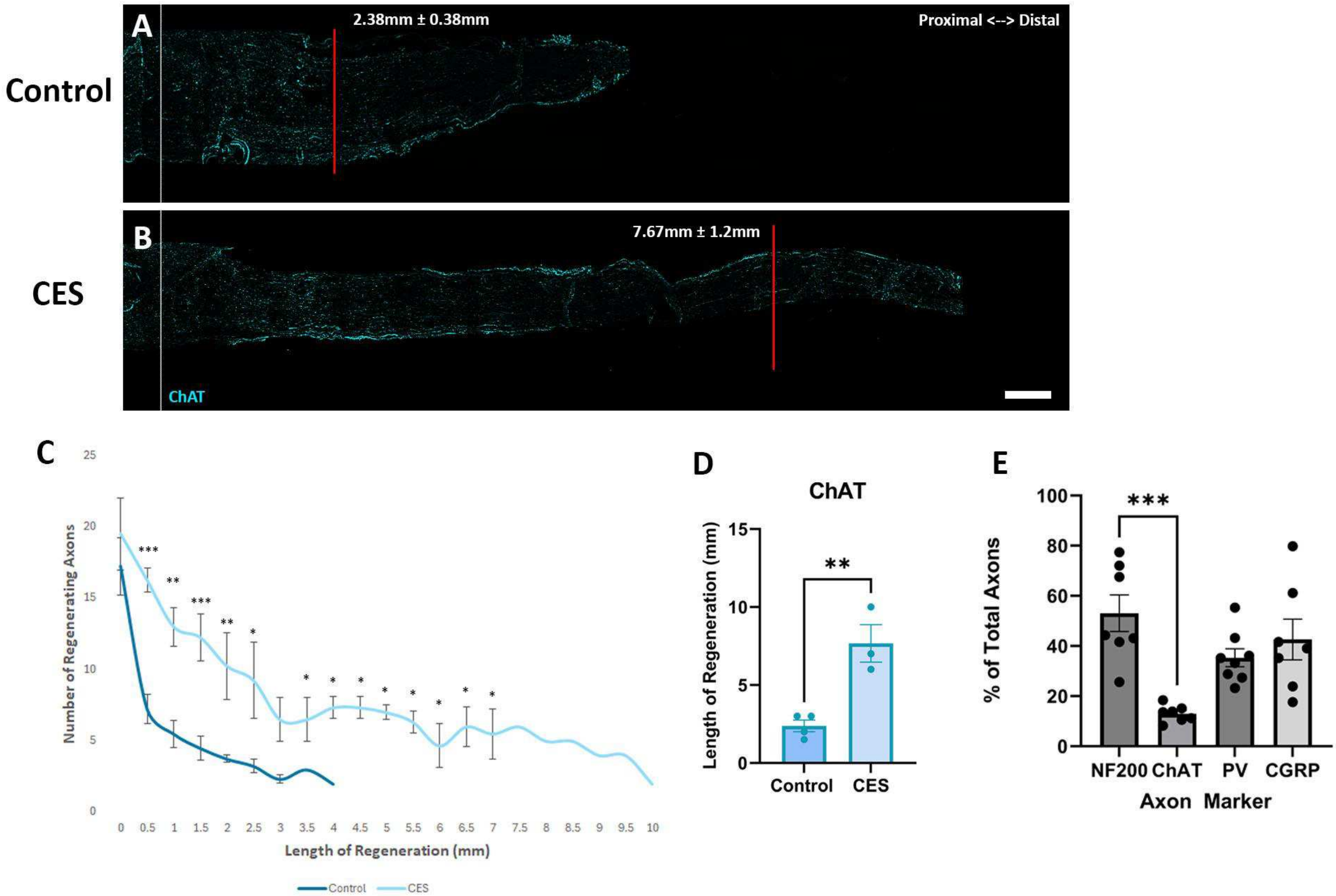

Figure 4.3.4 CES promotes regeneration in ChAT+ axons. (A-B) ChAT immunofluorescence on longitudinal tibial nerve sections depict nerves left unconditioned (A), or conditioned with CES for 1 hour (B). Red lines indicate the length at which less than 10 axons were counted. (C) Axon counts beginning at the nerve transection site, and quantified every 0.5mm until the end of regeneration. Statistical significance at each 0.5mm length where the number of axon counts of CES animals were different than the unconditioned axon counts is indicated on the graph (**p*<0.05, ***p*<0.01, ****p*<0.001). (D) CES promotes the length of regeneration in ChAT+ axons (***p*<0.01). (E) The proportion of ChAT+ axons is significantly smaller than the proportion of all other neuronal subtypes assessed (***p<0.001). Scale bar in B indicates a length of 0.5mm

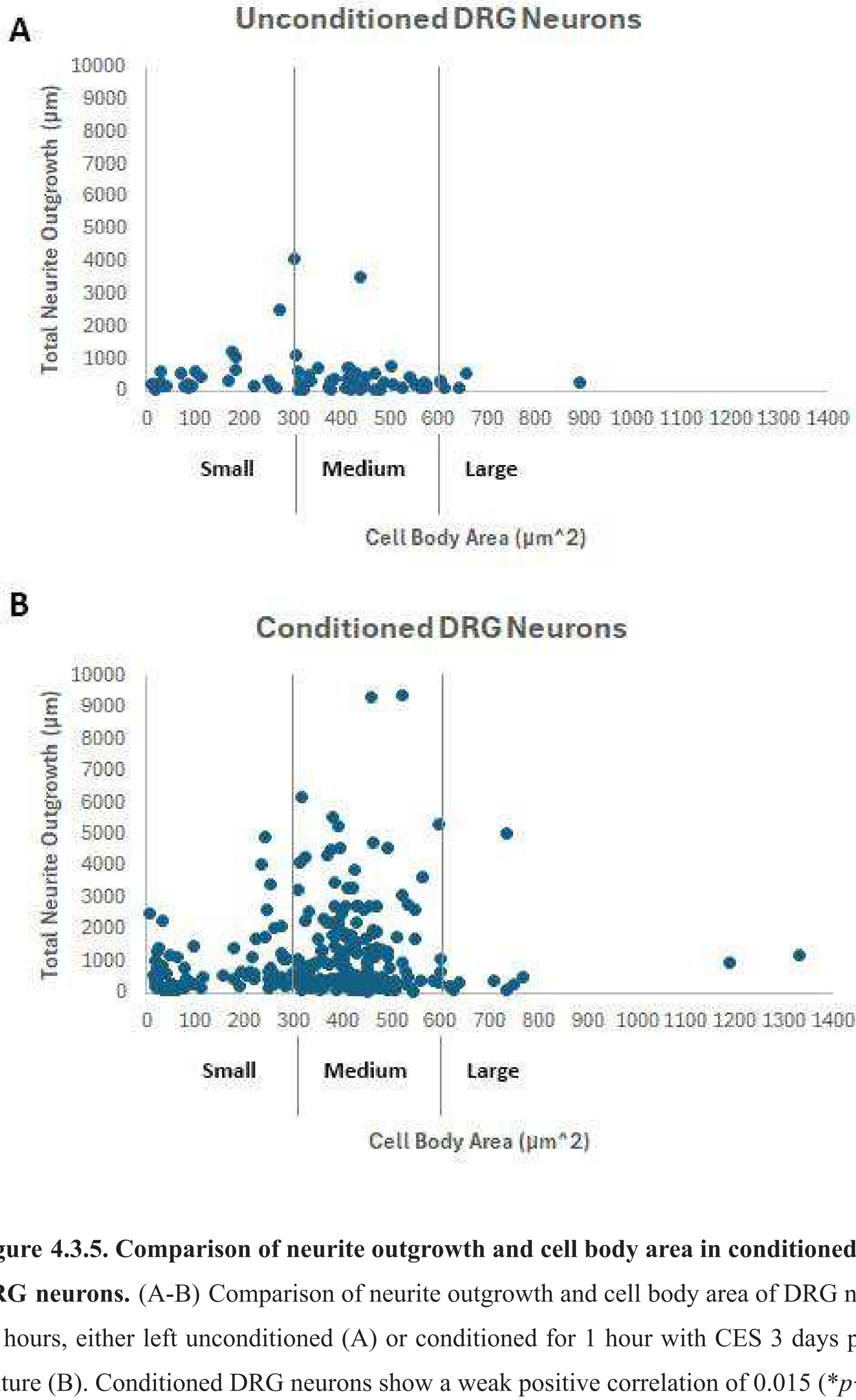

Figure 4.3.5. Comparison of neurite outgrowth and cell body area in conditioned and unconditioned DRG neurons. (A-B) Comparison of neurite outgrowth and cell body area of DRG neurons cultured over 48 hours, either left unconditioned (A) or conditioned for 1 hour with CES 3 days prior to DRG neuron culture (B). Conditioned DRG neurons show a weak positive correlation of 0.015 (**p*<0.05).

4.4 Discussion

4.4.1 CES promotes regeneration non-specifically

Our data suggests that CES elicits a nonspecific pro-regenerative response on all neuronal subpopulations assessed. Previously, only the regeneration of NF200+ axons was assessed following CES (Senger et al., 2018; 2019; 2020; 2022). NF200+ populations not only exclude small sensory fibers, but do not distinguish between medium and large diameter fibers or motor and sensory fibers; it is not known if CES specifically targets subpopulations within NF200+ axons. We assessed regeneration of total axons following CES, of which total axons demonstrated an increase in length of regeneration, and number of regenerating axons. Though no significant difference was observed between the length and number of axons compared to NF200+ axons, total axons consistently reported a longer length of regeneration and more regenerating axons, suggesting that more populations of axons responded to the pro-regenerative effects of CES. We have previously demonstrated CES to promote regeneration of CGRP+ axons. Total axons that do not express NF200+ may be CGRP+, though a proportion of CGRP+ and NF200+ axons overlap in medium diameter axons.

CES also promotes regeneration of large diameter PV+ and ChAT+ axons following injury. Both PV+ and ChAT+ axons overlap with NF200+ populations, as both populations are large diameter. PV+ and ChAT+ increased the length of regeneration and number of regenerating axons in response to CES, further suggesting the effects of CES are non-specific. Muscle mass and neuromuscular junction reinnervation is shown to improve following CES (Senger et al., 2019) to suggest improved regeneration of ChAT+ axons. However, my data is the first to demonstrate the effect of CES on the rate of regeneration directly. Further, the motor assessments conducted in Senger et al. (2019) only allude to PV+ axon recovery, while my data explicitly demonstrates that CES elicits pro-regenerative effects on PV+ axons.

These neuronal subpopulations do not account for NF200+ mechanoreceptors and medium diameter nociceptors, of which are not directly assessed. However, functional recovery studies in rats demonstrate accelerated recovery of mechanosensory and nociceptive function and improved sensory reinnervation with treatment of CES (Senger et al., 2019), strongly suggesting CES elicits pro-regenerative effects on these subpopulations as well.

To determine if CES elicits its pro-regenerative effects non-specifically on all neuronal populations, specific markers for mechanoreceptors and nociceptors should be identified. *Thy1* has previously been suggested to selectively label mechanoreceptors (Gangadharan et al., 2022), though it is not clear if this marker is also expressed in other large and medium diameter populations. Piezo2, a specific channel for mechanosensation, is expressed in all populations of mechanoreceptors, and would serve as a strong marker to identify LTMRs, though the ion channel is also present in proprioceptors (Song et al., 2019; Woo et al., 2015). IB-4 labels small diameter, nonpeptidergic nociceptors, a population excluded in our current assessment of peptidergic nociceptors (CGRP+) (Price et al., 2007). TRPV1 colocalizes with both peptidergic and nonpeptidergic nociceptors, although not completely (Price et al.., 2007). It remains difficult to comprehensively label entire mechanoreceptive and nociceptive populations while also differentiating between the subpopulations within. Silent nociceptors, itch-sensitive nociceptors, Aβ nociceptors, and C LTMRs all differ in protein expression, though likely also overlap largely within previously established subpopulations. Within our data, these populations remain hidden, and it is unknown if CES elicits pro-regenerative effects broadly within the specified populations, or if only certain subtypes respond to the pro-regenerative mechanism of CES. To best assess regeneration of different subpopulations in the future, combinations of markers should be used. Subpopulations of neurons are frequently evolving, further complicated by differences between species (Tavares-Ferreira et al., 2021; Olson et al., 2017). Axon diameter may prove to be a useful tool in combination with protein expression, and cross-sectional studies of regenerating axons may better facilitate measurement of axon diameter, as opposed to longitudinal analysis. Longitudinal sections best demonstrate length of regeneration; thus using both methods would allow for both an accurate depiction of length of regeneration, and number of regenerating axons at predetermined measurements at and past the nerve repair site.

Our data does not consider the innate differences between the rate of regeneration of neuronal subpopulations, or the proportions of neuronal subtypes within a nerve. Our lab is currently working on determining the composition of neuronal subpopulations within different sensory, motor, and mixed nerves, to then evaluate innate differences in the rate of regeneration. Though we assess the proportions of my neuronal populations out of the total axons, cross sectional analysis would likely give axon counts of higher accuracy. Thus, while my results accurately represent length of regeneration and the number of regenerating axons relative to my study, proportions of axon subtypes varied largely. Cross sectional studies should be used to accurately assess subtype proportions to allow a proper comparison between regeneration rates of different neuronal subtypes. While we demonstrate CES to promote regeneration in all assessed subtypes, our results do not speak to differences between subtypes. Further, identifying surface area of regenerating axons may better represent proportions of populations within nerves. ChAT+ axons had less axons regenerating with and without CES. Though ChAT+ axons make up much less of the total axons, these axons also likely represent a larger proportion of the surface area within the nerve. With a smaller initial proportion, it is possible that less motor reinnervation is needed for recovery of function. Despite sensory regeneration appearing to increase the number of regenerating axons substantially, sensory reinnervation may require more axons to elicit a similar degree of sensory functional recovery. Quantifying surface area of different neuronal subtypes in cross sections of the nerve at 0.5mm intervals distal to the injury site may provide a better representation of regeneration with and without CES.

4.4.2 Cell body area as a weak predictor of CES-mediated neurite outgrowth

Correlational analysis between cell body area and neurite outgrowth revealed a weak, positive linear relationship in conditioned DRG neurons, but not in unconditioned DRG neurons. Observational analysis reveals an overall increase in neurite outgrowth in DRG neurons compared to unconditioned, as previously demonstrated (Figure 3.5.3). When unconditioned, DRG neurons show little neurite extension across all size classifications, with some small and medium area neurons with spontaneous growth. Little to no large area neurons extend neurites. In comparison, conditioned DRG neurons show much more growth across all size classifications, suggesting a non-specific pro-regenerative effect. However, the weak positive correlation between neurite outgrowth and cell body size may suggest CES slightly favours larger DRG neurons to promote regeneration, whereas size does not appear to affect neurite outgrowth in unconditioned neurons. All size categories appear to increase outgrowth in response to CES, although not all neurons elicit a ‘conditioning effect,’ with the degree of neurite outgrowth overlapping between conditioned and unconditioned groups. Observational evidence also suggests the weak positive correlation may be due to the robust increase in neurite outgrowth of medium area neurons in particular; though large area neurons appear to also increase their outgrowth, the sample size of large area neurons is much smaller than either small or medium area neurons. This may be due to our use of 50kD poly-D-lysine to coat the plate. Poly-D-lysine is an artificial extracellular matrix used to facilitate cell adhesion to the culture dish. Our lab uses poly-D-lysine at a low molecular weight to allow for even coating on the dish. However, at lower molecular weights, larger DRG neurons do not adhere easily. Thus, while small and medium area DRG neurons adhere to the plate, much of the larger area DRG neuron population is washed away during tissue processing, along with their neurites. To better understand large area DRG neuron neurite extension in response to CES, we could increase the molecular weight of the poly-D-lysine used for substrate adhesion.

Our data may suggest that though CES promotes neurite extension in all neuronal subtypes, medium area DRG neurons appear the most susceptible to the pro-regenerative effects of CES. However, until a larger population of large area DRG neurons are included, it is unknown what the overall relationship between cell body area and neurite extension may be. To better understand this relationship, more DRG neurons in all categories should be assessed.

4.4.3 Implications of neuronal specificity on the molecular mechanism of CES

Determining the molecular mechanisms responsible for the pro-regenerative effects of CES may elucidate the neuronal specificity of CES. If the molecular mechanisms do not involve expression of proteins unique to specific subpopulations, the effect of CES is likely nonspecific. Alternatively, CES may promote regeneration in all neuronal populations to the same extent but may differ slightly in its mechanism between subtypes. As the mechanism of CES is still largely debated, this is unknown. BDNF has been largely implicated in the mechanism of CES (Yan et al., 2014). Though glial BDNF secretion from Schwann cells may differ between sensory and motor subtypes (Höke et al., 2006), motor and sensory axons alike express BDNF. Thus far, BDNF expression has only been noted to increase in DRG sensory neurons following CES (both *in vivo* and *in vitro*) (Senger et al., 2018b; Yan et al., 2014). Assessing the upregulation of RAGs and the DRG cell body area may begin to elucidate differences in neuronal specificity of CES. Future studies should differentiate between neuronal subtypes to assess neuronal specificity of CES.

CHAPTER 5: Investigating the Molecular Signaling Mechanism of Conditioning Electrical Stimulation

5.1 Introduction

As a recently developed intervention, the signaling pathways involved in CES remain elusive. Following our laboratory's differentiation between PES and CES paradigms and identification of signaling pathways involved in either intervention, we have identified gaps in the literature. Although cAMP has been widely accepted as an integral effector of ES (Chu et al., 2022; Javeed et al., 2021; Juckett et al., 2022; Willand et al., 2016; Zuo et al., 2020), it has only been indirectly implicated (and not proven) to play a role following CES. Though no study has specifically investigated the role of cAMP following CES, careful examination of the literature identified a single study that indicated upregulation of cAMP following ES; as ES was administered without injury, this is a CES-induced effect (Udina et al., 2008). Similarly, upregulation of BDNF and pCREB following CES is well characterized in sensory neurons (Senger et al., 2018; Singh et al., 2015). BDNF is a downstream target of cAMP and calcium signaling, given that cAMP mediated activation of pCREB promotes transcription of BDNF mRNA (McGregor & English, 2019). In turn, BDNF protein interactions with TrkB lead to the inhibition of phosphodiesterase activity, further upregulating cAMP (Mussen et al., 2023). Collectively, these studies suggest CES strongly implicates cAMP signaling, warranting further investigation into this pathway.

Traditionally, PKA has been recognized as the major effector of cAMP signaling, with its activation leading to pCREB activation and RhoA inhibition, and a subsequent increase in regenerative capacity in neurons (Hannila & Filbin, 2008). However, EPAC, a PKA-independent effector of cAMP has also been implicated in the regenerative capacity of neurons (Murray et al., 2008; Wei et al., 2016). The roles of either EPAC or PKA as cAMP effectors have not been clearly established in the context of CES.

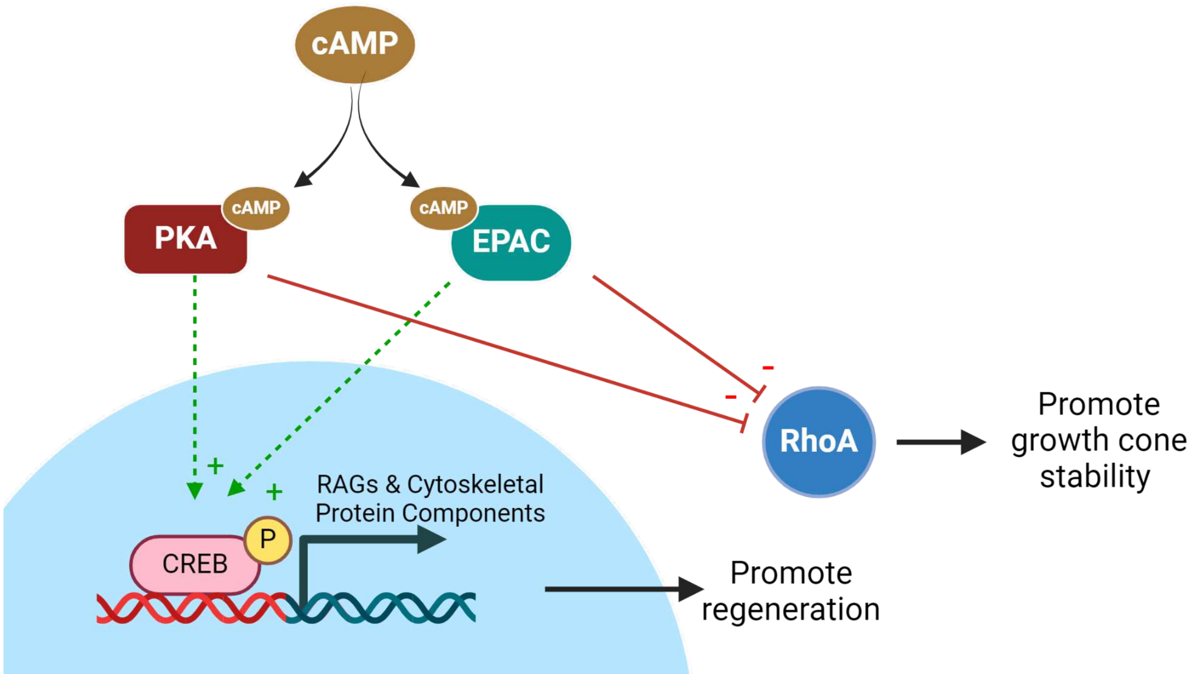

Figure 5.1.1 cAMP activates PKA and EPAC to promote CREB phosphorylation and RhoA inhibition to promote regeneration.

In a study that assessed the relationship between the two cAMP effectors in naive DRG neurons, researchers found that EPAC activation promoted neurite outgrowth, as previously established (Murray et al., 2008), but EPAC inhibition had little effect on outgrowth, and PKA inhibition had a slight positive effect on neurite outgrowth (Wei et al., 2016). The authors suggest PKA inhibition shunts cAMP signaling through the EPAC pathway as a compensatory, and potentially more effective regenerative mechanism. The combination of PKA and EPAC inhibitors eliminated the regenerative capacity of naive DRG neurons altogether (Wei et al., 2016). In a DRG growth cone turning assay, increased concentrations of EPAC induced attractive turning behaviour, akin to cAMP. PKA did not elicit the same turning behaviour in growth cones, suggesting slightly different roles for PKA and EPAC as cAMP effectors (Murray et al., 2008). PKA and EPAC thus far have not been investigated in the context of CES, and given the upregulation of cAMP, BDNF, and pCREB, these effectors pose as potential mediators of the intervention's pro-regenerative effects.

Our *in vitro* experimental design considers the timeline of the CES mechanism. We administer CES *in vivo* prior to DRG harvest and plating in culture, consistent with previously established methods (Udina et al., 2008). To appropriately target the enactors of the CES mechanism, we must consider both the timeline of the upregulation of signaling pathways and the necessary latency period to elicit the pro-regenerative effects *in vitro.* We have determined that a minimum latency period of 3 days is required, and that key RAGs including pCREB and BDNF, both downstream targets of cAMP effectors, are upregulated at 3 days post-conditioning. Due to our experimental design, we are unable to target cAMP pathway activation immediately. Thus, we choose the 3 day timepoint in order to ensure the pro-regenerative effects of CES sufficiently upregulate neurite extension, and to intercept and inhibit cAMP effectors early in their activation. To identify the contribution of cAMP signaling to the mechanism of CES, we administered EPAC and PKA inhibitors to neurons with and without CES after a 3 day latency period to determine the effect of EPAC and PKA on unconditioned and conditioned neurite extension.

5.2 Methods

5.2.1 Animals: Adult Sprague Dawley and *Thy-1-GFP* Sprague Dawley rats 8-12 weeks old, weighing 200g were housed with the Health Sciences Laboratory Animal Services (HSLAS) (AUP 00001871) at the University of Alberta. Animals were housed in flat-bottomed Greenline cages with ad libitum standard rat chow and water. Lighting was cycled with 12h on/off rotations. All experimental procedures were approved by the University of Alberta Animal Research Ethics Board.

5.2.2 Surgical Procedures: Animals were randomly divided into unconditioned (control) and CES (experimental) cohorts. Prior to all surgical interventions, animals were anesthetized with inhaled isoflurane (2% titrated at 1–2 L/min for maintenance of a surgical anesthetic plane) and received 0.01 mg/kg of subcutaneous buprenorphine. At the completion of all procedures, skin was closed with 4–0 Vicryl sutures (Ethicon Inc., Somerville, NJ). All surgeries were performed in a dedicated animal surgery facility at the University of Alberta.

5.2.3 Conditioning: Animals in the CES cohort received a 2 cm longitudinal incision at the right lower limb to isolate the sciatic nerve via blunt dissection proximal to the trifurcation point. CES animals received 20Hz electrical stimulation at 0.1 ms duration for 60 minutes to the sciatic nerve proximal to the trifurcation point, using an SD-9 stimulator (Grass Instruments, Quincy, MA) Settings were based on previous studies (Jo et al., 2019; Senger et al., 2018; 2019). Stainless-steel wire with bared ends was wrapped around the nerve, and the return electrode was placed into the tibialis anterior muscle; these were connected to the cathode and anode ports of an SD-9 stimulator. Excitation of the nerve was confirmed based on contractions of the foot. Unconditioned animals did not receive any experimental or surgical intervention. Sham electrical stimulation was not used as previous studies indicated no difference between unconditioned and sham animals (Senger et al., 2018; Senger et al., 2019).

5.2.4 Tissue Collection: Three days following conditioning for tissue culture, animals were euthanized with carbon dioxide and exsanguinated by opening the thoracic cavity and cutting the left ventricle of the heart. The sciatic nerve was re-exposed and traced to the L4-L5 level of the vertebral column. L4 and L5 DRGs were exposed and harvested, and placed into Hank's buffered salt solution (HBSS) modified medium (HyClone) and placed under a dissecting scope for removal of the epineurium and axon branches. Processed L4/L5 DRGs are transferred into sterile HBSS medium.

5.2.5 Tissue Culture: 1-7 days before culture, 500µL of 0.1 mg/mL poly-D-lysine suspended in sterile water (mol wt 70,000–100,000 kD) (Sigma) evenly distributed over bottom of well in a 24 well glass bottom plate (Cellvis). Solution left on wells for 15 minutes at room temperature, and wells washed 3x100µL with sterile water. Plate was allowed to dry for several hours in sterile hood, and stored sealed at 4°C. On the day of the culture, plates are coated with 500µL laminin (Mouse 1.0mg/mL) (Invitrogen) diluted in HBSS for a final concentration of 2µL/mL of HBSS. Plates are incubated at 37°C in tissue culture incubator for 2 hours. Laminin is removed immediately before plating cells. Dissected DRGs are washed by placing them into sterile HBSS and tilting to wash 3 times. Sterile 1 mg/mL collagenase (Sigma Aldrich) in HBSS medium is prepared and sterilized using a 0.22µm low protein binding syringe filter (Thermo Fisher Scientific). The washed DRGs were placed into collagenase solution and incubated in 37°C water bath for 1 hour. 0.05% of filter sterilized trypsin in HBSS (Sigma Aldrich) is added after 1 hour, and the incubation is continued for 15 minutes. Sterile 1mL pipette tips are used to aspirate DRGs with 10 passes through sterile tip for mechanical digestion. DRGs are incubated for 15 minutes in water bath if DRGs do not aspirate through 1mL tips. Aspiration continued with 1mL tips until DRGs passed easily through tips, then aspirated DRGs with 200µL tips for 10 passes. Incubated ganglia for 5 minutes in water bath. Repeated aspiration and incubation of ganglia until cells in suspension. 100µL fetal bovine serum (FBS) (Sigma Aldrich) was added to stop further enzyme reactions. Cell suspension then centrifuged at 800-1000 rpm for 7 minutes. Removed supernatant and resuspended cells in HBSS medium. Repeated centrifugation, removed supernatant, and resuspended cells in cell medium: Dulbecco's Modified Eagle Medium/F12 (DMEM) (Gibco), 1% N2 supplement (Thermo Fisher Scientific), and 1% pen-strep (HyClone). Plated cells with approximate concentration of 1000 neurons per well. Stored plate in 37°C tissue culture incubator for 48 hours or 5 days. Day of culture is considered Day 0. On Day 1 of the 48 hour cultures, 250µL of growth medium is pipetted out of each well and 250µL of fresh medium is pipetted in along with the full concentration of inhibitors for each respective treatment.

5.2.6 Immunocytochemistry for Tissue Culture: At experimental endpoints, an equivalent volume of 8% PFA was added to the media for an end concentration of 4%. Wells were incubated for 15-20 minutes at room temperature and wells washed with Dulbecco's phosphate buffered saline (DPBS) (Gibco) 3 times. Cells were permeabilized and blocked with 250µL 0.2% Triton X-100 in DPBS with 10% normal goat serum (NGS) (LifeTech) for 60 minutes at room temperature, then incubated overnight 4°C with primary antibody solution of β-III tubulin in DPBS (Table 5.5.1). The following day, cells were washed with DPBS 3 times, then incubated with DAPI (Invitrogen) and a secondary antibody solution of Cy3 in DPBS for 60 minutes at room temperature (Table 5.5.1). Following incubation, cells were washed 3 times with DPBS, and sealed and stored at 4°C.

5.2.7 Imaging: In vitro DRG neurons were imaged at 20X using High Content Screening Analysis ImageXpress Micro AI imaging system (MetaXpress XLS, Molecular Devices, San Jose, CA, USA). Total neurite outgrowth and length of primary neurite was analyzed using Image J software. Individual neurites were traced and measured to calculate total neurite outgrowth, and the longest neurite per DRG neuron was considered the primary neurite. DRG neurons overlapping neurite extension with other DRG neurons were excluded.

5.2.8 Statistical Analysis: Experimental results are written as the mean ± standard error mean *(s.e.m).* Significance of neurite outgrowth was determined using a one-way analysis of variance (ANOVA) to determine any differences in the mean between groups followed by a post-hoc Dunnett's test to compare experimental groups against unconditioned animals. A level of $p<0.05$ was the cut-off for statistical significance. Statistics were completed using Prism 9.3.1 (GraphPad Software, San Diego, CA).

Table 5.2.1 Primary and Secondary Antibody Protocols for Immunohistochemistry

Primary Antibody	**Antigen Retrieval** 40 minutes in 60 °C citrate buffer (10mM sodium citrate, 0.05% Tween-20, pH 6.0)	**Primary Antibody Dilution**	**Secondary Antibody**	**Secondary Antibody Dilution**
B Tubulin-III Sigma (rabbit) T2200	No	1:1000	Cy3 goat anti-rabbit Jackson Labs 111-167-003	1:1000

5.3 Results

5.3.1 EPAC and PKA co-inhibition does not impact neurite extension of naive DRG neurons.

Unconditioned Thy-1-*GFP* Sprague Dawley rat DRG neurons were placed *in vitro* for 48 hours (n=3) in the presence of EPAC and PKA pharmacological inhibitors. DRG neurons were imaged using MetaXpress software, and analyzed using Image J software following β-III tubulin immunohistochemistry Our triplicate *in vitro* experiments revealed treatment of naive DRG

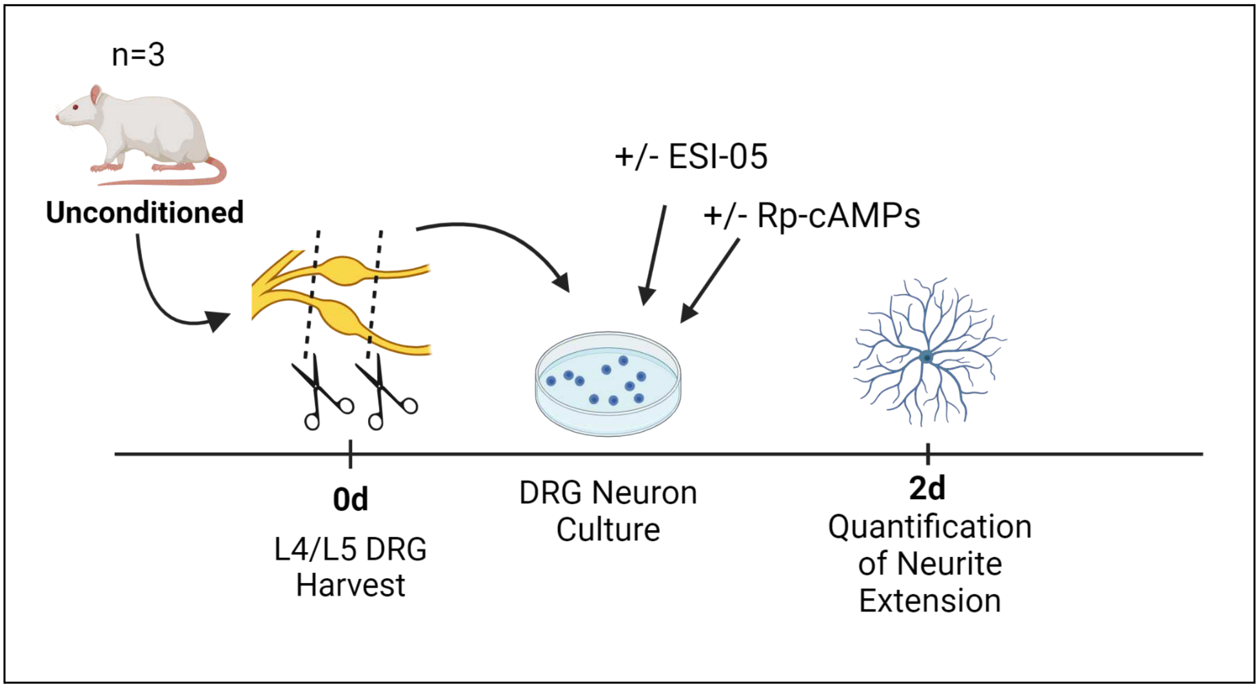

Figure 5.3.1 Experimental design of *in vitro* manipulation of cAMP signaling in naive DRG neurons.

neurons with 1µM ESI-05 (EPAC inhibitor), 10µM Rp-cAMPs (PKA inhibitor), or both, did not significantly impact total neurite extension or the longest neurite per DRG neuron. Untreated DRG neurons reported an average of 1839.4µm ± 510.7µm total neurite outgrowth, and an average length of the primary neurite of 323.6µm ± 11.4µm. ESI-05 treated DRG neurons showed no overall change in average total neurite outgrowth (76.6% ± 7.2% of control), or in average length of longest neurite (98.8% ± 12.2%) (p>0.05). Rp-cAMPs treated DRG neurons

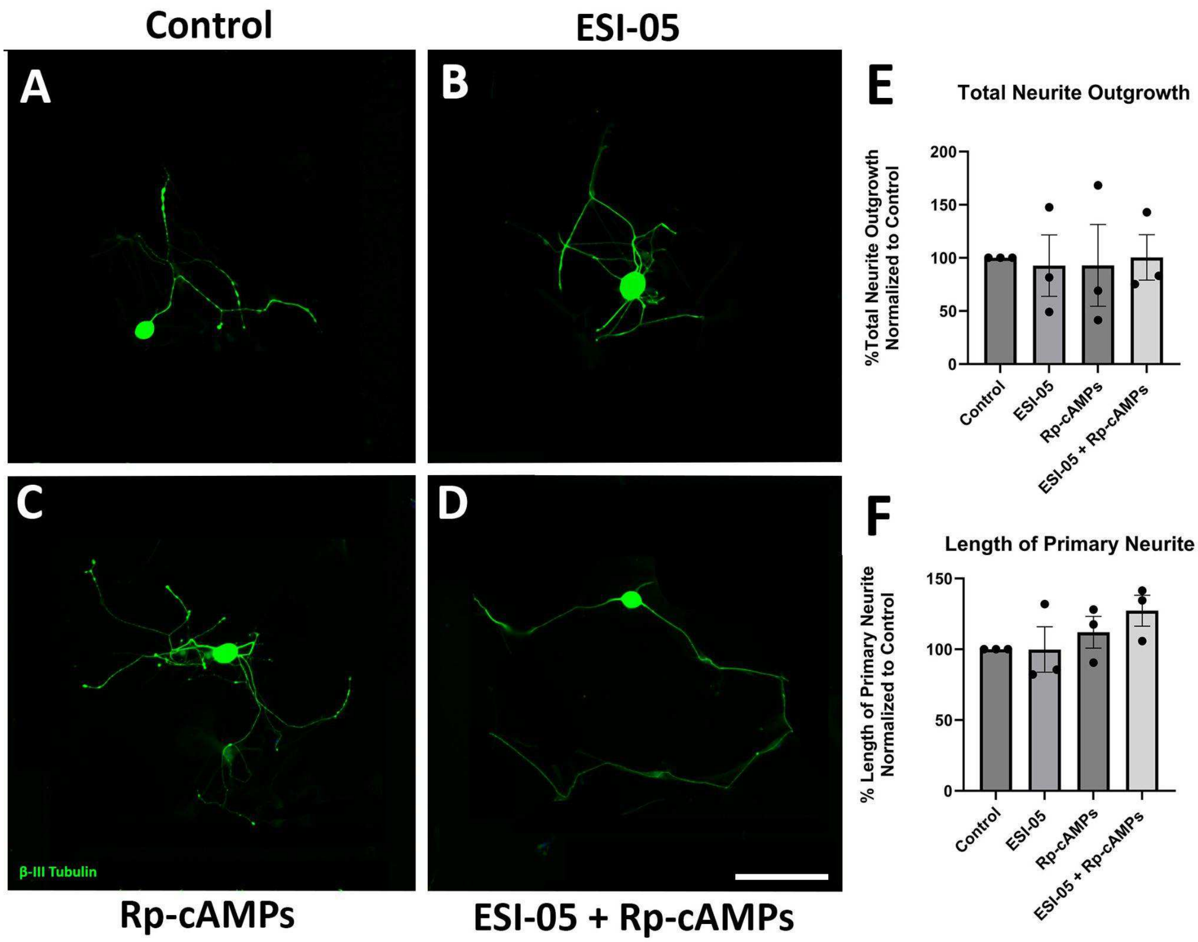

Figure 5.3.2 The inhibition of cAMP effectors EPAC and PKA do not affect the regenerative capacity of naive DRG neurons. (A-D) β-III tubulin immunostained 48 hour cultured DRG neurons in vitro treated with no inhibitors (A), 1μM ESI-05 (B), 10μM Rp-cAMPs (C), or 1μM ESI-05 and 10 μM Rp-cAMPs (D) (n=3). (E-F) Pharmacological inhibition of PKA and EPAC do not significantly affect total neurite outgrowth or length of primary neurite in naive DRG neurons cultured over 48 hours ($p<0.05$). Scale bar in D indicates a length of 100μm.

showed no overall change in average total neurite outgrowth (71.7% ± 6.63% of control), or in average length of longest neurite (111.6% ± 10.2% of control) (p>0.05). ESI-05 and Rp-cAMPs treated DRG neurons also revealed no change in average total neurite outgrowth (88.8% ± 7.9% of control) or average length of longest neurite (126.6% ± 10.9%) (p>0.05) (Figure 5.3.2).

5.3.2 EPAC and PKA co-inhibition prevents neurite extension in CES conditioned DRG neurons.

DRG neurons, conditioned by CES three days prior, were plated and left to grow for 48 hours with either no treatment, 1μM ESI-05, 10μM Rp-cAMPs, or both, before neurite extension

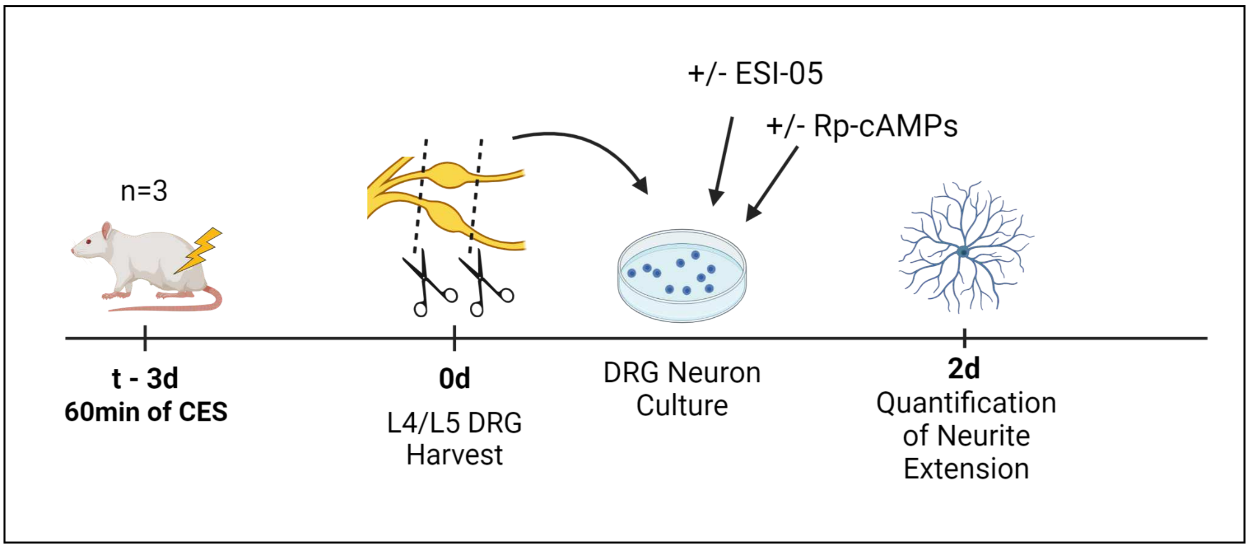

Figure 5.5.3 Experimental design of *in vitro* manipulation of cAMP signaling in naive DRG neurons.

was quantified. Conditioned neurons without inhibitor treatment were considered control DRG neurons, and outgrowth of conditioned and inhibitor treated DRG neurons was normalized to the outgrowth of control neurons within the respective triplicate experiment. Control DRG neurons reported an average total neurite outgrowth of 3363.7μm ± 797.5μm, and an average length of longest neurite of 692μm ± 100.2μm. ESI-05 treated conditioned DRG neurons revealed an average total neurite outgrowth of 65.9% ± 5.6% of control (p<0.05), and an average length of longest neurite of 88.2% ± 12.7% of control (*$p>0.05$). Rp-cAMPs treated conditioned DRG neurons revealed an average total neurite outgrowth of 81.1% ± 12% of control (*$p>0.05$), and an average length of longest neurite of 112.5% ± 28.6% of control (*$p>0.05$). ESI-05 and Rp-cAMPs treated conditioned DRG neurons revealed an average total neurite outgrowth of 39.7% ± 4.2% of control ***($p<0.001$), and an average length of longest neurite of 49.3% ± 4.6% of control (*$p<0.05$). (Figure 5.3.4). In summary, we demonstrated that CES DRG neurons treated with both ESI-05 and Rp-cAMPs blocked the CES conditioning effect on total neurite outgrowth, but treatment of ESI-05 or Rp-cAMPs alone did not.

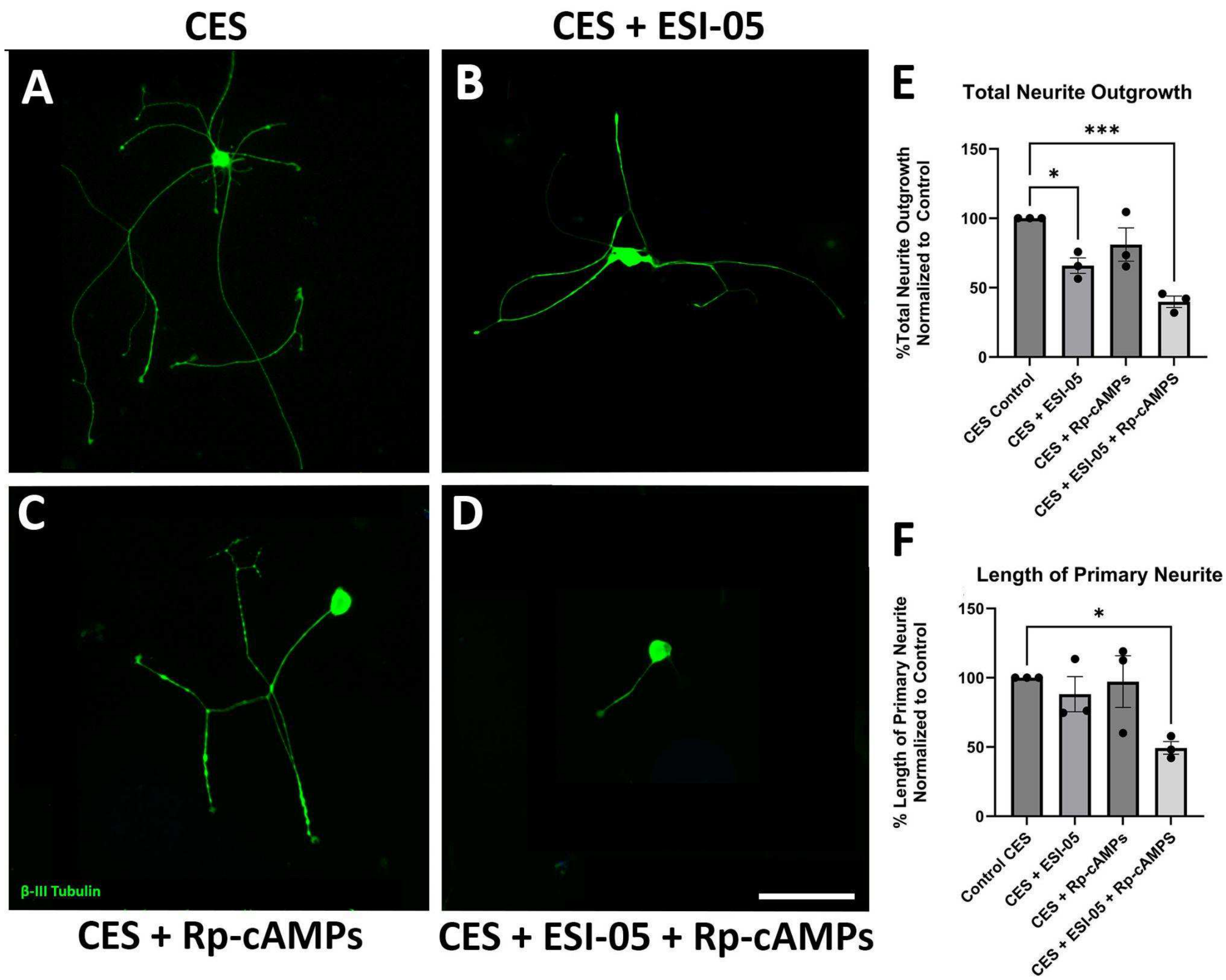

Figure 5.3.4 The inhibition of cAMP effectors EPAC and PKA eliminate the pro-regenerative effects of CES in DRG neurons. β-III tubulin immunostained 48 hour cultured DRG neurons *in vitro*, conditioned with 1 hour of CES *in vivo* with a 3 day latency period, and treated with no inhibitors (A), 1μM ESI-05 (B), 10μM Rp-cAMPs (C), or 1μM ESI-05 and 10μM Rp-cAMPs (D) (n=3). (E-F) The combination of ESI-05 and Rp-cAMPs ablates the pro-regenerative effects of CES, reducing both total neurite outgrowth (***$p<0.001$), and the length of the primary neurite (*$p<0.05$). Treatment of ESI-05 alone reduces total neurite outgrowth (*$p<0.05$), but not the length of the primary neurite ($p>0.05$). Scale bar in D indicates a length of 100μm.

5.4 Discussion

5.4.1 cAMP plays a minimal role in regeneration of naive DRG neurons

We found that EPAC and PKA inhibition did not interfere with the regenerative capacity (measured as total neurite outgrowth or the length of the primary neurite) of unconditioned DRG neurons. These data could be explained by the innate low levels of cAMP in unconditioned DRG neurons (Anderson et al., 2000). Our findings are contradictory to Wei et al., (2016) who demonstrated that EPAC and PKA co-inhibition decreased neurite extension of naive DRGs. The methodologies of these studies were different; our study investigated neurite extension of individual DRG neurons after 2 days, while Wei and colleagues measured DRG neurite outgrowth of the entire culture dish after 7 days. It is possible that our culture timeline was too short for the effect of cAMP inhibition to effectively impact neurite extension. Additionally, with lower levels of cAMP, inhibiting cAMP may have a smaller impact on naive growth, and any significant effects may be masked by a small sample size. The lack of inhibitory effect on naive DRG neurons cultured for 2 days suggests that the decrease in growth capacity observed in CES-treated DRG neurons is unique to the conditioning effect, rather than the effect of the inhibitors on innate growth capacity.

5.4.2 cAMP signaling mediates the effect of CES on regeneration in vitro

Total neurite outgrowth was significantly reduced in conditioned DRG neurons with treatment of both inhibitors, indicating a role for both cAMP effectors in the conditioning effect of CES. Surprisingly, EPAC inhibition alone reduced total neurite outgrowth, while inhibition of PKA alone did not affect outgrowth in conditioned DRG neurons. This is unlike naive outgrowth over 7 days, in which inhibiting PKA appeared to shunt cAMP activity to EPAC, thereby

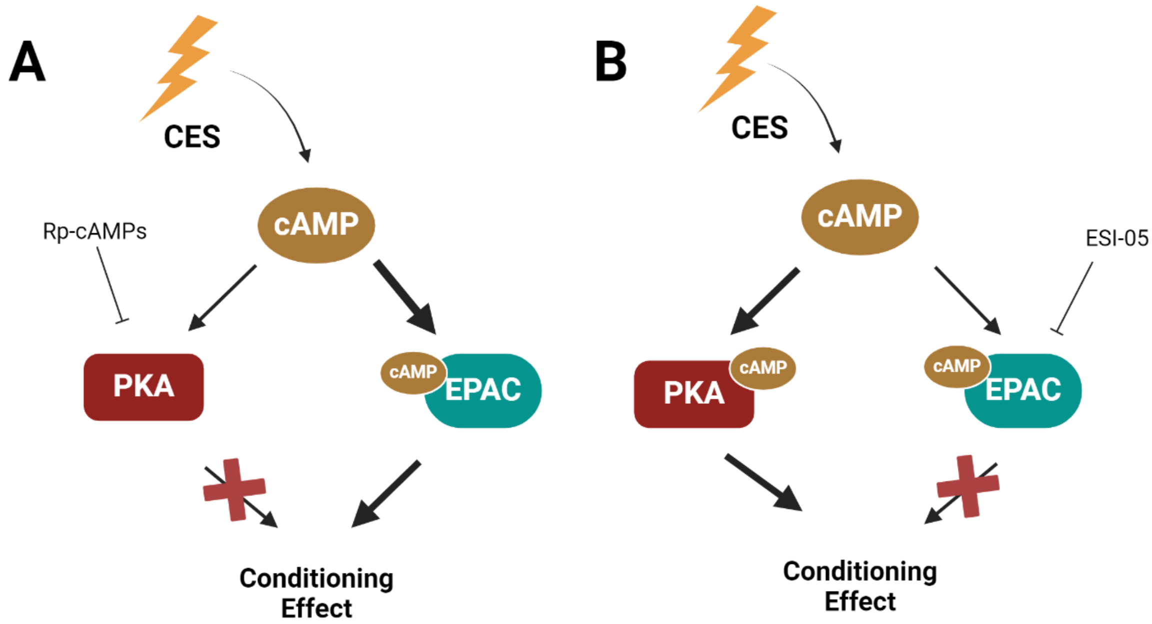

Figure 5.4.1 cAMP signaling elicits a conditioning effect of CES with a compensatory mechanism. (A) Rp-cAMPS inhibition of PKA and (B) ESI-05 inhibition of EPAC are insufficient to completely abolish the conditioning effect of CES alone.

promoting outgrowth (Wei et al., 2016). Though PKA inhibition does not promote outgrowth in conditioned DRG neurons, PKA also does not compensate for the loss of EPAC. Alternatively, EPAC compensates for the loss of PKA. Thus, similar to the conclusions of Wei and colleagues (2016) in unconditioned DRG neurons, our results suggest that EPAC may play a more significant role in the conditioning effect of CES compared to PKA. However, although EPAC adequately compensates for PKA, shunting all cAMP pathway activity through the EPAC pathway does not increase outgrowth. This suggests PKA may still play some integral role in conditioning, just to a lesser extent than EPAC. Furthermore, blocking both cAMP effector pathways abolishes the conditioning effect on total neurite outgrowth and the length of the primary neurite, unlike EPAC inhibition alone. Thus, EPAC and PKA together must be significantly involved in the mechanism of CES-mediated outgrowth.

5.4.3 EPAC and PKA may play different roles in CES

Though EPAC and PKA must both play integral roles in CES mediated outgrowth, these effectors may differ in their roles. PKA compensates for EPAC inhibition when the length of the primary neurite is assessed, but not total neurite outgrowth. Further, EPAC compensates completely for the loss of PKA. This may suggest that signaling between the effectors overlap, while EPAC further activates other signaling pathways to elicit a pro-regenerative response in CES that PKA is incapable of activating. pCREB and RhoA serve as known targets of PKA and EPAC to promote regeneration (Dong et al., 1998; Enserink et al., 2002; Lehmann et al., 1999; Wei et al., 2016) but the involvement of these effectors and other signaling pathways to promote regeneration is unknown in the context of CES. To garner complete understanding of the role of EPAC and PKA in CES, a mechanism for these effectors to elicit the conditioning effect of CES must be investigated.

EPAC and PKA have been found to elicit opposing effects on the PI3K pathway; in human embryonic kidney (HEK) cells, cAMP activation of EPAC results in increased Akt phosphorylation and activity, while PKA activation results in upregulation of unphosphorylated Akt protein levels (Mei et al., 2002). Rap1, as a main downstream target of EPAC, is found to activate PI3K, independent of PKA. Treating HEK cells with PKA inhibitors promotes Akt phosphorylation (Mei et al., 2002). The authors suggest that these diverging effects of EPAC and PKA may mediate cell-specific cAMP effects, based on either effector's expression. In the context of regeneration, the PI3K-Akt pathway mediates the pro-regenerative response to neurotrophins in DRG neurons (Singh et al., 2015), and deletion of PTEN, a known regenerative 'brake' of the PI3K-Akt pathway, results in enhanced axon regeneration (Christie et al., 2010). PTEN mRNA downregulates significantly following axotomy, but PTEN protein remains preserved in DRG neurons in both the axonal growth cone and cell body, and continues as a regenerative brake: promoting unphosphorylated GSK3-mediated growth cone collapse, and preventing activation of pro-regenerative genes in the cell body (Christie et al., 2010; Krishnan et al., 2016). Singh and colleagues (2015) have demonstrated that activation of PI3K partially mediates the conditioning effect of CES in DRG neurons *in vitro.* If EPAC activation promotes phosphorylation of Akt in DRG neurons, akin to HEK cells, CES-mediated activation of EPAC (and therefore Rap1) may target PI3K/Akt to facilitate regeneration; pAkt phosphorylates GSK3 to stabilize the growth cone, as well as to upregulate and phosphorylate Smad1, a factor responsible for transcription of pro-regenerative genes (Saijilafu et al., 2014; Singh et al., 2015). Alternatively, PKA inhibition of Akt may impede this pro-regenerative response. My results suggest that CES/cAMP-mediated PKA activation does not negatively impact regeneration overall. Thus, it is not likely that in CES, PKA completely inhibits the pro-regenerative response mediated by PI3K; instead, we propose that while PKA does contribute to PI3K inhibition, other molecules, including CES upregulated neurotrophins, counteract the effects of PKA. My data suggests PKA activates pro-regenerative pathways, as the combined inhibition of EPAC and PKA negatively affects regeneration, though these pathways are likely independent of PI3K. Together, we propose that PKA activation of PI3K-independent pathways compensates for any inhibitory effect of PKA on PI3K, resulting in a net pro-regenerative effect.

EPAC may serve as a more effective mediator of cAMP to promote regeneration, given that inhibition of EPAC alone slightly reduces the regenerative capacity. It is possible that EPAC mediated activation of Akt provides an alternate pathway for cAMP to promote regeneration, giving EPAC a broader range of pro-regenerative pathways to activate when compared to PKA. Potential activation of this pathway may explain differences between EPAC and PKA inhibition on naive and CES-treated DRG neurons; the PI3K pathway has previously been shown to play a role in the mechanism of CES (Singh et al., 2015). As neurotrophins also mediate the PI3K pathway, CES would upregulate PI3K activation regardless of cAMP activation. EPAC likely compensates for the loss of PKA as EPAC activates similar pathways, and potentially further activates PI3K. Loss of PKA may not affect outgrowth in conditioned DRG neurons as the PI3K pathway is also targeted by neurotrophins to combat PKA inhibition. However, a loss of EPAC may result in a more even activation and inhibition of PI3K between neurotrophins and PKA. Alternatively, naive DRG neurons likely have much lower activation of PI3K. It is possible that when PKA is inhibited in naive DRG neurons, as in Wei et al (2016), PI3K is released from PKA-mediated inhibition, and EPAC is free to combat PTEN mediated inhibition of PI3K, and promote PI3K signaling. Thus, inhibition of PKA results in newfound activation of PI3K in naive DRG neurons, and an increase in neurite outgrowth. Adding an EPAC agonist results in a similar increase in neurite outgrowth, which may indicate that increasing the proportion of EPAC relative to PKA may promote regeneration (Wei et al., 2016). Further studies should be conducted to determine whether EPAC promotes regeneration through activation of Akt to elicit the conditioning effect of CES.

EPAC and PKA both are implicated in regulation of the ERK1/2 pathway. EPAC directly activates Rap1, which activates ERK through either Raf1 alone, or B-Raf and Raf1, while PKA inhibits Raf1 (Dhillon et al., 2002; Enserink et al., 2002). Though PKA has also been shown to bind and activate Rap1 (Vossler et al., 1997), Rap1 activation in DRG neurons is specifically associated with EPAC, and Rap1-mediated activation of ERK is independent of PKA (de Rooij et al., 1998). ERK signaling has been shown to be involved in promoting regeneration following axotomy, but not in spontaneous regeneration, or the pro-regenerative effects of conditioning lesions (Hausot et al., 2022; Hausot & Klimaschewski, 2019; Traverse et al., 1992). However, ERK signaling has been associated with neurotrophin-mediated axon elongation in naive DRG culture (Atwal et al., 2000), and in CES-treated DRG culture (Yan et al., 2014). Downstream targets of ERK include cJun, pCREB, and Elk-1 (Enserink et al., 2002; Hausot & Klimaschewski, 2019; Perlson et al., 2005), potentially mediating the pro-regenerative effects associated with neurotrophins. cAMP effectors appear to produce a diverging effect on ERK, as EPAC appears to upregulate ERK while PKA inhibits ERK (Dhillon et al., 2002; Enserink et al., 2002). ERK has been shown to mediate CES-induced upregulation of BDNF expression (Yan et al., 2014). EPAC and PKA thus far have not demonstrated to activate ERK in the context of CES, and though ERK has been implicated, the upstream activators Rap1, Raf1 and B-Raf have not. However, if cAMP does elicit ERK activation following CES, ERK signaling may be a point of divergence for the roles of EPAC and PKA in CES. EPAC may act to contribute to ERK signaling, while PKA counteracts ERK signaling. Similar to the PI3K pathway, neurotrophin signaling that is likely induced following CES (as suggested by Yan et al., 2014) promote ERK signaling, and PKA inhibition of Raf1 is insufficient to block the resulting promotion of regeneration. However, EPAC may contribute significantly to the activation of ERK, providing another signaling pathway in which the roles of the cAMP effectors may differ. However, cAMP has been shown to both activate and inhibit ERK signaling in different contexts (Enserink et al., 2002). It is unknown in what contexts PKA will inhibit or EPAC activate ERK signaling.

Before considering potential signaling pathways that EPAC and PKA help to mediate the pro-regenerative effects of CES, the expression and activation profiles of the effectors should be determined. Udina (2008) has established that cAMP upregulation occurs as early as 24 hours following stimulation. However, we have previously established that a minimum of a 3 day latency period is required to elicit pro-regenerative effects in DRG neurons following *in vivo* CES. Thus far, we have not yet established a timeline for cAMP upregulation, or EPAC and PKA upregulation. In our studies, cAMP effectors were targeted between 3 and 5 days following conditioning to intercept the signaling pathways as early in their mechanism as possible, while ensuring the pro-regenerative effects of CES were elicited *in vitro*. Downstream targets of cAMP (pCREB and BDNF) upregulate as early as 1 day post-conditioning and are maintained until at least 7 days post-conditioning, suggesting that cAMP effectors remain active within the timeframe we target them pharmacologically. However, no studies have investigated a timeline for either cAMP activation or resulting EPAC or PKA activity post-CES. Thus, it is unknown when EPAC and PKA are optimally active; cAMP directly binds to both EPAC and PKA to induce conformational changes and expose the catalytic domain of both effectors (de Rooij et al., 1998) and as cAMP upregulates 24 hours following CES (Udina et al., 2008), EPAC and PKA are likely activated shortly after. EPAC and PKA are also known to activate pCREB (Wei et al., 2016), which I've demonstrated upregulates 1 day post-CES. Together, this suggests EPAC and PKA are active earlier than 3 days post-CES. To confirm this, a timeline of cAMP upregulation should be investigated, as EPAC and PKA activity likely directly follows that of cAMP. Alternatively, levels of EPAC and PKA activation could be directly assessed with immunohistochemistry using antibodies specific to their post-translationally modified active forms. It is unknown whether cAMP activates EPAC or PKA to different degrees, and determining a timeline and extent of activation may inform on differences in either effectors' role. If the optimal activity of these effectors precedes the pro-regenerative effects elicited *in vitro*, abolishing cAMP signaling *in vivo* before DRG neuron culture may better determine the extent of involvement of the cAMP pathway in CES. Further, cAMP activity should be abolished *in vivo* following CES prior to nerve transection and repair to confirm cAMP signaling is also involved in the pro-regenerative effects in *in vivo* regeneration, as well as the effects of cAMP signaling on RAG expression. Quantification of pCREB and BDNF following EPAC inhibition, PKA inhibition, or both will give further insight into whether these RAGs are upregulated in response to cAMP effectors.

Discussion

Establishing parameters for the clinical translation of CES

Our lab has previously demonstrated CES to be a non-inflammatory intervention (Senger et al., 2022) to promote regeneration in rat and mouse animal models, making the intervention an ideal candidate for clinical translation (manuscript in preparation). As CES clinical trials are underway, investigating the parameters necessary to elicit pro-regenerative effects of CES in preclinical models may guide the parameters investigated clinically. Many parameters used in CES protocols have been adapted from those of PES; PES has already been clinically validated (Barber et al., 2015; Gordon et al., 2010; Power et al., 2020), which suggests that parameters of CES may also translate accordingly. However, there remain challenges for use of either CES or PES in clinic. With limited time and resources, surgeons have opted for using as little as 10 minutes of PES in patients following nerve repair surgery. Preclinical evidence may suggest 10 minutes of PES sufficiently promotes regeneration in rats (Roh et al., 2022), though this is not yet backed by clinical evidence. Additionally, the SD-9 Grass Stimulator, traditionally used to administer both CES and PES preclinically and clinically, is not commercially available, and other stimulators have been proposed as alternatives. Our research seeks to establish a clinical precedent for the utilization of CES (with preclinical evidence), effectively balancing the time constraints of the operating room and the stimulation equipment available, with effective treatment for patients with peripheral nerve injury.

Our studies in CES suggest 10 minutes does not promote regeneration. As the duration of stimulation increases for CES, the conditioning effect strengthens. We establish 30 minutes as the minimum duration to elicit a conditioning effect, while 1 hour remains the most effective. Our results suggest CES to be a cumulative process, in which increasing the duration of stimulation upregulates key signaling pathways until key messengers are maximally active. Ten minutes elicits small changes, either not significant or unlikely to improve recovery of function. Ten minutes increases the number of regenerating axons capable of crossing the nerve repair site without affecting the length of regeneration, RAG protein expression, or the number of axons distal to the nerve repair site. This supports CES as a cumulative activation of signaling pathways, and reveals the initial effects of CES on regeneration. Studies to assess sensory and motor reinnervation and functional recovery should be conducted to further determine if 10 minutes sufficiently promotes regeneration.

Administering CES using Checkpoint stimulation sufficiently promotes regeneration, but only when 1 hour of CES is delivered, diverging from preclinical evidence suggesting 10 minutes of Checkpoint-delivered PES promotes regeneration (Roh et al., 2022). SD-9 and Checkpoint stimulators both deliver biphasic pulses, but only SD-9 stimulators allow for easy adjustment. Checkpoint stimulators are programmed to deliver 16Hz of stimulation, with options to adjust the amplitude to either 0.5mA, 2mA, or 20mA. Conversely, SD-9 stimulators allow adjustment for voltage, and voltage is titrated to elicit visible muscle twitch preclinically in CES, or to patient tolerance clinically in either PES or CES. Adjusting SD-9 stimulation to model that of Checkpoint may have more accurately assessed the efficacy of either stimulator. However, we chose to assess stimulator efficacy as they would be used in clinic. As these parameters did not seem to significantly affect the conditioning effect, there may be a degree of flexibility in stimulation equipment. Our evidence suggests that the length of stimulation remains a much more important factor in the efficacy of CES.

As the frequency of stimulation for CES has been adopted from that of PES, it may be prudent to investigate the effects of frequency on the pro-regenerative effects of CES. 20Hz was initially chosen as this is the average frequency of motor neuron action potentials (Burke, 1981). As motor neurons feature the fastest frequencies of action potentials, it follows that increasing the frequency of stimulation diminishes pro-regenerative effects found in PES (Lu et al., 2008; Udina et al., 2008). Lower frequencies than 20Hz also elicit pro-regenerative effects in PES (Lu et al., 2008; Ming et al., 2001; Yan et al., 2014; Yeh et al., 2010). Action potential conduction and frequency decreases as the degree of myelination also decreases, with differences in frequency proposed to segregate mechano-sensory information (Fischer et al., 2017). Different frequencies of stimulation may preferentially activate different neuronal subtypes; as opposed to large motor fibers, small diameter C-fibers feature lower neuronal firing rates (Burke, 1981). It is unknown how frequency of stimulation affects different neuronal subtypes.

CES has been demonstrated to promote regeneration in rat and mouse models (data not shown, manuscript in preparation). Though the evidence of CES in multiple species suggests the intervention may also promote regeneration in humans, other animal models may more closely represent the challenges of peripheral nerve regeneration, and the pro-regenerative effects of CES. A major discrepancy between rodent and human models is the distance for regeneration; small rodents feature much shorter distances for reinnervation when compared to humans. Due to the shorter distance required for reinnervation, rodents typically exhibit functional recovery even without intervention, and thus the chronic denervation phenotypes that limit regeneration and recovery in human models are not accurately represented. Larger models such as swine models may better represent the distances for regeneration that must occur following peripheral nerve injury, and therefore simulate the challenges commonly found in regeneration in humans (Kinsley et al., 2021). Investigation into CES in swine models may also reveal new aspects of the pro-regenerative mechanism not previously identified in rodent models. Ultimately, investigating

CES in swine models may provide us with stronger evidence to establish parameters of use for CES in clinic.

Mechanistic insights into CES: CES as a cumulative activation of signaling pathways to elicit a conditioning effect.

We propose that CES accelerates the innate rate of regeneration; by activating signaling pathways that enhance the capacity for cytoskeletal component transport and growth cone protrusion, regenerating axons are able to advance at a faster rate, reaching their target for reinnervation earlier. Evaluation of RAG protein expression lends to this hypothesis. BDNF and pCREB have been implicated in CES mechanism (Yan et al., 2014), and upregulation of both RAGs either precedes or coincides with the emergence of the conditioning effect. RAG expression is sustained until at least 7 days post-conditioning, according to our results, and previous studies have demonstrated RAG expression to remain upregulated as long as 14 days post-conditioning (Senger et al., 2018b). Similarly, the conditioning effect emerges between 3 and 7 days post-conditioning. It is unknown how long the conditioning effect persists after 7 days, though the accelerated rate of regeneration that allows for accelerated recovery of function in rodent models suggests the conditioning effect is sustained over weeks (Senger et al., 2019). More in depth timelines of activation of RAGs and emergence of the conditioning effect would allow for further comprehension of the mechanism of CES; evaluating the regenerative capacity at 12, 24, 36 and 48 hours may serve to establish the relative timeline of signaling pathway activation to culminate in the conditioning effect.

As CES is a relatively new intervention, previous literature has not differentiated between paradigms of CES and PES. In teasing out the different mechanisms of both CES and PES, 3 main signaling pathways appeared to mediate the pro-regenerative effects of CES; PI3K and ERK have been directly implicated in CES mediated neurite outgrowth (Singh et al., 2015; Yan et al., 2014), while our data implicates cAMP and its downstream effectors EPAC and PKA. Both PI3K and ERK signaling pathways have been demonstrated to overlap with cAMP signaling, though not in regenerative contexts. We propose that CES induced Ca^{2+} release (Hu et al., 2019; Singh et al., 2015; Wenjin et al., 2011; Yan et al., 2014; Yan et al., 2016) activates cAMP signaling, thereby activating EPAC and PKA to promote RhoA inhibition, and CREB phosphorylation, which in turn upregulates neuronal BDNF expression (McGregor & English, 2019) (Figure 6.1). Thus far, cAMP and Ca^{2+} signaling have not been linked in the context of CES; however, it is well established that cAMP upregulates in response to Ca^{2+}(Cooper et al., 1995) and both pCREB and BDNF expression following CES have been linked to Ca^{2+} release (Yan et al., 2014; Yan et al., 2016). Upregulation of these RAGs allows the neuron to shift to a regenerative phenotype prior to the injury sustained. It is likely that the phenotypic shift occurs between 1 and 3 days post-conditioning, with signaling pathways sufficiently upregulated at 3 days to elicit a conditioning effect. RhoA is present in uninjured peripheral nerves, RhoA significantly upregulates following injury (Webber & Zochodne, 2010), and CES (unpublished data). Further, cAMP mediated RhoA inhibition has primarily been found to be NGF/TrkA dependent at the growth cone (Gao et al., 2003), as opposed to Ca^{2+} release dependent. cAMP may elicit its pro-regenerative signaling through RhoA inhibition following injury, after the growth cone has formed and RhoA has been upregulated.

PI3K and ERK signaling has been demonstrated to be neurotrophin dependent, though Ca^{2+} signaling has also been implicated in ERK functions in CES (Yan et al., 2014). It is likely that CES induces axonal release of neurotrophins to act upon axonal neurotrophic receptors,

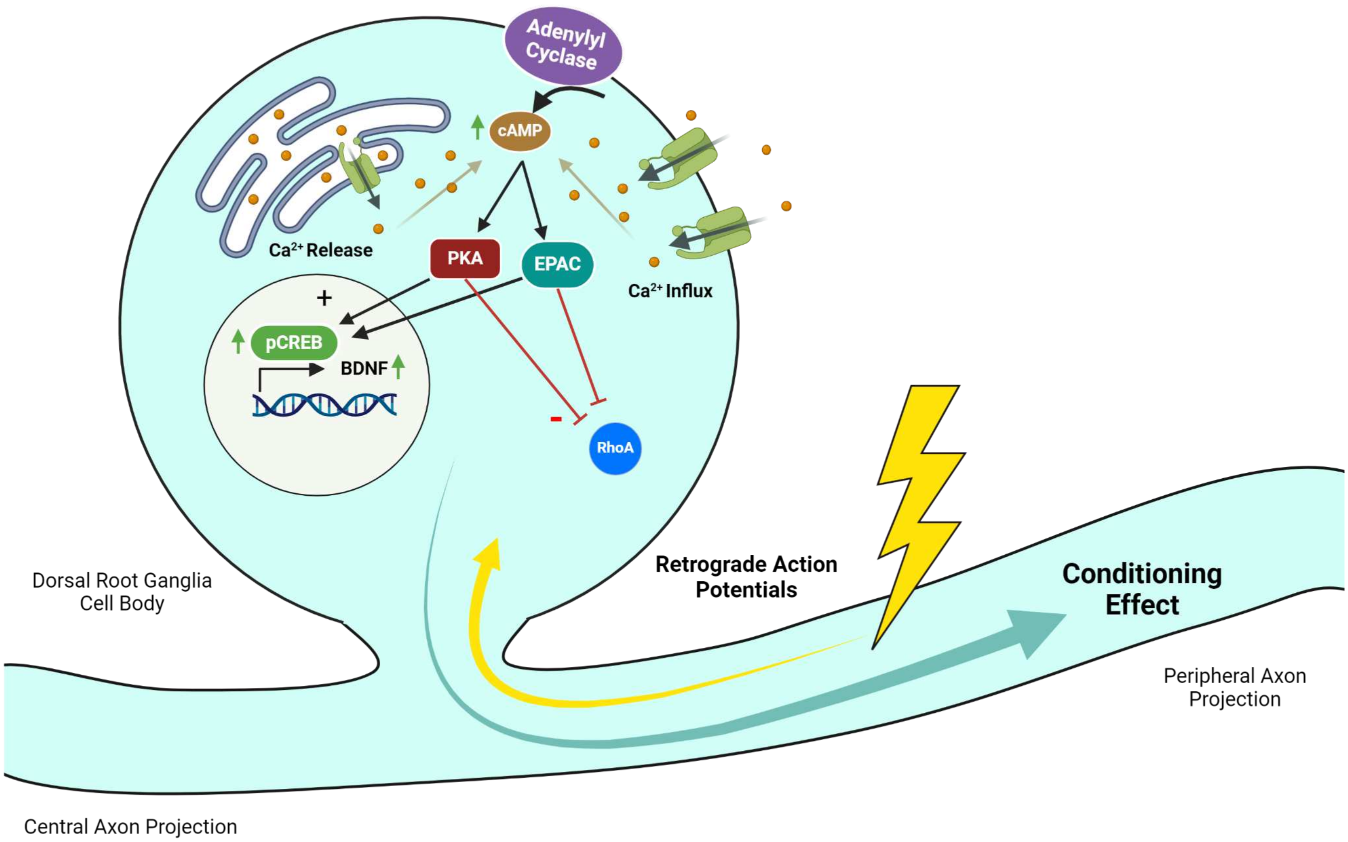

Figure 6.1 Proposed mechanism of CES mediated upregulation of cAMP to mediate its proregenerative effects. CES induces retrograde action potentials, causing Ca^{2+} influx and release into the cell body. Ca^{2+} signaling increases cAMP activation, which activates PKA and EPAC to phosphorylate CREB and inhibit RhoA. pCREB increases transcription of BDNF. Together this induces the conditioning effect elicited by CES.

particularly as BDNF expression increases following cAMP activation, further eliciting activation of PI3K, ERK, and cAMP pathways (Batty et al., 2020; Hausot & Klimaschewski, 2019; Saijilafu et al., 2014; Singh et al., 2015). Though each of these pathways have been implicated in the mechanism of CES, the specific signaling that elicits the conditioning effect is unknown. Both Ca^{2+} and neurotrophin signaling are understood to promote pro-regenerative transcription factors, polyamines, and cytoskeletal proteins necessary for regeneration, but it is not clear if PI3K, ERK and cAMP differ in their roles of promoting regeneration, or if they serve as a way to elicit a broad regenerative shift in phenotype through multiple pathways. If cAMP effector PKA is demonstrated to inhibit PI3K and ERK activation, as it has been demonstrated in other contexts, cAMP may serve as a regulatory pathway, rather than a purely pro-regenerative pathway.

Following injury, CES signaling pathways remain primed to promote regeneration, and injury signaling further activates key signaling pathways for regeneration, behaving as a conditioning strategy. Senger et al (2019) has demonstrated RAGs to remain upregulated following CES and injury combined, when compared to injured controls. cAMP, PI3K, and ERK pathways upregulate following injury. It is likely that these molecules and their pathways were to be compared between conditioned and unconditioned injured nerve, they would be upregulated in conditioned neurons, following the pattern of RAGs in Senger et al. (2019). The combination of accelerated cytoskeletal transport due to the early activation of signaling pathways, along with the upregulation of key pathways that may counteract any inhibitory signals to growth result in a robust conditioning response following injury. Further analysis is needed to confirm the roles of PI3K, ERK and cAMP signaling to promote regeneration following CES

Bibliography

Accornero, N., Bini, G., Lenzi, G. L., & Manfredi, M. (1977). Selective Activation of peripheral nerve fibre groups of different diameter by triangular shaped stimulus pulses. *The Journal of physiology*, *273*(3), 539–560. https://doi.org/10.1113/jphysiol.1977.sp012109

Ahlborn, P., Schachner, M., & Irintchev, A. (2007). One hour electrical stimulation accelerates functional recovery after femoral nerve repair. Experimental Neurology, 208(1), 137-144.

Aldrashan, M., Sung, M.-A., Kim Kwon, Y., Chung, H.-J., Kim, S.-J., & Lee, J.-H. (2011). Effects of combining electrical stimulation with BDNF gene transfer on the regeneration of crushed rat sciatic nerve. *Acta Neurochirurgica*, *153*(10), 2021–2029. https://doi.org/10.1007/s00701-011-1054-x

Al-Majed, A., Brushart, T., & Gordon, T. (2000a). Electrical stimulation accelerates and increases expression of BDNF and trkB mRNA in regenerating rat femoral motoneurons. European Journal of Neuroscience, 12(12), 4381-4390.

Al-Majed, A., Neumann, C., Brushart, T., & Gordon, T. (2000b). Brief electrical stimulation promotes the speed and accuracy of motor axonal regeneration. *The Journal of Neuroscience*, *20*(7), 2602–2608. https://doi.org/10.1523/jneurosci.20-07-02602.2000

Andersen, P. L., Webber, C. A., Kimura, K. A., & Schreyer, D. J. (2000). Cyclic AMP prevents an increase in GAP-43 but promotes neurite growth in cultured adult rat dorsal root ganglion neurons. *Experimental neurology*, *166*(1), 153–165. https://doi.org/10.1006/exnr.2000.7485

Asensio-Pinilla, E., Udina, E., Jaramillo, J., et al. (2009). Electrical stimulation combined with exercise increases axonal regeneration after peripheral nerve injury. Experimental Neurology, 219(1), 258-265.

Atwal, J. K., Massie, B., Miller, F. D., & Kaplan, D. R. (2000). The TrkB-Shc site signals neuronal survival and local axon growth via MEK and P13-kinase. *Neuron*, *27*(2), 265–277. https://doi.org/10.1016/s0896-6273(00)00035-0

Avraham, O., Deng, P.-Y., Jones, S., Kuruvilla, R., Semenkovich, C., Klyachko, V., & Cavalli, V. (2020). Satellite glial cells promote regenerative growth in sensory neurons. *Nature Communications*, *11*(4891). https://doi.org/10.1038/s41467-020-18642-y

Barabas, M. E., Kossyreva, E. A., & Stucky, C. L. (2012). TRPA1 is functionally expressed primarily by IB4-binding, non-peptidergic mouse and rat sensory neurons. *PloS one*, *7*(10), e47988. https://doi.org/10.1371/journal.pone.0047988

Barber, B., McNeely, M., Chan, K., Beaudry, R., Olson, J., Harris, J., Seikaly, H., & O'Connell, D. (2015). Intraoperative brief electrical stimulation (BES) for prevention of shoulder dysfunction after oncologic neck dissection: Study protocol for a randomized controlled trial. *Trials*, *16*.

Batty, N., Fenrich, K., & Fouad, K. (2016). The role of Camp and its downstream targets in neurite growth in the adult nervous system. *Neuroscience Letters*, *652*, 56–63. https://doi.org/10.1016/j.neulet.2016.12.033

Bautista, M., & Krishnan, A. (2022). Self-renewal of peripheral nerve resident macrophage: Does it represent a unique activation status? *Neural Regeneration Research*, *15*(5), 999–1000. https://doi.org/10.4103/1673-5374.324845

Blesch, A., Lu, P., Tsukada, S., Alto, L., Roet, K., Coppola, G., Geschwind, D., & Tuszynski, M. (2012). Conditioning lesions before or after spinal cord injury recruit broad genetic mechanisms that sustain axonal regeneration: Superiority to camp-mediated effects. *Experimental Neurology*, *235*(1), 162–173. https://doi.org/doi: 10.1016/j.expneurol.2011.12.037

Boivin, A., Pineau, I., Barrette, B., Filali, M., Vallières, N., Rivest, S., & Lacroix, S. (2007). Toll-like receptor signaling is critical for Wallerian degeneration and functional recovery after peripheral nerve injury. *Journal of Neuroscience*, *27*(46), 12565–12576. https://doi.org/DOI: 10.1523/JNEUROSCI.3027-07.2007

Bolívar, S., Navarro, X., & Udina, E. (2020). Schwann Cell Role in Selectivity of Nerve Regeneration. *Cells*, *9*(9), 2131. https://doi.org/10.3390/cells9092131

Bos, J. (2003). Epac: A new cAMP target and new avenues in cAMP research. *Nature Reviews Molecular Cell Biology*, *4*, 733–738. https://doi.org/10.1038/nrm1197

Bosse, F., Hasenpusch-Theil, K., Küry, P., & Müller, H. W. (2006). Gene expression profiling reveals that peripheral nerve regeneration is a consequence of both novel injury-dependent and reactivated developmental processes. *Journal of neurochemistry*, *96*(5), 1441–1457. https://doi.org/10.1111/j.1471-4159.2005.03635.x

Brushart, T., Hoffman, P., Royall, R., Murinson, B., Witzel, C., & Gordon, T. (2002). Electrical stimulation promotes Motoneuron regeneration without increasing its speed or conditioning the neuron. *The Journal of Neuroscience*, *22*(15), 6631–6638. https://doi.org/10.1523/jneurosci.22-15-06631.2002

Brushart, T., Jari, R., Verge, V., et al. (2005). Electrical stimulation restores the specificity of sensory axon regeneration. Experimental Neurology, 194(1), 221-229.

Brushart, T., & Gordon, T. (1995a). Contributing factors to poor functional recovery after delayed nerve repair: prolonged denervation. Journal of Neuroscience, 15(5), 3886-3895.

Brushart, T., & Gordon, T. (1995b). Contributing factors to poor functional recovery after delayed nerve repair: prolonged axotomy. Journal of Neuroscience, 15(5), 3876-3885.

Buki, A., & Povlishock, J. (2004). All roads lead to disconnection? – Traumatic axonal injury revisited. *Acta Neurochirurgica*, *148*, 181–194. https://doi.org/DOI 10.1007/s00701-005-0674-4

Burke D, Kiernan M, Mogyoros I, Bostock H. Susceptibility to conduction block: Differences in the biophysical properties of cutaneous afferents and motor axons. In: Kimura J, Kaji R, editors. *Physiology of ALS and Related Diseases.* Amsterdam: Elsevier; 1997. pp. 43–53.

Cai, D., Deng, K., Mellado, W., Lee, J., Ratan, R., & Filbin, M. (2002). Arginase I and polyamines act downstream from cyclic AMP in overcoming inhibition of axonal growth MAG and myelin in vitro. *Neuron*, *15*(35), 711–719. https://doi.org/doi: 10.1016/s0896-6273(02)00826-7

Cain, D. M., Khasabov, S. G., & Simone, D. A. (2001). Response properties of mechanoreceptors and nociceptors in mouse glabrous skin: an in vivo study. *Journal of neurophysiology*, *85*(4), 1561–1574. https://doi.org/10.1152/jn.2001.85.4.1561

Calvey, C., Zhou, W., Stakleff, K., Sendelbach-Sloan, P., Harkins, A., Lanzinger, W., & Willits, R. (2015). Short-term electrical stimulation to promote nerve repair and functional recovery in a rat model. *The Journal of Hand Surgery*, *40*(2), 314–322. https://doi.org/10.1016/j.jhsa.2014.10.002

Catala, M., & Kubis, N. (2013). Gross anatomy and development of the peripheral nervous system. *Handbook of Clinical Neurology*, 29–41. https://doi.org/10.1016/b978-0-444-52902-2.00003-5

Cheng, C., Webber, C. A., Wang, J., Xu, Y., Martinez, J. A., Liu, W. Q., McDonald, D., Guo, G. F., Nguyen, M. D., & Zochodne, D. W. (2008). Activated RHOA and peripheral axon regeneration. *Experimental neurology*, *212*(2), 358–369. https://doi.org/10.1016/j.expneurol.2008.04.023

Chhabra, A., Ahlawat, S., Belzberg, & Andreseik. (2014). Peripheral nerve injury grading simplified on MR neurography: As referenced to Seddon and Sunderland classifications. *The Indian Journal of Radiology & Imaging*, *24*(3), 217–224. https://doi.org/10.4103/0971-3026.137025

Christie, K. J., Webber, C. A., Martinez, J. A., Singh, B., & Zochodne, D. W. (2010). PTEN inhibition to facilitate intrinsic regenerative outgrowth of adult peripheral axons. *The Journal of neuroscience : the official journal of the Society for Neuroscience*, *30*(27), 9306–9315. https://doi.org/10.1523/JNEUROSCI.6271-09.2010

Chu, X.-L., Song, X.-Z., Li, Q., Li, Y.-R., He, F., Gu, X.-S., & Ming, D. (2022). Basic mechanisms of peripheral nerve injury and treatment via electrical stimulation. *Neural Regeneration Research*, *17*(10), 2185–2193. https://doi.org/10.4103/1673-5374.335823

Chung, D., Shum, A., & Caraveo, G. (2020). GAP-43 and BASP1 in Axon Regeneration: Implications for the Treatment of Neurodegenerative Diseases. *Frontiers in Cell and Developmental Biology*, *8*(567537). https://doi.org/doi: 10.3389/fcell.2020.567537

Coleman, M. P., & Höke, A. (2020). Programmed axon degeneration: from mouse to mechanism to medicine. *Nature reviews. Neuroscience*, *21*(4), 183–196. https://doi.org/10.1038/s41583-020-0269-3

Conforti, L., Gilley, J., & Coleman, M. (2014). Wallerian degeneration: An emerging axon death pathway linking injury and disease. *Nature Reviews Neuroscience*, *15*, 394–409. https://doi.org/10.1038/nrn3680

Cooper, D. M., Mons, N., & Karpen, J. W. (1995). Adenylyl cyclases and the interaction between calcium and camp signalling. *Nature*, *374*(6521), 421–424. https://doi.org/10.1038/374421a0

Crawford, L. K., & Caterina, M. J. (2019). Functional anatomy of the sensory nervous system: Updates from the Neuroscience Bench. *Toxicologic Pathology*, *48*(1), 174–189. https://doi.org/10.1177/0192623319869011

da Silva CF, Madison RD, Dikkes P, Chiu T-H, Sidman RL (1985) An in vivo model to quantify motor and sensory peripheral nerve regeneration using bioresorbable nerve guide tubes. Brain Research 342:307–315

de Rooij, J., Zwartkruis, F. J., Verheijen, M. H., Cool, R. H., Nijman, S. M., Wittinghofer, A., & Bos, J. L. (1998). Epac is a Rap1 guanine-nucleotide-exchange factor directly activated by cyclic AMP. *Nature*, *396*(6710), 474–477. https://doi.org/10.1038/24884

Dhillon, A. S., Pollock, C., Steen, H., Shaw, P. E., Mischak, H., & Kolch, W. (2002). Cyclic AMP-dependent kinase regulates Raf-1 kinase mainly by phosphorylation of serine 259. *Molecular and cellular biology*, *22*(10), 3237–3246. https://doi.org/10.1128/MCB.22.10.3237-3246.2002

Dietrich, S., Company, C., Song, K., Lowenstein, E. D., Riedel, L., Birchmeier, C., Gargiulo, G., & Zampieri, N. (2022). Molecular identity of proprioceptor subtypes innervating different muscle groups in mice. *Nature communications*, *13*(1), 6867. https://doi.org/10.1038/s41467-022-34589-8

Djouhri, L., & Lawson, S. N. (2004). Abeta-fiber nociceptive primary afferent neurons: a review of incidence and properties in relation to other afferent A-fiber neurons in mammals. *Brain research. Brain research reviews*, *46*(2), 131–145. https://doi.org/10.1016/j.brainresrev.2004.07.015

Dong, J. M., Leung, T., Manser, E., & Lim, L. (1998). cAMP-induced morphological changes are counteracted by the activated RhoA small GTPase and the Rho kinase ROKalpha. *The Journal of biological chemistry*, *273*(35), 22554–22562. https://doi.org/10.1074/jbc.273.35.22554

Dubin, A. E., & Patapoutian, A. (2010). Nociceptors: the sensors of the pain pathway. *The Journal of clinical investigation*, *120*(11), 3760–3772. https://doi.org/10.1172/JCI42843

Dubový, P., Klusáková, I., Hradilová-Svíženská, I., Brázda, V., Kohoutková, M., & Joukal, M. (2019). A Conditioning Sciatic Nerve Lesion Triggers a Pro-regenerative State in Primary Sensory Neurons Also of Dorsal Root Ganglia Non-associated With the Damaged Nerve. *Frontiers Cellular Neuroscience*, *13*(11). https://doi.org/doi: 10.3389/fncel.2019.00011

Eberhardt, K., Irintchev, A., Al-Majed, A., et al. (2006). BDNF/TrkB signaling regulates HNK-1 carbohydrate expression in regenerating motor nerves and promotes functional recovery after peripheral nerve repair. Experimental Neurology, 198(2), 500-510.

Elzinga, K., Tyreman, N., Ladak, K., et al. (2015). Brief electrical stimulation improves nerve regeneration after delayed repair in Sprague Dawley rats. *Exp Neurol*, 269, 142-153.

English, A., Schwartz, G., Meador, W., et al. (2007). Electrical stimulation promotes peripheral axon regeneration by enhanced neuronal neurotrophin signaling. Developmental Neurobiology, 67(2), 158-172.

Enserink, J. M., Christensen, A. E., de Rooij, J., van Triest, M., Schwede, F., Genieser, H. G., Døskeland, S. O., Blank, J. L., & Bos, J. L. (2002). A novel Epac-specific cAMP analogue demonstrates independent regulation of Rap1 and ERK. Nature cell biology, 4(11), 901–906. https://doi.org/10.1038/ncb874

Fischer, L., Scherbarth, F., Chagnaud, B., & Felmy, F. (2017). Intrinsic frequency response patterns in mechano-sensory neurons of the leech. *Biology open*, *6*(7), 993–999. https://doi.org/10.1242/bio.023960

Foeking, E., Fargo, K., Coughlin, L., Kim, J., Marzo, S., & Jones, K. (2012). Single session of brief electrical stimulation immediately following crush injury enhances functional recovery of rat facial nerve. *The Journal of Rehabilitation Research and Development*, *49*(3), 451. https://doi.org/10.1682/jrrd.2011.03.0033

Forman, D. S., & Berenberg, R. A. (1978). Regeneration of motor axons in the rat sciatic nerve studied by labeling with axonally transported radioactive proteins. *Brain research*, *156*(2), 213–225. https://doi.org/10.1016/0006-8993(78)90504-8

Forman DS, Wood DK, da Silva S (1979) Rate of regeneration of sensory axons in transected rat sciatic nerve repaired with epineurial sutures. Journal of the Neurological Sciences 44:55–59.

Fregnan, F., Muratori, L., Simões, A., Giacobini-Robecchi, M., & Raimondo, S. (2012). Role of inflammatory cytokines in peripheral nerve injury. *Neural Regeneration Research*, *7*(29), 2259–2266. https://doi.org/doi: 10.3969/j.issn.1673-5374.2012.29.003

Frey D, Laux T, Xu L, Schneider C, Caroni P. Shared and unique roles of CAP23 and GAP43 in actin regulation, neurite outgrowth, and anatomical plasticity. The Journal of cell biology. 2000 Jun 26;149(7):1443-54.

Frey, E., Valakh, V., Karney-Grobe, S., et al. (2015). An In Vitro Assay to Study Induction of the Regenerative State in Sensory Neurons. *Exp Neurol*, 263, 350-363.

Friese, A., Kaltschmidt, J. A., Ladle, D. R., Sigrist, M., Jessell, T. M., & Arber, S. (2009). Gamma and alpha motor neurons distinguished by expression of transcription factor Err3. *Proceedings of the National Academy of Sciences of the United States of America*, *106*(32), 13588–13593. https://doi.org/10.1073/pnas.0906809106

Fu, S., & Gordon, T. (1997). The cellular and molecular basis of peripheral nerve regeneration. *Molecular Neurobiology*, *14*, 67–116. https://doi.org/10.1007/BF02740621

Fu, S., & Gordon, T. (1995b). Contributing factors to poor functional recovery after delayed nerve repair: Prolonged axotomy. *The Journal of Neuroscience*, *15*(5), 3876–3885. https://doi.org/doi: 10.1523/JNEUROSCI.15-05-03876.1995.

Fu, S., & Gordon, T. (1995a). Contributing factors to poor functional recovery after delayed nerve repair: Prolonged denervation. *The Journal of Neuroscience*, *15*(5), 3886–3895. https://doi.org/doi: 10.1523/JNEUROSCI.15-05-03886.1995.

Galko, M. J., & Tessier-Lavigne, M. (2000). Function of an axonal chemoattractant modulated by metalloprotease activity. *Science (New York, N.Y.)*, *289*(5483), 1365–1367. https://doi.org/10.1126/science.289.5483.1365

Gangadharan, V., Zheng, H., Taberner, F. J., et al. (2022). Neuropathic pain caused by miswiring and abnormal end organ targeting. *Nature, 606*, 137–145. https://doi.org/10.1038/s41586-022-04777-z

Gao Y., Nikulina E., Mellado W., Filbin M.T. (2003). Neurotrophins elevate cAMP to reach a threshold required to overcome inhibition by MAG through extracellular signal-regulated kinase-dependent inhibition of phosphodiesterase. J. Neurosci., 23 (2003), pp. 11770-11777

Gaudet, A., Popovich, P., & Ramer, M. (2011). Wallerian degeneration: Gaining perspective on inflammatory events after peripheral nerve injury. *Journal of Neuroinflammation*, *110*. https://doi.org/10.1186/1742-2094-8-110

Geremia, N., Gordon, T., Brushart, T., et al. (2007). Electrical stimulation promotes sensory neuron regeneration and growth-associated gene expression. Experimental Neurology, 205(2), 347-359.

Gey, M., Wanner, R., Schilling, C., Pedro, M., Sinske, D., & Knoll, D. (2016). Atf3 mutant mice show reduced axon regeneration and impaired regeneration-associated gene induction after peripheral nerve injury. *Royal Society Open Science*, *6*(8). https://doi.org/10.1098/rsob.160091

Gordon, T., Amirjani, N., Edwards, D., & Chan, K. (2010). Brief post-surgical electrical stimulation accelerates axon regeneration and muscle reinnervation without affecting the functional measures in carpal tunnel syndrome patients. *Experimental Neurology*, *223*(1), 192–202. https://doi.org/10.1016/j.expneurol.2009.09.020

Gordon, T., Tyreman, N., & Raji, M. (2011). The Basis for Diminished Functional Recovery after Delayed Peripheral Nerve Repair. *Journal of Neurscience*, *31*(14), 5325–5334. https://doi.org/10.1523/JNEUROSCI.6156-10.2011

Grinsell, D., & Keating, C. (2014). Peripheral nerve reconstruction after injury: A review of clinical and experimental therapies. *BioMed Research International*, *2014*(698256lu).

Haastert-Talini, K., Schmitte, R., Korte, N., et al. (2011). Electrical stimulation accelerates axonal and functional peripheral nerve regeneration across long gaps. Journal of Neurotrauma, 28(4), 661-674.

Hadlock, T., Lindsay, R., Edwards, C., et al. (2010). The effect of electrical and mechanical stimulation on the regenerating rodent facial nerve. The Laryngoscope, 120(6), 1094-1102.

Han, S., Baig, H., & Hammarlund, M. (2016). Mitochondria localize to injured axons to support regeneration. Neuron, 92(6), 1308-1323.

Han, S., Kim, D., Sung, J., et al. (2019). Electrical stimulation accelerates neurite regeneration in axotomized dorsal root ganglion neurons by increasing MMP-2 expression. Biochemical and Biophysical Research Communications, 508(2), 348-353.

Hanani, M., & Spray, D. (2020). Emerging importance of satellite glia in nervous system function and dysfunction. *Nature Reviews Neuroscience*, *21*, 485–498. https://doi.org/10.1038/s41583-020-0333-z

Handler, A., & Ginty, D. D. (2021). The mechanosensory neurons of touch and their mechanisms of activation. *Nature reviews. Neuroscience*, *22*(9), 521–537. https://doi.org/10.1038/s41583-021-00489-x

Hannila, S., & Filbin, M. (2007). The role of cyclic AMP signaling in promoting axonal regeneration after spinal cord injury. *Experimental Neurology*, *209*(2), 321–332. https://doi.org/doi: 10.1016/j.expneurol.2007.06.020

Hanz, S., & Fainzilber, M. (2006). Retrograde signaling in injured nerve—The axon reaction revisited. *Journal of Neurochemistry*, *99*(1), 13–19. https://doi.org/doi: 10.1111/j.1471-4159.2006.04089.x

Hao, Y., Frey, E., Yoon, C., Wong, H., Nestorovski, D., Holzman, L., Giger, R., DiAntonio, A., & Collins, C. (2016). An evolutionarily conserved mechanism for cAMP elicited axonal regeneration involves direct activation of the dual leucine zipper kinase DLK. *eLife*, *5*. https://doi.org/10.7554/eLife.14048

Hausott, B., Glueckert, R., Schrott-Fischer, A., & Klimaschewski. (2022). Signal Transduction Regulators in Axonal Regeneration. *Cells*, *11*(9). https://doi.org/10.3390/cells11091537

Hausott, B., & Klimaschewski, L. (2019). Promotion of Peripheral Nerve Regeneration by Stimulation of the Extracellular Signal‐Regulated Kinase (ERK) Pathway. *The Anatomical Record*, *302*(8), 1261–1267. https://doi.org/doi: 10.1002/ar.24126

Hetzler, L., Sharma, N., Tanzer, L., Wurster, R., Leonetti, J., Marzo, S., Jones, K., & Foeking, E. (2008). Accelerating functional recovery after rat facial nerve injury: Effects of gonadal steroids and electrical stimulation. *Otolaryngology–Head and Neck Surgery*, *139*(1), 62–67. https://doi.org/10.1016/j.otohns.2008.02.006

Hill, C., Coleman, M., & Menon, D. (2016). Traumatic Axonal Injury: Mechanisms and Translational Opportunities. *Trends in Neurosciences*, *39*(5), 311–324. https://doi.org/10.1016/j.tins.2016.03.002

Höke, A., Redett, R., Hameed, H., Jari, R., Zhou, C., Li, Z. B., Griffin, J. W., & Brushart, T. M. (2006). Schwann cells express motor and sensory phenotypes that regulate axon regeneration. *The Journal of neuroscience : the official journal of the Society for Neuroscience*, *26*(38), 9646–9655. https://doi.org/10.1523/JNEUROSCI.1620-06.2006

Hu, M., Hong, L., Liu, C., et al. (2019). Electrical stimulation enhances neuronal cell activity mediated by Schwann cell derived exosomes. *Sci Rep*, 9(1).

Huang, J., Lu, L., Hu, X., et al. (2009). Electrical stimulation accelerates motor functional recovery in autograft-repaired 10mm femoral nerve gaps in rats. Journal of Neurotrauma, 26, 1805-1813.

Huang, J., Lu, L., Zhang, J., et al. (2012). Electrical stimulation to conductive scaffold promotes axonal regeneration and remyelination in a rat model of large nerve defect. PLoS ONE, 7(6).

Huang, J., Lu, L., Hu, X., Ye, Z., Peng, Y., Yan, X., Geng, D., & Luo, Z. (2010a). Electrical stimulation accelerates motor functional recovery in the rat model of 15-mm sciatic nerve gap bridged by scaffolds with longitudinally oriented microchannels. *Neurorehabilitation and Neural Repair*, *24*(8), 736–745. https://doi.org/10.1177/1545968310368686

Huang, J., Ye, Z., Hu, X., et al. (2010b). Electrical stimulation induces calcium-dependent release of NGF from cultured Schwann cells. *Glia*, 58, 622-631.

Huang, J., Zhang, Y., Lu, L., Hu, X., & Luo, Z. (2013). Electrical stimulation accelerates nerve regeneration and functional recovery in delayed peripheral nerve injury in rats. *European Journal of Neuroscience*, *38*(12), 3691–3701. https://doi.org/10.1111/ejn.12370

Huebner, E., & Strittmatter, S. (2009). Axon regeneration in the peripheral and central nervous systems. *Results and Problems in Cell Differentiation*, *48*, 339–351. https://doi.org/10.1007/400_2009_19

Ino, D., Sagara, H., Suzuki, J., et al. (2015). Neuronal Regulation of Schwann Cell Mitochondrial Ca(2+) Signaling during Myelination. Cell Reports, 12(12), 1951-1959.

Javeed, S., Faraji, A., Dy, C., Ray, W., & MacEwan, M. (2021). Application of electrical stimulation for peripheral nerve regeneration: Stimulation parameters and future horizons. *Interdisciplinary Neurosurgery*. https://doi.org/10.1016/j.inat.2021.101117

Jenq, C.-B., & Coggeshall, R. E. (1985). Numbers of regenerated axons in tributary nerves following neonatal sciatic nerve crush in rat. *Neuroscience Letters*, *61*(1–2), 43–48. https://doi.org/10.1016/0304-3940(85)90398-2

Jiang, H., Song, Q., Gill, B., et al. (2018). Electrical stimulation of the pudendal nerve promotes neuroregeneration and functional recovery from stress urinary incontinence in a rat model. *Am J Physiol-Ren Physiol*, 315(6).

Juckett, L., Saffari, T., Ormseth, B., Senger, J., & Moore, A. (2022). The Effect of Electrical Stimulation on Nerve Regeneration Following Peripheral Nerve Injury. *Biomolecules*, *12*(12), 1856. https://doi.org/10.3390/biom12121856

Kawasaki, Y., Yoshimura, K., Harii, K., & Park, S. (2000). Identification of myelinated motor and sensory axons in a regenerating mixed nerve. *The Journal of Hand Surgery*, *25*(1), 104–111. https://doi.org/10.1053/jhsu.2000.jhsu025a0104

Keane, G., Pan, D., Roh, J., et al. (2022). The Effects of Intraoperative Electrical Stimulation on Regeneration and Recovery After Nerve Isograft Repair in a Rat Model. HAND, 17(3), 540-548.

Keane, G., Marsh, E., Hunter, D., et al. (2023). Lidocaine Nerve Block Diminishes the Effects of Therapeutic Electrical Stimulation to Enhance Nerve Regeneration in Rats. *HAND*, 18(1), 119-125.

Khaitin, A. (2021). Calcium in Neuronal and Glial Response to Axotomy. *International Journal of Molecular Sciences*, *22*(24). https://doi.org/doi: 10.3390/ijms222413344

Kim, H., Ji, G., Kwan, K., et al. (2020). Electrical stimulation controls elongation and polarity of retinal Müller glial cells. Biochemical and Biophysical Research Communications, 527(1), 38-44.

Kim, H., Koo, T., & Ji, G. (2016a). Electrical stimulation promotes regenerative neurite outgrowth of cultured retinal ganglion cells. Biochemical and Biophysical Research Communications, 479(1), 18-23.

Kim, H., Park, S., & Ji, G. (2016b). Electrical stimulation modulates the Na(+)/K(+) pump function of retinal glial cells via activation of PKC. Biochemical and Biophysical Research Communications, 471(1), 31-36.

Kinsley, S. E., Fernicola, S. D., Dingle, M. E., Williams, M. S., Richardson, J. M., Taylor, D., de Vasconcellos, J. F., Malone, T. R., Blattner, M. R., Smith, J. K., Oliver, A., Koch, A. L., Riddle, L. E., Reiter, C., Culp, W. E., Caterson, E. J., Nesti, L. J., & Talbot, S. G. (2021). A Yorkshire swine (Sus scrofa domesticus) model for nerve regeneration and ischemia based on the sciatic nerve and femoral artery. *Annals of anatomy = Anatomischer Anzeiger : official organ of the Anatomische Gesellschaft*, *233*, 151587. https://doi.org/10.1016/j.aanat.2020.151587

Kiryu-Seo, S., Tamada, H., Kato, Y., et al. (2010). Neuronal injury-inducible gene is synergistically regulated by ATF3, c-Jun, and STAT3 through the interaction with Sp1 in damaged neurons. Journal of Biological Chemistry, 285(39), 29158-29170.

Klimaschewski, L., Hausott, B., & Angelov, D. (2013). The pros and cons of growth factors and cytokines in peripheral axon regeneration. *International Reviews of Neurobiology*, *108*, 131–171. https://doi.org/doi: 10.1016/B978-0-12-410499-0.00006-X

Koppes, A., Seggio, A., Thompson, D. (2011). Neurite outgrowth is significantly increased by the simultaneous presentation of Schwann cells and moderates exogenous electric fields. *J Neural Eng*, 8(4).

Koppes, A., Nordberg, A., Paolillo, G., et al. (2014). Electrical stimulation of Schwann cells promotes sustained increases in neurite outgrowth. *20*.

Krishnan, A., Duraikannu, A., & Zochodne, D. (2016). Releasing 'brakes' to nerve regeneration: Intrinsic molecular targets. *European Journal of Neuroscience*, *43*, 297–308. https://doi.org/doi:10.1111/ejn.13018

Larsson, M., & Nagi, S. S. (2022). Role of C-tactile fibers in pain modulation: Animal and human perspectives. *Current Opinion in Behavioral Sciences*, *43*, 138–144. https://doi.org/10.1016/j.cobeha.2021.09.005

Lauria, G., Devigili, G., & Smith, A. (2008). Skin biopsy as a diagnostic tool in peripheral neuropathy. Nature Clinical Practice Neurology, 4(10), 546-557.

Lehmann, M., Fournier, A., Selles-Navarro, I., Dergham, P., Sebok, A., Leclerc, N., Tigyi, G., & McKerracher, L. (1999). Inactivation of rho signaling pathway promotes CNS axon regeneration. *The Journal of Neuroscience*, *19*(17), 7537–7547. https://doi.org/10.1523/jneurosci.19-17-07537.1999

Li, X., Zhang, T., Li, C., et al. (2022). Electrical stimulation accelerates Wallerian degeneration and promotes nerve regeneration after sciatic nerve injury. *Glia*, 71(3), 758-774.

Lindwall, C., & Kanje, M. (2005). Retrograde axonal transport of JNK signaling molecules influence injury induced nuclear changes in p-c-Jun and ATF3 in adult rat sensory neurons. *Molecular and Cellular Neuroscience*, *29*(2), 269–282. https://doi.org/doi: 10.1016/j.mcn.2005.03.002

Lu, M.-C., Ho, C.-Y., Hsu, S.-F., Lee, H.-C., Lin, J.-H., Yao, C.-H., & Chen, Y.-S. (2008). Effects of electrical stimulation at different frequencies on regeneration of transected peripheral nerve. *Neurorehabilitation and Neural Repair*, *22*(4), 367–373. https://doi.org/10.1177/1545968307313507

Lu, M., Zhu, J., Jin, J., et al. (2015). Electrical stimulation enhances neuronal cell activity mediated by Schwann cell derived exosomes. Scientific Reports, 5.

Lundborg, G., Dahlin, L., & Danielsen, N. (1997). Nerve regeneration across an extended gap: a neurobiological view of nerve repair and the possible involvement of neuroma formation. Journal of Hand Surgery (British and European Volume), 22(5), 553-566.

Luo, J., Feng, J., Liu, S., Walters, E. T., & Hu, H. (2015). Molecular and cellular mechanisms that initiate pain and itch. *Cellular and molecular life sciences : CMLS*, *72*(17), 3201–3223. https://doi.org/10.1007/s00018-015-1904-4

Ma, T., Barco, A., Ratan, R., & Willis, D. (2014). cAMP-responsive Element-binding Protein (CREB) and cAMP Co-regulate Activator Protein 1 (AP1)-dependent Regeneration-associated Gene Expression and Neurite Growth. *Journal of Biological Chemistry*, *289*(47), 32914–32925. https://doi.org/doi: 10.1074/jbc.M114.582460

Ma, T., & Willis, D. (2015). What makes a RAG regeneration associated? *Frontiers in Molecular Neuroscience*, *8*(43). https://doi.org/doi: 10.3389/fnmol.2015.00043

Madorsky, S. J., Swett, J. E., & Crumley, R. L. (1998). Motor versus sensory neuron regeneration through collagen tubules. *Plastic and reconstructive surgery*, *102*(2), 430–438. https://doi.org/10.1097/00006534-199808000-00021

Mahar, M., & Cavalli, V. (2018). Intrinsic mechanisms of neuronal axon regeneration. *Nature Reviews Neurology*, *19*(6), 323–337. https://doi.org/doi: 10.1038/s41583-018-0001-8

Mandelosi, G., Madeddu, F., Bozzi, Y., Maffei, L., & Michele Ratto, G. (2004). Acute physiological response of mammalian central neurons to axotomy: Ionic regulation and electrical activity. *Federation of American Societies for Experimental Biology*, *18*(15), 1934–1936. https://doi.org/10.1096/fj.04-1805fje

McGlone, F., & Reilly, D. (2010). The cutaneous sensory system. *Neuroscience and biobehavioral reviews*, *34*(2), 148–159. https://doi.org/10.1016/j.neubiorev.2009.08.004

McLean, N., Popescu, B., Gordon, T., et al. (2014). Delayed nerve stimulation promotes axon-protective neurofilament phosphorylation, accelerates immune cell clearance and enhances remyelination in vivo in focally demyelinated nerves. *PLoS ONE*, 9(10).

McLean, N., Verge, V. (2016). Dynamic impact of brief electrical stimulation on the neural immune axis-polarization of macrophages toward a pro-repair phenotype in demyelinated peripheral nerve. *Glia*, 64(9), 1546-1561.

McGregor, C., & English, A. (2019). The Role of BDNF in Peripheral Nerve Regeneration: Activity-Dependent Treatments and Val66Met. *Frontiers in Cellular Neuroscience*, *12*(522). https://doi.org/10.3389/fncel.2018.00522

Mei, F. C., Qiao, J., Tsygankova, O. M., Meinkoth, J. L., Quilliam, L. A., & Cheng, X. (2002). Differential signaling of cyclic AMP. *Journal of Biological Chemistry*, *277*(13), 11497–11504. https://doi.org/10.1074/jbc.m110856200

Menorca, R., Fussell, T., & Elfar, J. (2013). Nerve physiology: Mechanisms of injury and recovery. *Hand Clinics*, *29*(3), 317–330. https://doi.org/10.1016/j.hcl.2013.04.002

Ming, G., Henley, J., Tessier-Lavigne, M., Song, H.-J., & Poo, M. (2001). Electrical activity modulates growth cone guidance by diffusible factors. *Neuron*, *29*(2), 441–452. https://doi.org/10.1016/s0896-6273(01)00217-3

Moldovan M (2006) Comparison of the fastest regenerating motor and sensory myelinated axons in the same peripheral nerve. Brain 129:2471–2483

Monaco, G., Brown, T., Burgette, R., et al. (2015). Electrical stimulation and testosterone enhance recovery from recurrent laryngeal nerve crush. *Restor Neurol Neurosci*, *(4)*, 571-578.

Murray, A., & Shewan, D. (2008). Epac mediates cyclic AMP-dependent axon growth, guidance and regeneration. *Molecular and Cellular Neuroscience*, *38*(4), 578–588. https://doi.org/10.1016/j.mcn.2008.05.006

Mussen, F., Broeckhoven, J. V., Hellings, N., Schepers, M., & Vanmierlo, T. (2023). Unleashing Spinal Cord Repair: The Role of cAMP-Specific PDE Inhibition in Attenuating Neuroinflammation and Boosting Regeneration after Traumatic Spinal Cord Injury. *International journal of molecular sciences*, *24*(9), 8135. https://doi.org/10.3390/ijms24098135

Naidu, M. (2009). The Role Of Cells, Neurotrophins, Extracellular Matrix And Cell Surface Molecules In Peripheral Nerve Regeneration. *Journal of Medical Sciences*, *16*(2), 10–14.

Nix, W., & Hopf, H. (1983). Electrical stimulation of regenerating nerve and its effect on motor recovery. Brain Research, 272(1), 21-25.

Olson, J., Power, H., Morhart, M., et al. (2018). Brief electrical stimulation accelerates axon regeneration in the peripheral nervous system and promotes sensory axon regeneration in the central nervous system. Experimental Neurology, 308, 198-207.

Pabari, A., Yang, S., Seifalian, A., & Mosahebi, A. (2010). Modern surgical management of peripheral nerve gap. *Journal of Plastic, Reconstructive & Aesthetic Surgery*, *63*(12), 1941–1948. https://doi.org/10.1016/j.bjps.2009.12.010

Palladino, S., Helton, E., Jain, P., Dong, C., Crowley, M., Crossman, D., & Ubogu, E. (2017). The Human Blood-Nerve Barrier Transcriptome. *Scientific Reports*, *7*(17477).

Pan, D., Li, Y., Gordon, T., et al. (2021). Intraoperative Brief Electrical Stimulation Promotes Recovery of Hand Function from Chronic Neurorrhaphy in a Rat Model. Plastic and Reconstructive Surgery, 147(3), 459e-467e.

Park, S., Liu, C., Ward, P., et al. (2019). Effects of repeated 20-Hz electrical stimulation on functional recovery following peripheral nerve injury. *Neurorehabil Neural Repair*, 33(9), 775-784.

Peace, & Shewan, D. (2011). New perspectives in cyclic AMP-mediated axon growth and guidance: The emerging epoch of Epac. *Brain Research Bulletin*, *10*(84), 280–288. https://doi.org/doi: 10.1016/j.brainresbull.2010.09.002.

Perlson, E., Hanz, S., Ben-Yaakov, K., Segal-Ruder, Y., Seger, R., & Fainzilber, M. (2005). Vimentin-Dependent Spatial Translocation of an Activated MAP Kinase in Injured Nerve. *Neuron*, *45*(5), 715–726. https://doi.org/10.1016/j.neuron.2005.01.023

Power, H., Morhart, M., Olson, J., & Chan, K. (2020). Postsurgical Electrical Stimulation Enhances Recovery Following Surgery for Severe Cubital Tunnel Syndrome: A Double-Blind Randomized Controlled Trial. *Neurosurgery*, *86*(6), 769–777. https://doi.org/doi: 10.1093/neuros/nyz322

Prato, V., Taberner, F. J., Hockley, J. R. F., Callejo, G., Arcourt, A., Tazir, B., Hammer, L., Schad, P., Heppenstall, P. A., Smith, E. S., & Lechner, S. G. (2017). Functional and Molecular Characterization of Mechanoinsensitive "Silent" Nociceptors. *Cell reports*, *21*(11), 3102–3115. https://doi.org/10.1016/j.celrep.2017.11.066

Price, T. J., & Flores, C. M. (2007). Critical evaluation of the colocalization between calcitonin gene-related peptide, substance P, transient receptor potential vanilloid subfamily type 1 immunoreactivities, and isolectin B4 binding in primary afferent neurons of the rat and mouse. *The journal of pain*, *8*(3), 263–272. https://doi.org/10.1016/j.jpain.2006.09.005

Quan, X., Huang, L., Yang, Y., et al. (2017). Potential Mechanisms of Neurite Outgrowth Enhanced by Electrical Stimulation: Involvement of MicroRNA-363-5p Targeting DCLK1 Expression in Rat. *Neurochem Res*, 42(2), 513-525.

Raslan, A., Salem, M., Al-Hussaini, A., et al. (2019). Brief electrical stimulation improves functional recovery after femoral but not after facial nerve injury in rats. *Anat Rec*, 302(8), 1304-1313.

Richardson, P. M., & Issa, V. M. (1984). Peripheral injury enhances central regeneration of primary sensory neurones. *Nature*, *309*(5971), 791–793. https://doi.org/10.1038/309791a0

Ring, D. (2013). Symptoms and disability after major peripheral nerve injury. Hand Clinics, 29(3), 421-425.

Roh, J., Schellhardt, L., Keane, G., Hunter, D., Moore, A., Snyder-Warwick, A., Mackinnon, S., & Wood, M. (2022). Short-Duration, Pulsatile, Electrical Stimulation Therapy Accelerates Axon Regeneration and Recovery Following Tibial Nerve Injury and Repair in Rats. *Plastic and Reconstructive Surgery*, *149*(4), 681–690. https://doi.org/doi: 10.1097/PRS.0000000000008924

Rotshenker, S. (2011). Wallerian degeneration: The innate-immune response to traumatic nerve injury. *Journal of Neuroinflammation*, *108*(8). https://doi.org/10.1186/1742-2094-8-109

Saijilafu, Hur, E.-M., Jiao, Z., Liu, C.-M., Xu, W.-L., & Zhou, F.-Q. (2013). PI3K-GSK3 signaling regulates mammalian axon regeneration by inducing the expression of Smad1. *Nature Communications*, *4*(2690). https://doi.org/doi: 10.1038/ncomms3690

Sajic, M., Mastrolia, V., Lee, C., et al. (2013). Impulse Conduction Increases Mitochondrial Transport in Adult Mammalian Peripheral Nerves in Vivo. *PLoS Biol*, 11(12), e1001754.

Sanger, J. R., Riley, D. A., Matloub, H. S., Yousif, N. J., Bain, J. L., & Moore, G. H. (1991). Effects of axotomy on the cholinesterase and carbonic anhydrase activities of axons in the proximal and distal stumps of rabbit sciatic nerves: a temporal study. *Plastic and reconstructive surgery*, *87*(4), 726–740.

Sayanagi, J., Acevedo-Cintron, J., Pan, D., et al. (2021). Brief Electrical Stimulation Accelerates Axon Regeneration and Promotes Recovery Following Nerve Transection and Repair in Mice. Journal of Bone and Joint Surgery, 103(20).

Scheib, J., & Höke, A. (2013). Advances in peripheral nerve regeneration. *Nature Reviews Neurology*, *9*(12), 668–676. https://doi.org/10.1038/nrneurol.2013.227

Seddon, H. (1942). A Classification of Nerve Injuries. *British Medical Journal*, *2*(4260), 237–239. https://doi.org/doi: 10.1136/bmj.2.4260.237

Senger, J., Chan, K., & Webber, C. (2020a). Conditioning electrical stimulation is superior to postoperative electrical stimulation, resulting in enhanced nerve regeneration and functional recovery. *Experimental Neurology*, *325*. https://doi.org/10.1016/j.expneurol.2019.113147

Senger, J., Macandili, H., Chan, K., & Webber, C. (2019). Conditioning electrical stimulation promotes functional nerve regeneration. *Experimental Neurology*, *315*, 60–71. https://doi.org/10.1016/j.expneurol.2019.02.001

Senger, J., Rabey, K., Acton, L., Lin, Y.-H., Lingrell, S., Chan, K., & Webber, C. (2022). Recovering the regenerative potential in chronically injured nerves by using conditioning electrical stimulation. *Journal of Neurosurgery*, *136*, 1442–1454. https://doi.org/DOI: 10.3171/2021.4.JNS21398

Senger, J., Rabey, K., Morhart, M., Chan, K., & Webber, C. (2020b). Conditioning electrical stimulation accelerates regeneration in nerve transfers. *Annals of Neurology*, *88*(2), 363–374. https://doi.org/10.1002/ana.25796

Senger, J., Verge, V., Chan, K., & Webber, C. (2018b). *The nerve conditioning lesion: A strategy to enhance nerve regeneration. 83*(4), 691–702. https://doi.org/10.1002/ana.25209

Senger, J., Verge, V., Macandili, H., Olson, J., Chan, K., & Webber, C. (2018a). Electrical stimulation as a conditioning strategy for promoting and accelerating peripheral nerve regeneration. *Experimental Neurology*, *302*, 75–84. https://doi.org/10.1016/j.expneurol.2017.12.013

Shapira, Y., & Midha, R. (2015). Shocking therapy: Brief electrical stimulation for delayed nerve repair. *Experimental Neurology*, *271*, 524–525. https://doi.org/10.1016/j.expneurol.2015.07.015

Shapira, Y., Sammons, V., Forden, J., et al. (2019). Brief electrical stimulation promotes nerve regeneration following experimental in-continuity nerve injury. *Neurosurgery*, 85(1), 156-163.

Shiers, S. I., Sankaranarayanan, I., Jeevakumar, V., Cervantes, A., Reese, J. C., & Price, T. J. (2021). Convergence of peptidergic and non-peptidergic protein markers in the human dorsal root ganglion and spinal dorsal horn. *The Journal of comparative neurology*, *529*(10), 2771–2788. https://doi.org/10.1002/cne.25122

Singh, B., Xu, G., Franz, C., et al. (2012). Accelerated axon outgrowth, guidance, and target reinnervation across nerve transection gaps following a brief electrical stimulation paradigm. *J Neurosurg*, 116(3), 498-512.

Sharma, N., Coughlin, L., Porter, R., et al. (2009). Effects of electrical stimulation and gonadal steroids on rat facial nerve regenerative properties. *Restor Neurol Neurosci*, 27(6), 635-646.

Sharma, N., Marzo, S., Jones, K., et al. (2010a). Electrical stimulation and testosterone differentially enhance expression of regeneration-associated genes. *Exp Neurol*, 223(1), 183-191.

Sharma, N., Moeller, C., Marzo, S., et al. (2010b). Combinatorial treatments enhance recovery following facial nerve crush. *The Laryngoscope*, 120(8), 1523-1530.

Shim, S., & Ming, G. L. (2010). Roles of channels and receptors in the growth cone during PNS axonal regeneration. *Experimental neurology*, *223*(1), 38–44. https://doi.org/10.1016/j.expneurol.2009.10.001

Shin, J., Cho, Y., Beirowski, B., Milbrandt, J., Cavalli, V., & DiAntonio, A. (2012). Dual leucine zipper kinase is required for retrograde injury signaling and axonal regeneration. *Neuron*, *74*(6), 1015–1022. https://doi.org/DOI: 10.1016/j.neuron.2012.04.028

Shin, J., Ha, H., Kim, Y., Cho, Y., & DiAntonio, A. (2019). DLK regulates a distinctive transcriptional regeneration program after peripheral nerve injury. *Neurobiology of Disease*, *127*, 178–192. https://doi.org/10.1016/j.nbd.2019.02.001

Singh, B., Krishnan, A., Micu, I., Koshy, K., Singh, V., Martinez, J., Koshy, D., Xu, F., Chandrasekhar, A., Dalton, C., Syed, N., Stys, P., & Zochodne, D. (2015). Peripheral neuron plasticity is enhanced by brief electrical stimulation and overrides attenuated regrowth in experimental diabetes. *Journal of Neurosurgery*, *83*, 134–151. https://doi.org/10.1016/j.nbd.2015.08.009

Sjöberg, J., & Kanje, M. (1990). Effects of repetitive conditioning crush lesions on regeneration of the rat sciatic nerve. *Brain Research*, *530*(1), 167–169. https://doi.org/10.1016/0006-8993(90)90676-3

Song, W., Cho, Y., Watt, D., & Cavalli, V. (2015). Tubulin-tyrosine Ligase (TTL)-mediated Increase in Tyrosinated α-Tubulin in Injured Axons Is Required for Retrograde Injury Signaling and Axon Regeneration. *Journal of Biological Chemistry*, *290*(23), 14765–14775. https://doi.org/10.1074/jbc.M114.622753

Song, Y., Li, D., Farrelly, O., Miles, L., Li, F., Kim, S. E., Lo, T. Y., Wang, F., Li, T., Thompson-Peer, K. L., Gong, J., Murthy, S. E., Coste, B., Yakubovich, N., Patapoutian, A., Xiang, Y., Rompolas, P., Jan, L. Y., & Jan, Y. N. (2019). The Mechanosensitive Ion Channel Piezo Inhibits Axon Regeneration. Neuron, 102(2), 373–389.e6. https://doi.org/10.1016/j.neuron.2019.01.050

Stork, P., & Schmitt, J. (2002). Crosstalk between cAMP and MAP kinase signaling in the regulation of cell proliferation. *Trends in Cellular Biology*, *12*(6), 258–266. https://doi.org/doi: 10.1016/s0962-8924(02)02294-8

Stucky, C. L., & Lewin, G. R. (1999). Isolectin B(4)-positive and -negative nociceptors are functionally distinct. *The Journal of neuroscience : the official journal of the Society for Neuroscience*, *19*(15), 6497–6505. https://doi.org/10.1523/JNEUROSCI.19-15-06497.1999

Sulaiman, W., & Gordon, T. (2013). Neurobiology of peripheral nerve injury, regeneration, and functional recovery: From bench top research to bedside application. *Ochsner Journal*, *13*(1), 100–108. https://doi.org/10.1093/brain/74.4.49

Sunderland. (1951). A classification of peripheral nerve injuries producing loss of function. *Brain*, *74*(4), 491–516. https://doi.org/10.1093/brain/74.4.491

Suzuki, G., Ochi, M., Shu, N., Uchio, Y., & Matsuura, Y. (1998). Sensory neurons regenerate more dominantly than motoneurons during the initial stage of the regenerating process after peripheral axotomy. *Neuroreport*, *9*(15), 3487–3492. https://doi.org/10.1097/00001756-199810260-00028

Tan, D., Zhang, H., Deng, J., Liu, J., Wen, J., Li, L., Wang, X., Pan, M., Hu, X., & Guo, J. (2020). RhoA-gtpase modulates neurite outgrowth by regulating the expression of Spastin and P60-Katanin. *Cells*, *9*(1), 230. https://doi.org/10.3390/cells9010230

Tavares-Ferreira, D., Shiers, S., Ray, P. R., Wangzhou, A., Jeevakumar, V., Sankaranarayanan, I., Cervantes, A. M., Reese, J. C., Chamessian, A., Copits, B. A., Dougherty, P. M., Gereau, R. W., 4th, Burton, M. D., Dussor, G., & Price, T. J. (2022). Spatial transcriptomics of dorsal root ganglia identifies molecular signatures of human nociceptors. *Science translational medicine*, *14*(632), eabj8186. https://doi.org/10.1126/scitranslmed.abj8186

Thompson, N., Sengelaub, D., & English, A. (2013). Enhancement of peripheral nerve regeneration due to treadmill training and electrical stimulation is dependent on androgen receptor signaling. *Dev Neurobiol*, 74(5), 531-540.

Traverse, S., Gomez, N., Paterson, H., Marshall, C., & Cohen, P. (1992). Sustained activation of the mitogen-activated protein (MAP) kinase cascade may be required for differentiation of PC12 cells. Comparison of the effects of nerve growth factor and epidermal growth factor. *Biochemical Journal*, *288*(2), 351–355. https://doi.org/10.1042/bj2880351

Triolo, D., Dina, G., Lorenzetti, I., Malaguti, M., Morana, P., Del Carro, U., Comi, G., Messing, A., Quattrini, A., & Previtali, S. (2006). Loss of glial fibrillary acidic protein (GFAP) impairs Schwann cell proliferation and delays nerve regeneration after damage. *Journal of Cell Science*, *119*(Pt 19), 3981–3993. https://doi.org/doi: 10.1242/jcs.03168

Udina, E., Furey, M., Busch, S., Silver, J., Gordon, T., & Fouad, K. (2008). Electrical stimulation of intact peripheral sensory axons in rats promotes outgrowth of their central projections. *Experimental Neurology*, *210*(1), 238–247. https://doi.org/10.1016/j.expneurol.2007.11.007

Verge VM, Gratto KA, Karchewski LA, Richardson PM (1996) Neurotrophins and nerve injury in the adult. Philos Trans R Soc Lond B Biol Sci 351(1338):423-430. doi:10.1098/rstb.1996.0038 PMID: 8730781

Vivó, M., Puigdemasa, A., Casals, L., et al. (2008). Immediate electrical stimulation enhances regeneration and reinnervation and modulates spinal plastic changes after sciatic nerve injury and repair. *Exp Neurol*, 211(1), 180-193.

Vossler, M. R., Yao, H., York, R. D., Pan, M. G., Rim, C. S., & Stork, P. J. (1997). cAMP activates MAP kinase and Elk-1 through a B-Raf- and Rap1-dependent pathway. *Cell*, *89*(1), 73–82. https://doi.org/10.1016/s0092-8674(00)80184-1

Wan, L., Ding, W., Xia, R., et al. (2010). Short-Term Low-Frequency Electrical Stimulation Enhanced Remyelination of Injured Peripheral Nerves by Inducing the Promyelination Effect of Brain-Derived Neurotrophic Factor on Schwann Cell Polarization. *J Neurosci Res*, 89(6), 2578-2587

Wang, W., Zhu, H., Li, F., et al. (2009). Electrical stimulation promotes motor nerve regeneration selectivity regardless of end-organ connection. *J Neurotrauma*, 26(4), 641-64

Wang, G., Simon, D., Wu, Z., Belsky, D., Heller, E., O'Rourke, M., Hertz, N., Molina, H., Zhong, G., Tessier-Lavigne, M., & Zhuang, X. (2019). Structural plasticity of actin-spectrin membrane skeleton and functional role of actin and spectrin in axon degeneration. *eLife*, *8*. https://doi.org/doi: 10.7554/eLife.38730

Wang, Y., Li, D., Wang, G., Chen, L., Chen, J., Liu, Z., Zhang, Z., Shen, H., Jin, Y., & Shen, Z. (2017). The effect of co-transplantation of nerve fibroblasts and Schwann cells on peripheral nerve repair. *International Journal of Biological Sciences*, *13*(12), 1507–1519. https://doi.org/doi:10.7150/ijbs.21976

Ward, P., Davey, R., Zajac, J., et al. (2021). Neuronal androgen receptor is required for activity dependent enhancement of peripheral nerve regeneration. *Dev Neurobiol*, 81(4), 411-423..

Webber, C. (2022a). Determining the mechanism through which conditioning electrical stimulation promotes nerve regeneration. Virtual Conference presented at: Proceedings of the American Society of Peripheral Nerve Conference; Jan 2022; Carlsbad, CA.

Webber, C. (2022b). Unlike a conditioning crush lesion, conditioning electrical stimulation promotes nerve regeneration in a non-injurious and non-inflammatory manner. Nanosymposium Presentation presented at: Society for Neuroscience Conference; Nov 2022; Miami, FL.

Wei, D., Hurd, C., Galleguillos, D., Singh, J., Fenrich, K., Webber, C., Sipione, S., & Fuoad, K. (2016). Inhibiting cortical protein kinase A in spinal cord injured rats enhances efficacy of rehabilitative training. *Experimental Neurology*, *283*, 365–374. https://doi.org/10.1016/j.expneurol.2016.07.001

Weng, Y.-L., An, R., Cassin, J., Joseph, J., Mi, R., Wang, C., Zhong, C., Jin, S.-G., Pfeifer, G., Bellacosa, A., Dong, X., Höke, A., He, Z., Song, H., & Ming, G.-L. (2017). An Intrinsic Epigenetic Barrier for Functional Axon Regeneration. *Neuron*, *19*(2), 37–346. https://doi.org/doi: 10.1016/j.neuron.2017.03.034

Willand, M., Nguyen, M.-A., Borschel, G., & Gordon, T. (2016). Electrical stimulation to promote peripheral nerve regeneration. *Neurorehabilitation and Neural Repair*, *30*(5), 490–496. https://doi.org/doi: 10.1177/1545968315604399

Wilson, D., Jagadeesh, P. (1976). Experimental regeneration in peripheral nerves and the spinal cord in laboratory animals exposed to a pulsed electromagnetic field. *Spinal Cord*, 14(1), 12-20.

Witzel, C., Koulaxouzidis, G., Brushart, T., & Infanger, M. (2009). Electrical stimulation enhances distal reinnervation without increasing regeneration speed. *Journal of Plastic, Reconstructive & Aesthetic Surgery*, *62*(6). https://doi.org/10.1016/j.bjps.2009.02.034

Witzel, C., Brushart, T., Koulaxouzidis, G., et al. (2016). Electrical Nerve Stimulation Enhances Perilesional Branching after Nerve Grafting but Fails to Increase Regeneration Speed in a Murine Model. *J Reconstr Microsurg*, 32(6), 491-497.

Wolf, A., Stys, P., Meaney, D., & Smith, D. (2001). Traumatic axonal injury induces calcium influx modulated by tetrodotoxin-sensitive sodium channels. *Journal of Neuroscience*, *21*(6), 1923–1930. https://doi.org/doi: 10.1523/JNEUROSCI.21-06-01923.2001

Wong, J., Olson, J., Morhart, M., et al. (2015). Electrical stimulation enhances sensory recovery: A randomized controlled trial. Annals of Neurology, 77(6), 996-1006.

Woo, S. H., Lukacs, V., de Nooij, J. C., Zaytseva, D., Criddle, C. R., Francisco, A., Jessell, T. M., Wilkinson, K. A., & Patapoutian, A. (2015). Piezo2 is the principal mechanotransduction channel for proprioception. *Nature neuroscience*, *18*(12), 1756–1762. https://doi.org/10.1038/nn.4162

Wood, M., Willits, R. (2009). Applied electric field enhances DRG neurite growth: influence of stimulation media, surface coating and growth supplements. *J Neural Eng*, 6(4).

Xu, C., Kou, Y., Zhang, P., et al. (2014). Electrical stimulation promotes regeneration of defective peripheral nerves after delayed repair intervals lasting under one month. *PLoS ONE*, 9(9).

Yan, X., Liu, J., Huang, J., et al. (2014). Electrical stimulation induces calcium-dependent neurite outgrowth and immediate early genes expressions of dorsal root ganglion neurons. *Neurochem Res*, 39(1), 129-141.

Yan, X., Liu, J., Ye, Z., et al. (2016). CaMKII-mediated CREB phosphorylation is involved in Ca2+-induced BDNF mRNA transcription and neurite outgrowth promoted by electrical stimulation. *PLoS ONE*, 11(9).

Yang, X., Liu, R., Xu, Y., Ma, X., & Bing, Z. (2021). The Mechanisms of Peripheral Nerve Preconditioning Injury on Promoting Axonal Regeneration. *Neural Plasticity*. https://doi.org/10.1155/2021/6648004

Yang, Z., & Wang, K. (2015). Glial fibrillary acidic protein: From intermediate filament assembly and gliosis to neurobiomarker Zhihui Yang 1, Kevin K W Wang 2. *Trends in Neuroscience*, *38*(6), 364–374. https://doi.org/doi: 10.1016/j.tins.2015.04.003

Yao, J., Sasaki, Y., Wen, Z., Bassell, G., & Zheng, J. (2006). An essential role for beta-actin mRNA localization and translation in Ca2+-dependent growth cone guidance. *Nature Neuroscience*, *9*(10), 1265–1273. https://doi.org/doi: 10.1038/nn1773

Zhang, J., Huang, J., Zhang, C., et al. (2013). Electrical stimulation-induced neuronal outgrowth from human gingiva-derived mesenchymal stem cells. Artificial Cells, Nanomedicine, and Biotechnology, 41(4), 217-225.

Zhang, Y., Zhang, J., Jin, C., et al. (2020). Brief electrical stimulation accelerates axon regeneration through Schwann cells via modulation of the transforming growth factor-beta signaling pathway. Journal of Neurochemistry, 154(6), 650-664.

Zhang, Y., Yu, C., Jin, C., et al. (2021). Brief Electrical Stimulation Accelerates Peripheral Nerve Regeneration by Enhancing Neuronal TGF-β Expression. Frontiers in Neuroscience, 15.

Zhu, J., Lu, K., Zhang, N., et al. (2016). Electrical stimulation affects neural stem cell fate and function in vitro. Experimental and Therapeutic Medicine, 12(2), 779-784.

Ziv, N., & Spira, M. (1995). Axotomy induces a transient and localized elevation of the free intracellular calcium concentration to the millimolar range. *Journal of Neurophysiology*, *74*(6), 2625–2637. https://doi.org/doi: 10.1152/jn.1995.74.6.2625

Zochodne, D. (2008). *Neurobiology of Peripheral Nerve Regeneration*. Cambridge University Press.

Zuo, K., Shafa, G., Antonyshyn, K., Chan, K., Gordon, T., & Borschel, G. (2020). . A single session of brief electrical stimulation enhances axon regeneration through nerve autografts. *Experimental Neurology*, *322*. https://doi.org/10.1016/j.expneurol.2019.113074

Appendix A

LABORATORY RESEARCH

A Direct Comparison of Targeted Muscle Reinnervation and Regenerative Peripheral Nerve Interfaces to Prevent Neuroma Pain

Jenna-Lynn B. Senger, MD, PhD[*,‡], Paige Hardy, BSc[*], Aline Thorkelsson, BSc[*], Shirley Duia, BSc[*], Ralph Hsiao, MSc[*], Stephen W. P. Kemp, PhD[§], Gustavo Tenorio, BSc[¶], Mithun Rajshekar, PhD[#], Bradley J. Kerr, PhD[¶], K. Ming Chan, MD[#], Karyne N. Rabey, PhD[*,**], Christine A. Webber, PhD[*]

[*]Department of Surgery, Division of Anatomy, University of Alberta, Edmonton, AB, Canada; [‡]Division of Plastic & Reconstructive Surgery, University of British Columbia, Vancouver, BC, Canada; [§]Department of Surgery, Section of Plastic Surgery, University of Michigan, Ann Arbor, Michigan, USA; [||]Department of Biomedical Engineering, University of Michigan, Ann Arbor, Michigan, USA; [¶]Department of Anesthesiology, University of Alberta, Edmonton, AB, Canada; [#]Division of Physical Medicine and Rehabilitation, University of Alberta, Edmonton, AB, Canada; [**]Department of Anthropology, University of Alberta, Edmonton, AB, Canada

The abstract, objectives and results (including figures) were presented at the Canadian Society of Plastic Surgeons, June 20, 2022, Quebec, Canada.

Correspondence: Christine A. Webber, PhD, Department of Surgery, Division of Anatomy, University of Alberta, #5-01 Medical Sciences Building, Edmonton, AB, Canada.
Email: webber2@ualberta.ca

Received, January 23, 2023; **Accepted,** March 29, 2023; **Published Online,** June 2, 2023.

BACKGROUND AND OBJECTIVES: Targeted muscle reinnervation (TMR) and regenerative peripheral nerve interface (RPNI) surgeries manage neuroma pain; however, there remains considerable discord regarding the best treatment strategy. We provide a direct comparison of TMR and RPNI surgery using a rodent model for the treatment of neuroma pain.

METHODS: The tibial nerve of 36 Fischer rats was transected and secured to the dermis to promote neuroma formation. Pain was assessed using mechanical stimulation at the neuroma site (direct pain) and von Frey analysis at the footpad (to assess tactile allodynia from collateral innervation). Once painful neuromas were detected 6 weeks later, animals were randomized to experimental groups: (a) TMR to the motor branch to biceps femoris, (b) RPNI with an extensor digitorum longus graft, (c) neuroma excision, and (d) neuroma in situ. The TMR/RPNIs were harvested to confirm muscle reinnervation, and the sensory ganglia and nerves were harvested to assess markers of regeneration, pain, and inflammation.

RESULTS: Ten weeks post-TMR/RPNI surgery, animals had decreased pain scores compared with controls ($P < .001$) and they both demonstrated neuromuscular junction reinnervation. Compared with neuroma controls, immunohistochemistry showed that sensory neuronal cell bodies of TMR and RPNI showed a decrease in regeneration markers phosphorylated cyclic AMP receptor binding protein and activation transcription factor 3 and pain markers transient receptor potential vanilloid 1 and neuropeptide Y ($P < .05$). The nerve and dorsal root ganglion maintained elevated Iba-1 expression in all cohorts.

CONCLUSION: RPNI and TMR improved pain scores after neuroma resection suggesting both may be clinically feasible techniques for improving outcomes for patients with nerve injuries or those undergoing amputation.

KEY WORDS: Neuroma, Peripheral nerve, Targeted muscle reinnervation, Regenerative peripheral nerve interface, Rat, Nerve regeneration, Pain

Neurosurgery 00:1–12, 2023 https://doi.org/10.1227/neu.0000000000002541

Although the earliest evidence for surgical amputations can be traced to 31 000 years ago,[1] we continue to struggle with preventing and managing the postoperative sequelae associated with amputations, including painful neuromas.[2] Reports range with some indicating up to 80% of patients develop painful neuromas after amputation, significantly affecting quality of life.[3-5] It is not understood why some neuromas remain asymptomatic and further investigation into the pathophysiology is needed. Components of the nociceptive response of painful neuromas have been identified, including central sensitization, accumulation of ion channels, and an

ABBREVIATIONS: ATF3, activation transcription factor 3; **CGRP,** calcitonin gene-related peptide; **DAPI,** 4′,6-diamidino-2-phenylindole; **DRG,** dorsal root ganglion; **EDL,** extensor digitorum longus; **iDISCO,** immuno-enabled three-dimensional imaging of surgical constructs; **NMJ,** neuromuscular junctions; **NPY,** neuropeptide Y; **pCREB,** phosphorylated cyclic AMP receptor binding protein; **RPNI,** regenerative peripheral nerve interface; **SEM,** standard error of the mean; **TMR,** targeted muscle reinnervation.